

Toward ab initio density functional theory for nuclei

J.E. Drut, R.J. Furnstahl, L. Platter

Department of Physics, Ohio State University, Columbus, OH 43210

September 11, 2009

Abstract

We survey approaches to nonrelativistic density functional theory (DFT) for nuclei using progress toward *ab initio* DFT for Coulomb systems as a guide. *Ab initio* DFT starts with a microscopic Hamiltonian and is naturally formulated using orbital-based functionals, which generalize the conventional local-density-plus-gradients form. The orbitals satisfy single-particle equations with multiplicative (local) potentials. The DFT functionals can be developed starting from internucleon forces using wave-function based methods or by Legendre transform via effective actions. We describe known and unresolved issues for applying these formulations to the nuclear many-body problem and discuss how *ab initio* approaches can help improve empirical energy density functionals.

Keywords: Density functional theory, nuclear structure, many-body perturbation theory

Contents

1	Introduction	2
1.1	Overview	2
1.2	Basic features/ingredients of DFT	3
1.3	Coulomb vs. nuclear DFT	8
1.4	Scope and plan of review	10
2	Orbital-based DFT	11
2.1	Hartree-Fock in coordinate representation	11
2.2	Motivation for orbital-dependent functionals	13
2.3	Derivation of the optimized effective potential	17
2.4	OEP from total energy minimization or density invariance	19
2.5	Approximations	21
3	DFT and ab initio wave function methods	22
3.1	Goldstone many-body perturbation theory	22
3.2	Improved perturbation theory	25
3.3	Low-momentum interactions	28
3.4	Density matrix expansion	30
4	DFT as Legendre transform	38
4.1	Analogy to Legendre transform in thermodynamics	40
4.2	Effective actions for composite operators	42
4.3	EFT and power counting for functionals	46
4.4	Additional comments	48

5 Topics for nuclear DFT	49
5.1 Pairing	49
5.2 Broken symmetries	53
5.3 Single-particle energies	55
5.4 Improving empirical EDF's	56
6 Summary and outlook	58
References	62

1 Introduction

1.1 Overview

Density functional theory (DFT) has been applied to the Coulomb many-body problem with great phenomenological success in predicting properties of atoms, molecules, and solids [1, 2, 3, 4, 5, 6]. DFT calculations are comparatively simple to implement yet often very accurate and have a computational cost that makes them at present the only choice for systems with large numbers of electrons [7]. For these same reasons (with nucleons rather than electrons), large-scale collaborations of nuclear physicists in the SciDAC UNEDF [8, 9] (“Universal Nuclear Energy Density Functional”) and FIDIPRO [10] projects, as well as many other individuals, are working on further developing DFT for the nuclear many-body problem. Questions in astrophysics and the advent of new experimental facilities to study nuclei at the limits of existence, as well as societal needs, are driving multi-pronged efforts to calculate nuclear properties and reactions across the full table of the nuclides more accurately and reliably than what is currently possible with existing energy density functional (EDF) methods (e.g., those based on Skyrme, Gogny, or relativistic mean-field functionals [11]).

A principal strategy is to exploit the substantial and ongoing progress in *ab initio* nuclear structure calculations, which are primarily based on approximating the many-nucleon wave function. This progress is the consequence of synergistic advances in the construction of internucleon interactions, in methods to calculate properties of many-nucleon systems, and in the ability to effectively use growing computational power [8]. Because these approaches will be limited in scope for the foreseeable future, a natural goal is to develop *ab initio* DFT for nuclei. In this context, “*ab initio*” is taken to mean a formalism based directly on a microscopic nuclear Hamiltonian that describes two-nucleon and few-body scattering and bound-state observables, in analogy to calculations in quantum chemistry or condensed matter physics that start from the Coulomb interaction. This contrasts with many nuclear EDF approaches [11] that fit a functional without relying on an explicit underlying Hamiltonian [12]. Efforts to construct bridges between *ab initio* few-body calculations and the largely empirical nuclear EDF's are bringing together diverse theorists and formal techniques using insights from other fields. The language and formalism differences are a barrier to progress. We hope to lessen this barrier with this review by setting up *ab initio* DFT as an intermediary.

There are multiple possible paths to *ab initio* DFT and the optimal choice for describing nuclei is not clear. In confronting the limitations of the most widely used conventional Coulomb DFT implementations (such as so-called “generalized gradient approximation” or GGA functionals), condensed matter physicists and quantum chemists have made extensive developments toward *ab initio* Coulomb DFT based on wave-function methods. We would like to exploit these advances. This means understanding what can be borrowed directly for nuclei and where modifications are needed. At the same time, DFT based on effective actions may suggest alternative approximations as well as connections to effective field theory (EFT). The goal of this review is to outline various strategies that are being adopted (or

may be explored soon), identify common features and challenges, and generally make them more accessible to the various communities of nuclear physicists attacking these problems. We restrict ourselves to a definition of *ab initio* DFT that is consistent with usage in Coulomb systems (see Section 1.2) but which is a subset of the full range of efforts pointing toward non-empirical nuclear EDF (e.g., see Refs. [13, 14, 15, 16]).

The focus on *ab initio* DFT does not mean we propose abandoning the successes of the empirical EDF's, which already achieve an accuracy for known nuclear masses that will be hard to reach directly with *ab initio* functionals. Furthermore, it will only be possible in the near future to make *ab initio* calculations of a limited subset of all nuclei. DFT was originally formulated and is still typically described in terms of existence proofs. These proofs imply that it is *possible* to find a functional (or functionals) that depends only explicitly on the density and which is minimized at the ground state energy with the ground state density. While these proofs are not constructive, they can be taken to justify empirical nuclear EDF approaches. An important prong of the nuclear DFT effort seeks to make the EDF's less empirical and therefore more reliable for extrapolation to unmeasured nuclear properties by generalizing or constraining the functionals based on *ab initio* input. This can be done directly using constraints from accurate *ab initio* nuclear structure calculations (e.g., fitting the theoretical neutron matter equation of state) but also through insights from *ab initio* DFT about the form and characteristics of the functionals.

1.2 Basic features/ingredients of DFT

Our discussion is based on the nuclear many-body problem formulated in terms of a nonrelativistic Schrödinger equation for protons and neutrons, with a Hamiltonian of the form

$$\hat{H}_N = \hat{T} + \hat{V} \equiv \hat{T} + \hat{V}_{NN} + \hat{V}_{NNN} + \dots , \quad (1)$$

where \hat{T} is the kinetic energy and \hat{V} is the sum of two- and three- and higher-body forces in a decreasing hierarchy, which is truncated at three-body forces in the most complete present-day calculations. (Effects from relativity and other degrees of freedom are absorbed into the potentials either explicitly or implicitly.) Such Hamiltonians are derived in low-energy effective theories of quantum chromodynamics (QCD) with varying degrees of model dependence. The development of better Hamiltonians, and of many-body forces in particular, is an on-going enterprise [17]. We emphasize that “Hamiltonians” is plural because there is not a unique or even preferred form of the short-distance parts of the potentials (the longest-ranged part, pion exchange, *does* have a common, local form in almost all potentials). Contrast this with the electronic case, where the long-range Coulomb potential is for many systems the entire story.

For most of our discussion it is irrelevant whether the Hamiltonian being used results from a systematic effective field theory (EFT) expansion [17] or a more phenomenological form [18], as long as it reproduces few-body observables. What *is* relevant is that the initial Hamiltonian can be transformed (e.g., with renormalization group methods) to maintain observables while making it more suitable for particular many-body methods (see below). We argue that transformations to soften the potential will be critical in making DFT a feasible framework for nuclei; that is, DFT implies an organization of the many-body problem that will not work well with all nuclear Hamiltonians.

We can classify microscopic nuclear structure methods into two broad categories, wave function and Green's function methods. In the former, one solves in some approximation the A -body Schrödinger equation for the A -body wave function $\Psi(x_1, \dots, x_A)$, where x_i is shorthand for all of the variables of nucleon i (e.g., \mathbf{x}_i , spin, isospin). If the operators are known, this allows the calculation of any nuclear observable. Methods in this category include Green's function¹ and auxiliary field Monte Carlo

¹Despite the name, GFMC is not a Green's function method in the sense it is used here.

(GFMC/AFMC) [19, 20], no-core shell model (NCSM) [21], and coupled cluster (CC) [22, 23]. The computational cost of such calculations rises rapidly with A . Nevertheless, most of the recent progress in *ab initio* nuclear structure physics has come from pushing these techniques to higher A [24, 21, 25].

Our *ab initio* DFT discussion will connect to wave-function based formulations that use a single-particle basis and can handle non-local interactions (e.g., NCSM and CC but not GFMC). In principle, such a formulation solves the problem of finding the ground-state energy E_{gs} of a given \hat{H}_N (for a specified number of nucleons A) by minimizing $\langle \Psi | \hat{H}_N | \Psi \rangle$ over all normalized anti-symmetric A -particle wave functions [4]:

$$E_{\text{gs}} = \min_{\Psi} \langle \Psi | \hat{H}_N | \Psi \rangle . \quad (2)$$

In practice, of course, the Hilbert space (i.e., the basis size) is finite and E_{gs} is found approximately. (The calculation is also not variational in many cases, such as CC, but that is not an issue here.)

An alternative to working with the many-body wave function is density functional theory (DFT) [1, 4, 26], which as the name implies, has fermion densities as the fundamental “variables”. We will start with DFT as it is typically introduced, citing a theorem of Hohenberg and Kohn (HK) [27]: There exists an energy functional $E_v[\rho]$ of the density $\rho(\mathbf{x})$,² labeled by a (static) external potential $v_{\text{ext}}(\mathbf{x})$ such that

$$E_v[\rho] = F[\rho] + \int d\mathbf{x} v_{\text{ext}}(\mathbf{x})\rho(\mathbf{x}) , \quad (3)$$

which is minimized at the ground-state energy E_{gs} with the ground-state density $\rho_{\text{gs}}(\mathbf{x})$. An example of v_{ext} is the electrostatic potential from ions in atoms and molecules, as in Eq. (30). The functional F , often designated F_{HK} in the literature, is independent of the external potential v_{ext} and has the same form for any A . In this sense it is said to be *universal*. The HK theorem offers no help in constructing F , but is useful in that it gives a license to search for (or guess) approximate energy functionals. This would serve as justification for nuclear EDF’s except for the disquieting feature that there is no v_{ext} for self-bound nuclei, which makes the meaning of Eq. (3) unclear.

A constrained search derivation [28] is a more illuminating alternative to the proof-by-contradiction approach to DFT used by Hohenberg and Kohn. We start as before with the minimization in Eq. (2), adding an external potential, but now we separate the minimization into two steps [4]:

1. First minimize over all Ψ that yield a given density $\rho(\mathbf{x})$:

$$\min_{\Psi \rightarrow \rho} \langle \Psi | \hat{H}_N + \hat{V}_{\text{ext}} | \Psi \rangle = \min_{\Psi \rightarrow \rho} \langle \Psi | \hat{T} + \hat{V} | \Psi \rangle + \int d\mathbf{x} v_{\text{ext}}(\mathbf{x})\rho(\mathbf{x}) , \quad (4)$$

where \hat{V} is the full internucleon interaction and $\hat{V}_{\text{ext}} = \int d\mathbf{x} v_{\text{ext}}(\mathbf{x})\hat{\rho}(\mathbf{x})$. Define $F[\rho]$ as the resulting contribution of the first term:

$$F[\rho] \equiv \langle \Psi_{\rho}^{\text{min}} | \hat{T} + \hat{V} | \Psi_{\rho}^{\text{min}} \rangle . \quad (5)$$

2. Then minimize over $\rho(\mathbf{x})$:

$$E = \min_{\rho} E_v[\rho] \equiv \min_{\rho} \left\{ F[\rho] + \int d\mathbf{x} v_{\text{ext}}(\mathbf{x})\rho(\mathbf{x}) \right\} . \quad (6)$$

where the external potential $v_{\text{ext}}(\mathbf{x})$ is held fixed.

In principle one works at fixed A by introducing a chemical potential μ :

$$\delta \left\{ F[\rho] + \int d\mathbf{x} v_{\text{ext}}(\mathbf{x})\rho(\mathbf{x}) - \mu \int d\mathbf{x} \rho(\mathbf{x}) \right\} = 0 , \quad (7)$$

²As discussed below, we will have multiple densities in practice but considering the fermion density only suffices for now.

which implies

$$\frac{\delta F[\rho]}{\delta \rho(\mathbf{x})} + v_{\text{ext}}(\mathbf{x}) = \mu . \quad (8)$$

The chemical potential is adjusted until the density ρ resulting from solving Eq. (8) yields the desired particle number A . Or one minimizes only over ρ that satisfy $\int d\mathbf{x} \rho(\mathbf{x}) = A$.

As noted by Kutzelnigg [29], the presentation of the HK theorem as an existence proof is often accompanied by misleading statements such as “all information about a quantum mechanical ground state is contained in its electron density ρ ” or that “the energy is completely expressible in terms of the density alone.” These claims seem at odds with the observation that while the external potential energy is expressible in terms of ρ (if there is a v_{ext}), the kinetic energy is given in terms of the one-particle density matrix and interaction energies require two-particle and higher density matrices. How do we reconcile this? The key is that the usual wave-function treatment of the many-body problem as in Eq. (2) has in mind a *single, fixed Hamiltonian*. In that case, to make a variational calculation of the ground-state wave function Ψ , the energy E must be made stationary to variations in the relevant density matrices and not just the density. This corresponds to variations of the normalized A -body wave function Ψ .

To understand DFT we should consider instead a *family* of Hamiltonians $\hat{H}[v]$, each characterized by a potential v for which we know the corresponding ground state energy $E[v]$. We might ask, if we know $E[v]$, why not just evaluate at $v = v_{\text{ext}}$ and avoid more complications? But if we do know $E[v]$, then we can construct the functional Legendre transform [29],

$$-F[\rho] = \min_v \left\{ \int d\mathbf{x} v(\mathbf{x})\rho(\mathbf{x}) - E[v] \right\} , \quad (9)$$

where the minimization is over an appropriate domain of v (really the infimum or greatest lower bound) rather than just considering a fixed v_{ext} [29]. Thus we obtain the dependence of the internal energy on the density. This justifies the suggestive notation of Eq. (3): If $v(\mathbf{x})$ is set to a constant, it acts as a chemical potential and the equation expresses a Legendre transform between two thermodynamic potentials. (An expanded version of the thermodynamic analogy is given in Section 4.) If the Legendre transform is possible (see Ref. [30, 29]), we can also obtain with a second Legendre transformation that

$$E[v] = \min_\rho \left\{ \int d\mathbf{x} v(\mathbf{x})\rho(\mathbf{x}) + F[\rho] \right\} \equiv \min_\rho \left\{ E_v[\rho] \right\} , \quad (10)$$

which is the energy for fixed v expressed as a minimization over a trial set of densities. Thus we reproduce Eq. (6) and show the origin of the HK expression in Eq. (3).

This perspective shows that DFT and Eq. (3) are really in the spirit of the other major category of microscopic nuclear structure methods, namely Green’s functions. Instead of the many-body wave function, the Green’s function approach considers the response of the ground state to adding or removing particles [31, 32, 33]. The underlying idea is that knowing the most general response of the ground state (or the partition function in the presence of the most general sources) gives a complete specification of the many-body problem. Observables such as the ground state energy, densities, single-particle excitations, and more can be expressed in terms of Green’s functions (with one-body operators needing the single-particle Green’s function, two-body operators generally needing the two-particle Green’s function, and so on). The special case considered here starts with the response of the energy to a “source” $v(\mathbf{x})$, which is coupled to the density. Instead of non-local sources that individually create particles in one place and destroy them elsewhere, here the perturbation by the source is a local shift in the density. Because it is a more limited response than the usual Green’s functions, the corresponding observables probed are also limited, but include the ground-state energy. A natural mathematical framework for such responses and other Legendre transforms is the effective action formalism using path integrals. We

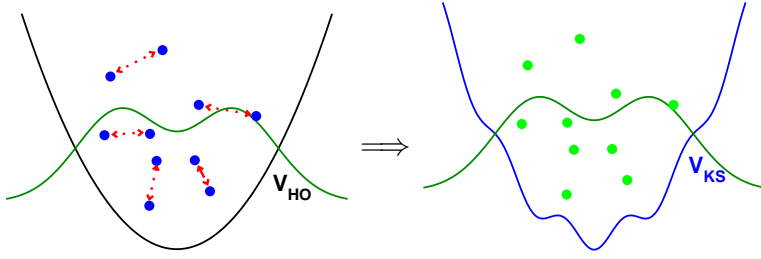


Figure 1: Kohn-Sham DFT for a $v_{\text{ext}} = V_{\text{HO}}$ harmonic trap. On the left is the interacting system and on the right the Kohn-Sham system. The density profile is the same in each.

give more details in Section 4 on how this works. (This perspective also shows that taking $v = 0$ is not a problem in principle; such sources are usually set equal to zero at the end, although in this case there are related issues with self-bound systems such as nuclei.)

In practice, DFT is rarely implemented as a pure functional of the density, such as a generalized Thomas-Fermi functional, because no one has succeeded in constructing one that yields the desired accuracy (an immediate problem is finding an adequate functional of density only for the kinetic energy). Instead, the most successful procedure is to introduce single-particle orbitals that are used in what appears to be an auxiliary problem, but which still leads to the minimization of the energy functional for the ground-state energy E_{gs} and density ρ_{gs} . This is called Kohn-Sham (KS) DFT, and is illustrated schematically in Fig. 1 for fermions in a harmonic trap. The characteristic feature is that the interacting density for A fermions in the external potential v_{ext} is equal (by construction) to the non-interacting density in another single-particle potential. This is achieved by orbitals $\{\phi_i(\mathbf{x})\}$ in the *local* potential $v_{\text{KS}}([\rho], \mathbf{x}) \equiv v_{\text{KS}}(\mathbf{x})$, which are solutions to

$$[-\nabla^2/2m + v_{\text{KS}}(\mathbf{x})]\phi_i(\mathbf{x}) = \varepsilon_i\phi_i(\mathbf{x}), \quad (11)$$

and determine the density by

$$\rho(\mathbf{x}) = \sum_i n_i |\phi_i(\mathbf{x})|^2 = \sum_{i=1}^A |\phi_i(\mathbf{x})|^2, \quad (12)$$

where the sum is over the lowest A states with $n_i = \theta(\varepsilon_F - \varepsilon_i)$ here. When we include pairing, the sum is generalized to be over all orbitals with appropriate occupation numbers (see Section 5.1). The magic Kohn-Sham potential $v_{\text{KS}}([\rho], \mathbf{x})$ is in turn determined from $\delta E_v[\rho]/\delta\rho(\mathbf{x})$ (see below). Thus the Kohn-Sham orbitals depend on the potential, which depends on the density, which depends on the orbitals, so we must solve self-consistently (for example, by iterating until convergence). We will return later to address the meaning of the KS eigenvalues ε_i . The ground-state energy is $E_{\text{gs}} = E_{v_{\text{ext}}}[\rho_{\text{gs}}]$.

We will define orbital-based density functional theory (DFT) broadly as *any* many-body method based on a local (“multiplicative”) background potential (what we called v_{KS} above) used to calculate the ground-state energy and density of inhomogeneous systems in the manner just described. That is, there will be a single-particle, non-interacting component of the problem that involves solving for orbitals with a local (diagonal in coordinate space) potential. We will also require that there are no corrections to the density obtained from these occupied orbitals (as in usual Kohn-Sham DFT). It is not obvious at this point that this is a necessary feature, because it is not essential to the numerical simplicity or good scaling behavior. We will see in later sections how it arises. This characterization of DFT can be realized in seemingly very different approaches, such as a particular organization of (possibly resummed) many-body perturbation theory (MBPT) and effective actions for composite operators (based on functional Legendre transformations). The DFT formalism is often said to be a mean-field approach because of the Kohn-Sham potential and this applies to our general definition as well. The point is that it is not a

mean-field *approximation* but an organization that takes a mean-field state as a reference state, which if solved completely includes all many-body correlations. (The real issue is how much correlation is included in a given approximation to the exact functional.)

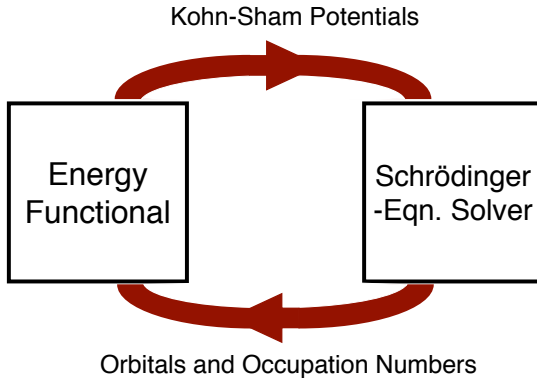


Figure 2: Generic self-consistency cycle for Kohn-Sham DFT. The energy functional takes orbital wave functions and eigenvalues (with occupation numbers) as inputs. The outputs are the local Kohn-Sham potentials from the functional derivative of the energy functional. These could be directly evaluated as with a Skyrme or density matrix expansion functional, or solved from OEP equations.

Implementations of orbital-based DFT will have a self-consistency cycle of the form shown in Fig. 2. The code that solves the KS single-particle Schrödinger equations (“Schrödinger-Eqn. Solver”) can be generic (if generalized to include pairing) because the same equations are solved for different energy functionals (only the potentials change). This part of the calculation is generally the key to the computational scaling because the cost goes up gently with A and it also means that we can adapt the well-developed tools used for Skyrme calculations. The “Energy Functional” will be particular to the implementation, ranging from simple function evaluation to solving complicated integral equations. If the cost of evaluating this box, which includes calculating the functional derivative defining v_{KS} , can be kept under control, the computational advantage will hold. (Conversely, in full calculations of orbital-based DFT, one has to consider seriously the computational scaling when comparing to alternative strategies.) It is often the case that the energy functional is taken to be of the local or semi-local³ form:

$$E[\rho_i, \tau_i, \dots] = \int d\mathbf{x} \mathcal{E}(\rho_i(\mathbf{x}), \tau_i(\mathbf{x}), \dots), \quad (13)$$

where we have allowed different types of densities such as the kinetic energy density τ_i and where dependence on gradients of the densities is also allowed. For example, the Skyrme functional in Eq. (101) has this structure. We emphasize that *this is not a general form*, but requires significant approximations to be derived from a non-local orbital-based functional (such as by applying the density matrix expansion, see Section 3.4).

We also emphasize that the Kohn-Sham *potentials* v_{KS} are always local no matter how non-local the energy density becomes. This is different from some nuclear EDF approaches that feature finite-range effective interactions in the form of a Hartree-Fock functional (e.g., Gogny), for which the single-particle equations have non-local exchange potentials [11]. While the locality of Kohn-Sham potentials eases the computational burden, it is a constraint that may ultimately prove to be too limiting for nuclear energy functionals [13, 16].

We can separate our subsequent discussion of *ab initio* DFT into two parts:

³“Semi-local” in this context means that the energy density at \mathbf{x} depends only on the electron density and orbitals in an infinitesimal neighborhood of \mathbf{x} [34]. So \mathcal{E} has only a finite number of gradients.

1. Given an energy functional, what is the associated Kohn-Sham potential?

2. How do we construct an *ab initio* energy functional systematically?

The second question is more fundamental but the first one is more generic, so we begin with it in Section 2; two approaches to the second question are described in Sections 3 and 4. We stress that Kohn-Sham DFT, with orbitals, is in fact a natural development in each of these approaches, rather than simply a “trick” to better approximate the kinetic energy. Further, we find that keeping the densities fixed entirely from the Kohn-Sham orbitals either follows as a consequence of the DFT minimization conditions or can be used as an imposed condition to derive a functional. In our working definition of DFT we allow complete freedom in defining the Kohn-Sham system, which permits more physics to be shifted into the potential (“mean field”), making the DFT functional more effective (e.g., a perturbative expansion will converge more rapidly). One way of doing this is to allow *any* local densities paired with corresponding sources.

1.3 Coulomb vs. nuclear DFT

We will rely heavily on the progress made in *ab initio* DFT for Coulomb systems, but we should always keep in mind the differences between Coulomb and nuclear many-body problems, which will introduce substantial challenges. For most Coulomb applications, the Hamiltonian is well known and takes a simple, two-body local form (that is, it is diagonal in coordinate representation and has no spin dependence). While in principle one could modify the interaction at short distances, e.g., with unitary transformations, the original local form is clearly preferred. Because the interaction is to good approximation $1/r$, it does not make sense to transform it.

The $1/r$ potential follows in a straightforward manner from the underlying theory of quantum electrodynamics (QED).⁴ A directly analogous *ab initio* calculation of the strong interaction would have to start with the quark and gluon interactions of quantum chromodynamics (QCD). But because quarks and gluons are not efficient low-energy degrees of freedom because of confinement, low-energy effective theories of QCD are used to construct interactions between protons and neutrons. These interactions may be systematic (e.g., using EFT) or more phenomenological. But as effective interactions they are not unique and transformations may result in forms more amenable to the DFT formulation.

The weak strength and long range of the Coulomb potential means that the binding energies of atoms and molecules are numerically dominated by the Hartree contribution [6]. This dominance would make the problem simple except that while the exchange-correlation energy (what is beyond Hartree) is often a small fraction of the total binding energy of atoms, molecules, and solids, it is of the same size as the chemical bonding or atomization energy [4]. Thus an accurate DFT functional for this contribution (called E_{xc}) is essential and this is the principal challenge of Coulomb DFT, although there are complications in certain electron systems (e.g., from pseudopotentials, relativity, etc.).

It might be supposed that the dominance of Hartree-Fock contributions to the energy, so that correlations are small corrections treatable in (possibly resummed) perturbation theory, is an important reason why Coulomb DFT works so well. In contrast, for typical realistic NN interactions, correlations are much greater than the Hartree-Fock contribution! This may mean that DFT fails for these Hamiltonians. But we can use the possibility of modifying the interactions by renormalization group methods [35, 36] (and related methods [37, 38]) to change the “perturbativeness” of nuclei. There are several sources of nonperturbative physics for typical nucleon-nucleon interactions.⁵

1. Strong short-range repulsion (“hard-core” for short).

⁴If heavier atoms are being considered there will be in practice a more involved potential and possibly the need to treat the system fully relativistically.

⁵There is also pairing, which we consider separately.

2. Iterated tensor interactions (e.g., from pion exchange).
3. Near zero-energy bound states (e.g., the deuteron and near bound state in the 1S_0 channel).

However, the first two sources depend on the resolution (i.e., the degree of coupling to high-energy physics), and the third one is affected by Pauli blocking. Thus we can use the freedom of low-energy theories to simplify calculations by lowering the resolution, which softens the potential and makes the nonperturbative nuclear physics more perturbative. That is, the convergence rate of perturbative expansions such as the Born series for free-space scattering or the in-medium sum of particle-particle ladder diagrams improves at lower resolution. This is demonstrated using a quantitative measure of the convergence in Ref. [39].

In general, transformations to low-resolution interactions that are compatible with the natural resolution scale of nuclear bound states make the nuclear problem look in some ways more like the Coulomb problem. Not entirely, of course, but generally much more perturbative with weaker tensor correlations. For example, Hartree-Fock plus second-order many-body perturbation theory may be well converged for the bulk energy of the uniform system [39, 40]. Residual issues include how to handle contributions from mixing into the ground state of low-lying excitations in finite nuclei, which could require a nonperturbative treatment. In addition, we might expect that such contributions to the energy functional are significantly non-local, which may be why empirical nuclear EDF's (which are semi-local) have problems incorporating this physics and typically rely on additional procedures to handle these corrections [41]. Testing whether orbital-based DFT can accommodate this physics will be an important area for study.

The conventional DFT for Coulomb systems takes as its starting point precision calculations of the uniform electron gas. These are *ab initio* numerical calculations (e.g., using GFMC) combined with well-controlled analytic limits. This solid starting point for a local density approximation (LDA) is combined with constrained gradient terms to construct semi-local functionals (GGA) that are not microscopic but are also not fit to data.⁶ For any DFT, the uniform system is special, because E vs. ρ is a limiting case for the functional that is an observable function. (In general, the functional evaluated with a density that is not at the minimum is not an observable, see Section 4.1.) At present, *ab initio* nuclear calculations of the uniform system with equal numbers of protons and neutrons (“symmetric nuclear matter”) are much less controlled than the electron gas counterpart. As a result, present-day nuclear EDF's are often purely empirical (e.g., most Skyrme interactions): a parametrized form has constants fit to properties such as binding energies and radii of a set of nuclei. Indeed, the most stringent constraints on the saturation properties of symmetric nuclear matter come from taking the uniform limit of the fitted EDF's. Other nuclear EDF's take guidance from the best possible nuclear matter calculations but then fine tune to yield quantitatively accurate properties of finite nuclei (e.g., see Refs. [44, 45] and references cited therein).

The calculation of nuclei also has features without direct parallel in the basic Coulomb systems, which complicates the formulation of DFT. Perhaps most apparent is the role of symmetries. Atoms and molecules can generally be treated in Born-Oppenheimer approximation, where the slow nuclear degrees of freedom provide an external (Coulomb) potential (this is $v_{\text{ext}}!$) for the fast electronic degrees of freedom. The basic Coulomb problem for DFT is to find the minimal energy given a configuration of nuclei, treated as fixed in space, and the related distribution of electrons (the density or, more generally, the spin densities). This external potential means that symmetries of the Hamiltonian such as translational and rotational invariance are not realized in the physical ground state. In contrast, ordinary nuclei are self-bound and should reflect these symmetries.

But the nuclear Kohn-Sham potential $v_{\text{KS}}(\mathbf{x})$ breaks these symmetries, so that the system being calculated is an intrinsic “deformed” state. This is familiar from any mean-field based calculation

⁶These are called “non-empirical” [42, 43] because the additional parameters are determined by constraints rather than data; quantum chemists also construct empirical Kohn-Sham DFT functionals that are less microscopic.

of nuclei [46, 47]; in general, the organization of the problem about a mean-field inevitably breaks symmetries. Handling the restoration of symmetries is well known from a wave-function point of view through the use of projection. How we should deal with it for *ab initio* DFT has only recently been considered and may require significant developments [12, 48, 49]. The fact that nuclei are self-bound presents not only practical problems but conceptual problems, because there is no external field in the case of interest. In the face of symmetry breaking, is the Kohn-Sham approach even well defined? This issue has been considered by various authors recently and will be reviewed in Section 5.2. This is a situation where an alternative formulation, in this case using effective actions, lends a somewhat complementary interpretation that can suggest different ideas for approximation.

Bulk nuclear matter is superfluid and the treatment of pairing is found to be crucial in the accurate reproduction of experimental trends in finite nuclei by empirical energy density functionals. For Skyrme-type EDF's, pairing has been accommodated by generalizing from zero-range Hartree-Fock equations (equivalent to Hartree) to zero-range Hartree-Fock-Bogoliubov equations [50], with empirical fits of the pairing parameters. This requires the inclusion of “anomalous” densities, which is not physics that arises for atoms and molecules, and the use of *local* anomalous potentials leads to divergences. Bulgac and collaborators [51, 52] have clarified the corresponding renormalization issues and developed procedures that could be incorporated into *ab initio* orbital-based DFT (see Section 5.1). An alternative path has been followed for Coulomb DFT applied to bulk superconductivity, where non-local Kohn-Sham potentials avoid the new divergences. Similarly, nuclear EDF's with finite-range pairing potentials (e.g., Gogny) and recent non-empirical pairing based on low-momentum microscopic interactions in non-local form [15, 16] have natural high-momentum cutoffs. While we focus in this review on methods with local Kohn-Sham potentials, we stress that the best way to incorporate pairing is an open question.

All of these features of nuclei impact the energy functional at the same level of accuracy as we are trying to achieve, so they cannot be ignored. This further motivates a multi-pronged attack to be able to have complementary calculations and to cross-check results, as well as the need to be open to alternatives to strict orbital-based DFT.

1.4 Scope and plan of review

Our target audience for this review spans several communities of nuclear physicists. Those who do wave-function based many-body theory, such as coupled cluster, are likely most familiar with second quantization formalism and many-body perturbation theory (MBPT). The practitioners of effective field theory, who often come from a particle physics background, are generally more fluent in the language of path integrals and effective actions (although probably not in the form directly analogous to DFT). The users of EDF's are experts in the language and techniques of mean-field approximations and broken symmetries, dealing with pairing and the like. Rather than concentrate on only one of these formalisms, we consider both effective action and many-body perturbation theory perspectives as well as discuss how to make empirical approaches less empirical. We believe this will make each more understandable, help focus on the key issues, and suggest approximations and generalizations.

However, it is clear that a complete treatment of these various formalisms would require detailed reviews on each topic. Because of space limitations, our discussions will necessarily be rather schematic, but we will indicate where to find more details in the literature. Fortunately, there are many fine articles targeted at the Coulomb many-body problem that can fill in details. We hope that our treatment here will make these articles more accessible to a nuclear physics audience (or, more precisely, audiences).

Our intention is to provide a guide to possible pathways to improved DFT for nuclei based on the *ab initio* ideas that result in local Kohn-Sham potentials rather than to make an assessment of the current status of alternative approaches. Therefore we provide limited details on the successes and problems with present-day DFT (or EDF) for nuclei, except for pointers to the literature. We also omit various topics, including the many developments in covariant density functional theory, which builds upon the

phenomenologically successful relativistic mean-field calculations, time-dependent DFT, the superfluid local density approximation (SLDA), and efforts to analyze and improve EDF's without reference to an underlying Hamiltonian. At the end we return to provide brief perspectives on some of these topics.

The plan of the review is as follows. In Section 2, the formalism for orbital-based DFT is derived several ways to help clarify its nature. We also present simplifying approximations that have proven notably effective in Coulomb applications. In Section 3, the connection to *ab initio* wave function methods is explored through conventional nuclear MBPT and an improved perturbation approach for Coulomb DFT. The critical role of low-momentum potentials to make MBPT for nuclei viable and how this can be exploited in a semi-local expansion is also examined. The idea of DFT based on Legendre transformations as formulated using effective actions is reviewed in Section 4, with connections to effective field theory (EFT) for DFT and conventional Green's function methods. The issues of symmetry breaking for self-bound systems, pairing, and single-particle energies are addressed in Section 5, along with an overview of efforts to make empirical nuclear EDF's closer to *ab initio*. Section 6 summarizes our perspective on the paths to *ab initio* DFT and points out some alternative routes.

2 Orbital-based DFT

In this section, we introduce the general motivation for orbital-based DFT using the experience of Coulomb systems as a guide and derive in several ways how to go from an energy functional to multiplicative (local) Kohn-Sham potentials within the optimized effective potential (OEP) method. We rely heavily on the reviews by Engel, which appears in Ref. [4], and by Kümmel and Kronik [53] (see also Refs. [54, 6] and Kurth/Pittalis in Ref. [55]), but annotate the presentation with comments on differences expected for applications to nuclei. We defer discussion of the *construction* of appropriate energy functionals to later sections. To provide a point of comparison for the OEP method, we start with a brief review of the Hartree-Fock (HF) approximation in coordinate representation, which is the simplest version of the wave-function microscopic approach. While the exchange-only OEP has close similarities to HF, there are important distinctions that persist when OEP includes correlations.

For simplicity, we present formulas as if the microscopic interactions were always finite-ranged but local (i.e., diagonal in coordinate representation), spin-isospin independent, and two-body only. We caution the reader that for the nuclear case we will have to deal with non-local forces and (at least) three-body forces, all with spin-isospin dependence (see Section 3.4 for examples of these generalizations).

2.1 Hartree-Fock in coordinate representation

The distinction between the usual wave-function description based on many-body perturbation theory (resummed or not) and orbital-based DFT is already evident with Hartree-Fock. As noted earlier, HF is a natural starting place for any Coulomb calculation and, with low-momentum interactions, the same is now true for nuclei (although Hartree-Fock plus second-order may be a fairer comparison). Further, most nuclear EDF's have been viewed at least originally as arising from Hartree-Fock calculations of effective interactions (which might be zero-ranged as with Skyrme or finite-ranged as with Gogny) [11].

Hartree-Fock is the simplest approximate realization of Eq. (2), with single Slater determinants of orbitals ϕ_i :

$$|\Psi_{\text{HF}}\rangle \longrightarrow \det\{\phi_i(\mathbf{x}), i = 1 \cdots A\} \quad (14)$$

as the wave functions over which the energy is minimized. The spin-isospin dependence of the nuclear interaction is critical to the physics but not to the structure of the equations, where it is a distraction. So in order to keep the notation from getting cumbersome, through much of this review we let \mathbf{x} represent the coordinate variable and, when relevant, also the spin-isospin indices. (Similarly, $\int d\mathbf{x}$ includes a summation over spin and isospin when relevant.)

The Hartree-Fock energy in coordinate representation for a *local* two-body potential $V(\mathbf{x}, \mathbf{y})$ in the presence of an external potential is [47]

$$\begin{aligned} \langle \Psi_{\text{HF}} | \hat{H} | \Psi_{\text{HF}} \rangle &= \sum_{i=1}^A \frac{\hbar^2}{2M} \int d\mathbf{x} \nabla \phi_i^\dagger \cdot \nabla \phi_i + \frac{1}{2} \sum_{i,j=1}^A \int d\mathbf{x} \int d\mathbf{y} |\phi_i(\mathbf{x})|^2 V(\mathbf{x}, \mathbf{y}) |\phi_j(\mathbf{y})|^2 \\ &\quad - \frac{1}{2} \sum_{i,j=1}^A \int d\mathbf{x} \int d\mathbf{y} \phi_i^\dagger(\mathbf{x}) \phi_i(\mathbf{y}) V(\mathbf{x}, \mathbf{y}) \phi_j^\dagger(\mathbf{y}) \phi_j(\mathbf{x}) + \sum_{i=1}^A \int d\mathbf{y} v_{\text{ext}}(\mathbf{y}) |\phi_i(\mathbf{y})|^2 , \end{aligned} \quad (15)$$

where the sums are over occupied states. Note that this energy functional of the orbitals is non-local in that there are integrals over \mathbf{x} and \mathbf{y} . The minimization of the energy is achieved by a variation of Eq. (15) with respect to the ϕ_i :

$$\frac{\delta}{\delta \phi_i^*(\mathbf{x})} \left(\langle \Psi_{\text{HF}} | \hat{H} | \Psi_{\text{HF}} \rangle - \sum_{j=1}^A \varepsilon_j \int d\mathbf{y} |\phi_j(\mathbf{y})|^2 \right) = 0 , \quad (16)$$

with the HF eigenvalues ε_j introduced as Lagrange multipliers to constrain the orbitals to be normalized. There are no other subsidiary conditions, such as imposed below in the OEP. The result is the familiar coordinate-space equation for $\phi_i(\mathbf{x})$:

$$-\frac{\hbar^2}{2M} \nabla^2 \phi_i(\mathbf{x}) + \sum_{j=1}^A \int d\mathbf{y} V(\mathbf{x}, \mathbf{y}) \phi_j^*(\mathbf{y}) \{ \phi_j(\mathbf{y}) \phi_i(\mathbf{x}) - \phi_j(\mathbf{x}) \phi_i(\mathbf{y}) \} = \varepsilon_i \phi_i(\mathbf{x}) , \quad (17)$$

or, after defining the local Hartree potential and the non-local exchange or Fock potential,

$$\Gamma_H(\mathbf{x}) \equiv \int d\mathbf{y} V(\mathbf{x}, \mathbf{y}) \sum_{j=1}^A |\phi_j(\mathbf{y})|^2 = \int d\mathbf{y} V(\mathbf{x}, \mathbf{y}) \rho(\mathbf{y}) \quad (18)$$

$$\Gamma_F(\mathbf{x}) \equiv -V(\mathbf{x}, \mathbf{y}) \sum_{j=1}^A \phi_j^*(\mathbf{y}) \phi_j(\mathbf{x}) = -V(\mathbf{x}, \mathbf{y}) \rho(\mathbf{x}, \mathbf{y}) , \quad (19)$$

we find the non-local Schrödinger equation:

$$\left\{ -\frac{\hbar^2}{2M} \nabla^2 + \Gamma_H(\mathbf{x}) \right\} \phi_i(\mathbf{x}) + \int d\mathbf{y} \Gamma_F(\mathbf{x}, \mathbf{y}) \phi_i(\mathbf{y}) = \varepsilon_i \phi_i(\mathbf{x}) . \quad (20)$$

The equations for the Hartree-Fock orbitals are solved with the same self-consistency cycle as in Fig. 2. This is more involved than solving the Kohn-Sham equations (11) because of the non-local Fock potential, but it is drastically simpler than solving for the full wave function. (A typical numerical solution method is to introduce a basis, e.g. the harmonic oscillator basis, which reduces the calculation to a straightforward linear algebra problem.)

The coordinate-space HF equations become significantly more complicated with non-local NN potentials, such as the soft low-momentum NN potentials, and with three-body potentials. With non-local potentials, even the Hartree piece is no longer a multiplicative potential. Indeed, working in coordinate representation is not particularly natural in this case, which may raise questions about the appropriateness of the DFT focus on locality [56]. The treatment of non-local, momentum-space potentials at HF is outlined below in Section 3.4.

At the opposite extreme, if the interaction is taken to be zero ranged (contact interactions) so that $V(\mathbf{x}, \mathbf{y}) \rightarrow V(\mathbf{x}) \delta(\mathbf{x} - \mathbf{y})$, then the Hartree and Fock terms reduce to the same multiplicative form.

This is why “Skyrme-Hartree-Fock” is not only equivalent to a Hartree functional, but has the same form as Kohn-Sham functionals that include correlations beyond exchange. This is also why a ladder of approximations leading to full orbital-based DFT (as described in Section 6) naturally involves Skyrme functionals on the lower rungs. (However, we emphasize that the microscopic functionals described below *do not* assume zero-range interactions.)

Finally, we comment on the interpretation of orbital eigenvalues. The Kohn-Sham eigenvalues in Eq. (11) appear to be analogs of the HF orbital energies in Eq. (20). The latter are well-defined approximations to the separation energies:

$$E_\alpha^{A+1} - E_0^A \quad \text{for} \quad \alpha > A \quad (\text{particle}) \quad (21)$$

$$E_0^A - E_\alpha^{A-1} \quad \text{for} \quad \alpha \leq A \quad (\text{hole}) . \quad (22)$$

The interpretation of the corresponding KS eigenvalues that appear in the orbital-based DFT treatment is less clear, as there is no Koopman’s theorem to identify the difference of $A + 1$ and A body ground-state energies with the eigenvalues [53]. However, Görling [57] has shown that differences of Kohn-Sham eigenvalues are well-defined approximations to excitation energies. In addition, Janak’s theorem holds that the ionization potential equal to the chemical potential is given by the highest occupied KS eigenvalue [6]. (This follows in most cases simply from the large-distance fall-off of the physical density as dictated by the contribution of the least bound particle, whose wave function falls off according to its energy.) The viability of a physical interpretation for the KS eigenvalues is an important topic for nuclear DFT and we return to it below.

2.2 Motivation for orbital-dependent functionals

The motivation given in the literature for orbital-dependent DFT functionals for Coulomb systems is based on some characteristic failures of semi-local functionals as well as the need for greater accuracy in some applications. Both of these points are relevant to nuclear DFT, where EDF’s of the Skyrme type are also semi-local and where greater accuracy is sought globally and greater reliability is sought for extrapolations. Before considering the motivation in more detail, we first review some of the standard Coulomb DFT formalism, indicating where our treatment for nuclei will differ. Following Engel [4], we restrict our discussion to non-relativistic, time-independent, spin-saturated systems; this is for simplicity and is not a limitation of the formalism.

The total energy functional is generally decomposed for Coulomb systems as (except that n is typically used for density instead of ρ ; other details of the notation also vary in the literature)

$$E_{\text{tot}}[\rho] = T_s[\rho] + E_{\text{ext}}[\rho] + E_H[\rho] + E_{\text{xc}}[\rho] , \quad (23)$$

where T_s is the KS kinetic energy, E_{ext} is the external potential energy, E_H is the Hartree energy, and E_{xc} (“xc” stands for “exchange-correlation”) is defined to be everything that is left over; i.e., it is *implicitly* defined by specifying the other pieces. (Note: We have omitted a piece describing the energy of the ions themselves.) For Coulomb systems with just a $1/r$ potential there are explicit expressions in terms of KS orbitals for all but E_{xc} , namely

$$T_s[\rho] = -\frac{1}{2m} \sum_{i=1}^A \int d\mathbf{x} \phi_i^\dagger(\mathbf{x}) \nabla^2 \phi_i(\mathbf{x}) , \quad (24)$$

$$E_{\text{ext}}[\rho] = \int d\mathbf{x} v_{\text{ext}}(\mathbf{x}) \rho(\mathbf{x}) , \quad (25)$$

$$E_H[\rho] = \frac{1}{2} \int d\mathbf{x} \int d\mathbf{y} \rho(\mathbf{x}) V_c(\mathbf{x}, \mathbf{y}) \rho(\mathbf{y}) \quad \text{where} \quad V_c(\mathbf{x}, \mathbf{y}) = \frac{e^2}{|\mathbf{x} - \mathbf{y}|} . \quad (26)$$

As before (and throughout this review), these orbitals satisfy

$$\left[-\frac{\nabla^2}{2m} + v_{\text{KS}}(\mathbf{x}) \right] \phi_i(\mathbf{x}) = \varepsilon_i \phi_i(\mathbf{x}) , \quad (27)$$

where the KS potential $v_{\text{KS}}(\mathbf{x}) = \delta(E_{\text{ext}} + E_{\text{H}} + E_{\text{xc}})/\delta\rho(\mathbf{x})$.⁷ The signature features for *ab initio* DFT (in our broad definition) is that $v_{\text{KS}}(\mathbf{x})$ appears multiplicatively in the KS equation and that the density is given completely by summing up the occupied (defined as the energetically lowest here) KS states:

$$\rho(\mathbf{x}) = \sum_i n_i |\phi_i(\mathbf{x})|^2 . \quad (28)$$

At finite temperature or when pairing is introduced, the sum will be extended to all orbitals with appropriate occupation numbers n_i (see Section 5.1).

Given Eq. (23), the KS potential $v_{\text{KS}}(\mathbf{x})$ is the sum of three pieces,

$$v_{\text{KS}}(\mathbf{x}) = v_{\text{ext}}(\mathbf{x}) + v_{\text{H}}(\mathbf{x}) + v_{\text{xc}}(\mathbf{x}) , \quad (29)$$

where

$$v_{\text{ext}}(\mathbf{x}) = - \sum_{\alpha=1}^{N_{\text{ion}}} \frac{Z_{\alpha} e^2}{|\mathbf{x} - \mathbf{x}_{\alpha}|} , \quad (30)$$

$$v_{\text{H}}(\mathbf{x}) = \frac{\delta E_{\text{H}}[\rho]}{\delta \rho(\mathbf{x})} = e^2 \int d\mathbf{x}' \frac{\rho(\mathbf{x}')}{|\mathbf{x} - \mathbf{x}'|} , \quad (31)$$

and

$$v_{\text{xc}}(\mathbf{x}) = \frac{\delta E_{\text{xc}}[\rho]}{\delta \rho(\mathbf{x})} . \quad (32)$$

These formulas for $v_{\text{ext}}(\mathbf{x})$ and $v_{\text{H}}(\mathbf{x})$ are particular to the Coulomb problem, but the structure of these terms is more general, as is the expression of $v_{\text{xc}}(\mathbf{x})$ as a functional derivative.

Some comments about these formulas:

- While real nuclei usually do not have external potentials, it can be useful to theoretically put the nucleus in a trap for comparisons of empirical functionals to *ab initio* calculations. However, the external potential should be viewed more generally as a *source* that is varied and then set to zero at the end, such as those used in field theory with path integrals. Therefore we can add more general sources coupled to local densities, such as the kinetic energy, spin-orbit, and pairing densities found in Skyrme EDF theory and expect to have better energy functionals. In this case, we have a series of Kohn-Sham potentials, each equal to a functional derivative of the corresponding density. We will see how this works explicitly for the kinetic energy and anomalous (pairing) densities in Sections 4.2 and 5.1, respectively.
- If a functional in the semi-local form of Eq. (13) is constructed (e.g., from a local density approximation plus gradient corrections), then v_{xc} can be evaluated trivially from Eq. (32) and the self-consistency cycle of Fig. 2 can be carried out directly. This is the form of Kohn-Sham DFT that is most widely used (e.g., GGA and its variations for the Coulomb problem and Skyrme, SLDA, etc. for the nuclear problem).
- The success of Kohn-Sham compared to Thomas-Fermi (for which the kinetic energy is a functional of the density) followed from the introduction of orbitals to treat the kinetic energy, with manifest improvements such as the reproduction of oscillations from shell structure [26]. Thus, in this sense

⁷The KS potential, density, etc. are often denoted v_s , ρ_s , and so on in the Coulomb DFT literature.

orbital-based functionals are already inevitable and making the potential energy orbital dependent is not a major step conceptually [4]. Note that the kinetic energy contribution here is just a definition and, while a good approximation, it is *not* the many-body kinetic energy (which would be expressed in terms of the full single-particle Green's function or the one-body density matrix). The exchange-correlation part has to absorb the difference between these kinetic energies.

- For Coulomb systems the Hartree contribution is dominant and the Hartree energy functional takes a special form that depends *explicitly* on the density only. These are the reasons for singling it out. For nuclear systems the Hartree piece is neither the dominant contribution nor simple in general with low-momentum potentials, which are non-local and require integrals over quantities that do not reduce to the density (e.g., the one-particle density matrix). So singling it out is not generally helpful. It *is* advantageous in some approximations such as the density matrix expansion (DME) to isolate the long-range part of the potential, which is local, and to treat this part of the Hartree potential explicitly.
- The exchange part can also be singled out for Coulomb because of the possibility of a precise formula in terms of the KS orbitals and the Coulomb potential. But isolating particular parts of the functional is not *necessary*, because

$$v_H(\mathbf{x}) + v_{xc}(\mathbf{x}) \equiv v_{Hxc}(\mathbf{x}) = \frac{\delta}{\delta\rho(\mathbf{x})} \{E_H[\rho] + E_{xc}[\rho]\} \equiv \frac{\delta E_{Hxc}[\rho]}{\delta\rho(\mathbf{x})}, \quad (33)$$

so all the interaction terms can simply be combined (and we use the “Hxc” subscript to indicate when this is done). This is the form we generally use for the application to nuclei.

As is well documented, the conventional Kohn-Sham DFT with semi-local functionals has been extremely successful for Coulomb systems. However, there are failures and these help motivate the development of orbital-dependent functionals. It is not yet clear to what extent these failures have analogs for nuclear-based system, but we summarize the list of arguments (taken largely from Engel’s review in Ref. [4]; look there for specific references) along with some speculations about nuclei:

- **Heavy Elements.** For heavy constituents (e.g., gold), the local density approximation (LDA) tends to work better than the generalized gradient approximation (GGA) and this is not attributable to relativistic effects. The suggestion is that GGA has trouble with higher angular momentum (*d* and *f*). If this is a generic problem it would certainly be relevant for nuclei. The fact that GGA is not a systematic improvement over LDA is also motivation for *ab initio* DFT — to develop a hierarchy of approximations that do systematically improve, as for the coupled cluster method [58, 59].
- **Negative Ions.** The fall-off of the Kohn-Sham potential does not have the $1/r$ asymptotic form needed for negative ions and Rydberg states. The physical picture is that if one electron is far away from the others, it should see the net charge of the remaining system of $N - 1$ electrons and N protons. But because v_H still always has the Coulomb repulsion of the far electron, it has to be removed by v_x , but this does not happen with LDA or GGA functionals. Engel emphasizes that the exchange functional needs to be rather non-local to cancel the self-interaction in the Hartree potential [4]. For the nuclear case, the impact of the self-interaction problem was considered long ago in Ref. [60] but only recently reconsidered along with the additional problem of self-pairing in Refs. [12, 48, 49].
- **Dispersion Forces.** Dispersion forces are a type of van der Waals force. The problem here is the locality of the exchange-correlation functional. If two atoms are so separated such that there is no

overlap in the densities, then the density is the sum of the two atomic densities. But we expect virtual dipole excitations leading to molecular bonding (this is called the London dispersion force). This does not work for LDA because the binding energy from the correlation functional is

$$E_b = E_c^{\text{LDA}}[\rho_A + \rho_B] - E_c^{\text{LDA}}[\rho_A] - E_c^{\text{LDA}}[\rho_B], \quad (34)$$

which vanishes because only regions with non-zero density contribute to the correlation energy (so the first term on the right side is the sum of the other two terms). The same result holds for GGA because the density only in the near vicinity of \mathbf{x} contributes to the energy density at \mathbf{x} . So we need non-locality for virtual excitations. Analogous issues for nuclei may arise from coupling to low-lying vibrations.

- **Strongly Correlated Systems.** Here there are failures for certain systems, such as some 3d transition metal monoxides, which the LDA and GGA either predict are metallic when they are actually Mott insulators or else greatly underestimate the band gap. Indications are that the incorrect treatment of self-interaction correction is the problem (although this is not proven).

The self-interaction problem can be illustrated by considering the “exact exchange” functional E_x of DFT, which is defined to be the Fock term as in Eq. (15) written with KS orbitals. So for a local potential $V(\mathbf{x}, \mathbf{x}')$, this is simply

$$E_x \equiv -\frac{1}{2} \sum_{kl} n_k n_l \int d\mathbf{x} \int d\mathbf{x}' \phi_k^\dagger(\mathbf{x}) \phi_l(\mathbf{x}) V(\mathbf{x}, \mathbf{x}') \phi_l^\dagger(\mathbf{x}') \phi_k(\mathbf{x}'). \quad (35)$$

This is *not* the usual HF exchange contribution, because while it agrees in *form* with Eq. (15), it does not have orbitals that satisfy the non-local HF equations. Just like the difference in the kinetic part, the difference between HF and KS exchange is absorbed into the correlation functional by construction. The functional E_x is a density functional in that the orbitals are uniquely determined by the density, but it is implicit in the density dependence. The more general $E_{\text{Hxc}}[\rho]$ will also depend on the KS eigenvalues.

The form of E_x ensures exact cancellation of the self-interaction energy in E_H [4]. Suppose we split E_x into two pieces according to whether or not $k = l$ in the double sum. Then

$$\begin{aligned} E_x &= -\frac{1}{2} \sum_{k \neq l} n_k n_l \int d\mathbf{x} \int d\mathbf{x}' \phi_k^\dagger(\mathbf{x}) \phi_l(\mathbf{x}) V(\mathbf{x}, \mathbf{x}') \phi_l^\dagger(\mathbf{x}') \phi_k(\mathbf{x}') \\ &\quad - \frac{1}{2} \sum_k n_k \int d\mathbf{x} \int d\mathbf{x}' \phi_k^\dagger(\mathbf{x}) \phi_k(\mathbf{x}) V(\mathbf{x}, \mathbf{x}') \phi_k^\dagger(\mathbf{x}') \phi_k(\mathbf{x}'). \end{aligned} \quad (36)$$

Note that the integrand in the second term *does not* reduce to the product of densities because there is only one k sum. However, this second term does cancel the corresponding part of the Hartree functional if we rewrite the latter in a similar form:

$$\begin{aligned} E_H &= \frac{1}{2} \sum_{k \neq l} n_k n_l \int d\mathbf{x} \int d\mathbf{x}' \phi_k^\dagger(\mathbf{x}) \phi_k(\mathbf{x}) V(\mathbf{x}, \mathbf{x}') \phi_l^\dagger(\mathbf{x}') \phi_l(\mathbf{x}') \\ &\quad + \frac{1}{2} \sum_k n_k \int d\mathbf{x} \int d\mathbf{x}' \phi_k^\dagger(\mathbf{x}) \phi_k(\mathbf{x}) V(\mathbf{x}, \mathbf{x}') \phi_k^\dagger(\mathbf{x}') \phi_k(\mathbf{x}'). \end{aligned} \quad (37)$$

This cancellation is familiar from ordinary Hartree-Fock. But if E_x is expanded in semi-local form as in the LDA or GGA for Coulomb systems or the DME for the nuclear case (see Sect. 3.4), this cancellation is lost.

Kümmel and Kronik [53] emphasize the formal deficiencies that can lead to qualitative failures of the LDA and GGA predictions. These include not only the non-cancellation of self-interaction but the lack of a derivative discontinuity in E_{xc} . The latter issue starts with the DFT definition of a chemical potential μ :

$$\mu \equiv \frac{\delta E_{\text{tot}}[\rho]}{\delta \rho(\mathbf{x})}, \quad (38)$$

which is position independent when evaluated at the ground-state density. Perdew et al. argued [61] that this chemical potential must have a discontinuity: if the integer number of electrons is approached from below its absolute value should be the ionization potential while if from above it should equal the electron affinity. The derivative discontinuities at integer particle numbers in general comes from both the noninteracting kinetic energy and E_{xc} . But the LDA and GGA E_{xc} 's are continuous in the density and its gradient, so there is no particle number discontinuity. Ref. [53] has more details on why this is an important issue for Coulomb DFT. We know of no investigation, however, into its impact on nuclear EDF's.

In the end, a basic issue is that any full DFT energy functional *must* have non-localities and it may be problematic for nuclear structure to expand in a semi-local functional [12, 48, 49]. The only way we know to test this is by comparing such functionals derived from microscopic interactions (e.g., through the density matrix expansion, see Section 3.4) to a full orbital-based functional. A program to carry out such comparisons was recently initiated as part of the UNEDF project [8, 9].

2.3 Derivation of the optimized effective potential

The fundamental problem in extracting the Kohn-Sham potential is to calculate the functional derivative with respect to the density as in Eq. (33). (More generally, we will need to take functional derivatives with respect to other densities, such as the kinetic energy density and the anomalous density for pairing for nuclear applications.) Starting from an *ab initio* energy functional, one way to proceed is an expansion such as the density matrix expansion (DME), which results in functionals with the densities explicit (see Section 3.4). In the absence of such approximations, the density is naturally explicit only in the Hartree energy functional (and in this case only for local interactions). Therefore, we need an *implicit* calculation of the derivatives [4].

The most direct procedure is to use the chain rule [4]. As reviewed in later sections, the energy functional can be built from the KS orbitals and eigenvalues (e.g., with Kohn-Sham MBPT as in Section 3), so we express the density derivative in terms of those. As an intermediate derivative we vary the KS potential v_{KS} :

$$\begin{aligned} \frac{\delta E_{\text{xc}}[\phi_k, \varepsilon_k]}{\delta \rho(\mathbf{x})} &= \int d\mathbf{x}' \frac{\delta E_{\text{xc}}}{\delta v_{\text{KS}}(\mathbf{x}')}\frac{\delta v_{\text{KS}}(\mathbf{x}')}{\delta \rho(\mathbf{x})} \\ &= \int d\mathbf{x}' \frac{\delta v_{\text{KS}}(\mathbf{x}')}{\delta \rho(\mathbf{x})} \sum_k \left\{ \int d\mathbf{x}'' \left[\frac{\delta \phi_k^\dagger(\mathbf{x}'')}{\delta v_{\text{KS}}(\mathbf{x}')} \frac{\delta E_{\text{xc}}}{\delta \phi_k^\dagger(\mathbf{x}'')} + \text{c.c.} \right] + \frac{\delta \varepsilon_k}{\delta v_{\text{KS}}(\mathbf{x}')} \frac{\partial E_{\text{xc}}}{\partial \varepsilon_k} \right\}. \end{aligned} \quad (39)$$

Note that in all of the expressions given here the sum over orbitals k is *not* restricted to occupied states unless n_k explicitly appears. (We assume filled shells here and refer the reader to the cited literature for the case of unfilled shells.) Now we need to find the functional derivatives introduced in this expression.⁸

For the exchange functional defined in Eq. (35) with a local potential, we obtain

$$\frac{\delta E_x}{\delta \phi_k^\dagger(\mathbf{x}')} = -n_k \sum_l n_l \phi_l(\mathbf{x}') \int d\mathbf{x} \phi_l^\dagger(\mathbf{x}) \phi_k(\mathbf{x}) V(\mathbf{x}, \mathbf{x}'), \quad (40)$$

⁸In general one also needs to vary the occupation numbers, although this is not needed if there is fixed particle number [62].

and $\partial E_x / \partial \varepsilon_k = 0$. The functional derivatives $\delta \phi_k^\dagger / \delta v_{\text{KS}}$ and $\delta \epsilon_k / \delta v_{\text{KS}}$ follow from simple first-order (non-degenerate) perturbation theory with δv_{KS} as the perturbation. That is, we treat the KS equation for the orbitals just like in conventional quantum mechanics. So we start with the change in the eigenvalue:

$$\delta \varepsilon_k [\delta v_{\text{KS}}] = \int d\mathbf{x}' \phi_k^\dagger(\mathbf{x}') \delta v_{\text{KS}}(\mathbf{x}') \phi_k(\mathbf{x}') , \quad (41)$$

which directly implies the functional derivative

$$\frac{\delta \varepsilon_k}{\delta v_{\text{KS}}(\mathbf{x})} = \phi_k^\dagger(\mathbf{x}) \phi_k(\mathbf{x}) . \quad (42)$$

Similarly, for the wave function,

$$\delta \phi_k(\mathbf{x}) = \sum_{l \neq k} \frac{\phi_l(\mathbf{x})}{\varepsilon_k - \varepsilon_l} \int d^3 \mathbf{x}'' \phi_l^\dagger(\mathbf{x}'') \delta v_{\text{KS}}(\mathbf{x}'') \phi_k(\mathbf{x}'') , \quad (43)$$

and

$$\delta \phi_k^\dagger(\mathbf{x}) = \sum_{l \neq k} \int d^3 \mathbf{x}'' \phi_k^\dagger(\mathbf{x}'') \delta v_{\text{KS}}(\mathbf{x}'') \phi_l(\mathbf{x}'') \frac{\phi_l^\dagger(\mathbf{x})}{\varepsilon_k - \varepsilon_l} , \quad (44)$$

which imply the functional derivatives

$$\frac{\delta \phi_k(\mathbf{x})}{\delta v_{\text{KS}}(\mathbf{x}')} = \sum_{l \neq k} \frac{\phi_l(\mathbf{x}) \phi_l^\dagger(\mathbf{x}')}{\varepsilon_k - \varepsilon_l} \phi_k(\mathbf{x}') = -G_k(\mathbf{x}, \mathbf{x}') \phi_k(\mathbf{x}') , \quad (45)$$

and

$$\frac{\delta \phi_k^\dagger(\mathbf{x})}{\delta v_{\text{KS}}(\mathbf{x}')} = \phi_k^\dagger(\mathbf{x}') \sum_{l \neq k} \frac{\phi_l(\mathbf{x}') \phi_l^\dagger(\mathbf{x})}{\varepsilon_k - \varepsilon_l} = -\phi_k^\dagger(\mathbf{x}') G_k(\mathbf{x}', \mathbf{x}) , \quad (46)$$

where (note the sign change in the denominator, which can differ in the literature)

$$G_k(\mathbf{x}, \mathbf{x}') \equiv \sum_{l \neq k} \frac{\phi_l(\mathbf{x}) \phi_l^\dagger(\mathbf{x}')}{\varepsilon_l - \varepsilon_k} . \quad (47)$$

Note that to construct the Green's function for every state requires explicit solutions for all the orbitals. Below we discuss approximations that avoid the complication of unoccupied orbitals.

To complete the chain rule we need to evaluate $\delta v_{\text{KS}} / \delta \rho$. To do so, we focus first on the inverse function, which is the static response function of the KS system,

$$\frac{\delta \rho(\mathbf{x})}{\delta v_{\text{KS}}(\mathbf{x}')} = \chi_s(\mathbf{x}, \mathbf{x}') = - \sum_k n_k \phi_k^\dagger(\mathbf{x}) G_k(\mathbf{x}, \mathbf{x}') \phi_k(\mathbf{x}') + \text{c.c.} . \quad (48)$$

This follows directly by applying our functional derivative formulas to the expression for $\rho(\mathbf{x})$ in terms of orbitals. Note that only the terms with l unoccupied in G_k will contribute to χ_s , because those with l occupied will cancel (e.g., pick an l and a k and note that the complex conjugate term is the same but with the opposite sign energy denominator).

By multiplying $\delta E_{\text{xc}} / \delta \rho(\mathbf{x})$ by χ_s and integrating over \mathbf{x} , the OEP or OPM (optimized potential method) integral equation is obtained:⁹

$$\int d\mathbf{x}' \chi_s(\mathbf{x}, \mathbf{x}') v_{\text{xc}}(\mathbf{x}') = \Lambda_{\text{xc}}(\mathbf{x}) , \quad (49)$$

⁹The names OEP and OPM are used in the literature by different authors to describe either this equation or more generally the orbital-based approach.

where

$$\Lambda_{\text{xc}}(\mathbf{x}) = \sum_k \left\{ - \int d\mathbf{x}' \left[\phi_k^\dagger(\mathbf{x}) G_k(\mathbf{x}, \mathbf{x}') \frac{\delta E_{\text{xc}}}{\delta \phi_k^\dagger(\mathbf{x}')} + \text{c.c.} \right] + |\phi_k(\mathbf{x})|^2 \frac{\partial E_{\text{xc}}}{\partial \varepsilon_k} \right\}. \quad (50)$$

This is a Fredholm integral equation of the first kind. Note that because Eqs. (49) and (50) are linear in E_{xc} , we can consider separate equations for different pieces of E_{xc} . It is common to introduce the “orbital shifts” [53]

$$\psi_k^\dagger(\mathbf{x}) \equiv \int d\mathbf{x}' \phi_k^\dagger(\mathbf{x}') [u_{\text{xc},k}(\mathbf{x}') - v_{\text{xc}}(\mathbf{x}')] G_k(\mathbf{x}', \mathbf{x}), \quad (51)$$

where

$$u_{\text{xc},k} \equiv \frac{1}{\phi_k^\dagger(\mathbf{x}')} \frac{\delta E_{\text{xc}}}{\delta \phi_k(\mathbf{x}'s)}, \quad (52)$$

so that we can write the OPM integral equation compactly as

$$\sum_k (\psi_k^\dagger(\mathbf{x}) \phi_k(\mathbf{x}) + \text{c.c.}) = 0. \quad (53)$$

In carrying out the self-consistency loop (Fig. 2), the solution for the orbitals when given a Kohn-Sham potential proceeds the same as always. Given the new orbitals and eigenvalues, we first find $G_k(\mathbf{x}, \mathbf{x}')$ and $u_{\text{xc},k}$, and then the new KS potential by solving the OPM equation, and the loop repeats. As discussed in Section 2.5, this is numerically difficult and comparatively inefficient, but there are also good approximations that simplify the solution significantly.

2.4 OEP from total energy minimization or density invariance

To get more insight into the physics of the OEP, we turn to the original derivation of the OPM integral equation, which is based on the minimization of the energy functional with respect to the density [4]. Without explicit dependence on the density we do not know how to do that minimization, but the Hohenberg-Kohn theorem that tells us that v_{KS} and ρ are directly related. In particular, this implies that we can replace the minimization with respect to ρ by a minimization with respect to v_{KS} (for fixed particle number),

$$\frac{\delta E_{\text{tot}}[\phi_k, \varepsilon_k]}{\delta v_{\text{KS}}(\mathbf{x})} = 0. \quad (54)$$

Now we apply the chain rule as before:

$$\frac{\delta E_{\text{tot}}[\phi_k, \varepsilon_k]}{\delta v_{\text{KS}}(\mathbf{x})} = \sum_k \left\{ \int d\mathbf{x}' \left[\frac{\delta \phi_k^\dagger(\mathbf{x}')}{\delta v_{\text{KS}}(\mathbf{x})} \frac{\delta E_{\text{tot}}}{\delta \phi_k^\dagger(\mathbf{x}')} + \text{c.c.} \right] + \frac{\delta \varepsilon_k}{\delta v_{\text{KS}}(\mathbf{x}')} \frac{\partial E_{\text{xc}}}{\partial \varepsilon_k} \right\}. \quad (55)$$

The functional derivatives of E_{tot} with respect to the orbitals and eigenvalues are given by

$$\frac{\delta E_{\text{tot}}}{\delta \phi_k^\dagger(\mathbf{x})} = n_k \left[-\frac{\nabla^2}{2M} + v_{\text{ext}}(\mathbf{x}) + v_H(\mathbf{x}) \right] \phi_k(\mathbf{x}) + \frac{\delta E_{\text{xc}}}{\delta \phi_k^\dagger(\mathbf{x})}, \quad (56)$$

$$\frac{\partial E_{\text{tot}}}{\partial \varepsilon_k} = \frac{\partial E_{\text{xc}}}{\partial \varepsilon_k}, \quad (57)$$

with the remaining derivatives given by previous expressions. The first term on the right side of Eq. (56) can be rewritten because $\phi_k(\mathbf{x})$ satisfies the KS orbital equation,

$$\frac{\delta E_{\text{tot}}}{\delta \phi_k^\dagger(\mathbf{x})} = n_k [\varepsilon_k - v_{\text{xc}}(\mathbf{x})] \phi_k(\mathbf{x}) + \frac{\delta E_{\text{xc}}}{\delta \phi_k^\dagger(\mathbf{x})}. \quad (58)$$

Plugging everything into Eq. (55) gives the minimization condition:

$$\sum_k \int d\mathbf{x}' \left\{ \phi_k^\dagger(\mathbf{x}) G_k(\mathbf{x}, \mathbf{x}') \left[n_k \phi_k(\mathbf{x}) (v_{\text{xc}} - \varepsilon_k) + \frac{\delta E_{\text{xc}}}{\delta \phi_k^\dagger(\mathbf{x}')} \right] + \text{c.c.} \right\} + \sum_k |\phi_k(\mathbf{x})|^2 \frac{\partial E_{\text{xc}}}{\partial \varepsilon_k} = 0 . \quad (59)$$

Finally, the OPM integral equation is recovered after identifying $\chi_s(\mathbf{x}, \mathbf{x}')$ and $\Lambda_{\text{xc}}(\mathbf{x})$ and using

$$\int d\mathbf{x} \phi_k^\dagger(\mathbf{x}) G_k(\mathbf{x}, \mathbf{x}') = \int d\mathbf{x}' G_k(\mathbf{x}, \mathbf{x}') \phi_k^\dagger(\mathbf{x}') = 0 . \quad (60)$$

(Note that Eq. (60) means there will be complications with inverting χ_s .)

If we just include the direct and exchange terms in the functional then E_{tot} looks just like an HF functional. The key difference is that the HF approach corresponds to a *free* (unconstrained) minimization of the total energy functional with respect to the ϕ_k and ε_k . But the minimization here is not free; rather, the ϕ_k and ε_k have to satisfy the KS equations with a multiplicative potential. This is a *subsidiary* condition to the minimization of E_{tot} , which is implemented by the OPM equation. Because this means the variational calculation is over a more limited set of states, the OEP applied to exchange only will always give a higher energy than Hartree-Fock [4].

The OPM equation can be derived yet another way, which is based on the point-by-point equivalence of the KS and interacting densities [63, 64, 65]:

$$\rho_s(\mathbf{x}) - \rho(\mathbf{x}) = 0 . \quad (61)$$

This is perhaps the least obvious feature of Kohn-Sham DFT. It might appear in the context of a perturbative expansion (see Section 3) to be simply a *choice* of the Kohn-Sham potential that makes higher order corrections to the density vanish. However, in fact it implies the energy minimization that is common to all DFT applications, that is, that the KS exchange-correlation potential is the variationally best local approximation to the exchange-correlation energy [64]. The basic demonstration starts with expressing Eq. (61) in terms of traces over the KS and full single-particle Green's functions evaluated at equal times and the same coordinate arguments:

$$-i\text{Tr}\{G_s(\mathbf{x}t, \mathbf{x}t^+) - G(\mathbf{x}t, \mathbf{x}t^+)\} = 0 , \quad (62)$$

where the Green's functions are defined as usual as time-ordered products of the field operators in the KS or fully interacting ground states:

$$G_s(\mathbf{x}t, \mathbf{x}'t') = -i\langle \Phi_{\text{KS}} | T\psi(\mathbf{x}t)\psi^\dagger(\mathbf{x}'t') | \Phi_{\text{KS}} \rangle \quad (63)$$

$$G(\mathbf{x}t, \mathbf{x}'t') = -i\langle \Psi_0 | T\psi(\mathbf{x}t)\psi^\dagger(\mathbf{x}'t') | \Psi_0 \rangle . \quad (64)$$

The specification t^+ serves to order the field operators as $\psi^\dagger\psi$. The full Green's function is related to the KS Green's function by a Dyson equation [using a four-vector notation $x = (\mathbf{x}, t)$]:

$$G(x, x') = G_s(x, x') + \int dy dy' G_s(x, y) \left[\Sigma_{\text{Hxc}}(y, y') - \delta(y - y') v_{\text{Hxc}}(\mathbf{y}) \right] G(y', x') , \quad (65)$$

which follows from the separate Dyson equations for G_s and G by forming G^{-1} and G_s^{-1} and subtracting, solving for G^{-1} , and then taking the inverse [4]. Note that the Hartree parts of the irreducible self-energy $\Sigma_{\text{Hxc}}(y, y')$ and the Kohn-Sham self-energy $\delta(y - y') v_{\text{Hxc}}(\mathbf{y})$ cancel for local potentials, leaving the difference of Σ_{xc} and v_{xc} . This is known as the Sham-Schlüter equation and is a nonlinear equation for v_{xc} , which can be shown to be equivalent to the OPM equation. We leave the details of showing this equivalence to the references, but give a schematic demonstration in Section 4.

2.5 Approximations

While the preceding demonstrations illustrate formal constructions that suffice to carry out orbital-based DFT (given appropriate energy functionals), solving the equations can be numerically difficult and there are also efficiency issues. (For recent work on numerically stable methods to solve the OEP equations using Gaussian basis sets, see Refs. [59, 66].) In Coulomb applications, OPM calculations are found to take one or two orders of magnitude longer than corresponding GGA calculations. The source of this inefficiency is the need for the Kohn-Sham Green's function, which requires knowledge of all the unoccupied as well as occupied orbitals. An approximation (and subsequent variations) by Krieger, Li and Iafrate (KLI) [67] based on a closure approximation avoids this problem and seems in practice (for Coulomb cases) to be quite accurate, at least for the exchange part of the functional.

The key is to replace the energy denominator in the Green's function by an averaged difference:

$$G_k(\mathbf{x}, \mathbf{x}') \approx \sum_{l \neq k} \frac{\phi_l(\mathbf{x})\phi_l^\dagger(\mathbf{x}')}{\Delta\bar{\epsilon}} = \frac{1}{\Delta\bar{\epsilon}} [\delta^3(\mathbf{x} - \mathbf{x}') - \phi_k(\mathbf{x})\phi_k^\dagger(\mathbf{x}')] . \quad (66)$$

Upon substituting into the OPM integral equation, one obtains

$$v_{xc}(\mathbf{x}) = \frac{1}{2\rho(\mathbf{x})} \sum_k \left\{ \left[\phi_k^\dagger(\mathbf{x}) \frac{\delta E_{xc}}{\delta \phi_k^\dagger(\mathbf{x})} + \text{c.c.} \right] + |\phi_k(\mathbf{x})|^2 \left[\Delta v_k - \Delta\bar{\epsilon} \frac{\partial E_{xc}}{\partial \varepsilon_k} \right] \right\} \quad (67)$$

$$\Delta v_k = \int d\mathbf{x} \left\{ n_k |\phi_k(\mathbf{x})|^2 v_{xc}(\mathbf{x}) - \phi_k^\dagger(\mathbf{x}) \frac{\partial E_{xc}}{\partial \varepsilon_k} \right\} + \text{c.c.} . \quad (68)$$

Consistent with the closure approximation, the derivative $\partial E_{xc}/\partial \varepsilon_k$ is neglected, which finally yields

$$v_{xc}^{\text{KLI}}(\mathbf{x}) = \frac{1}{2\rho(\mathbf{x})} \sum_k \left\{ \left[\phi_k^\dagger(\mathbf{x}) \frac{\delta E_{xc}}{\delta \phi_k^\dagger(\mathbf{x})} + \text{c.c.} \right] + |\phi_k(\mathbf{x})|^2 \Delta v_k^{\text{KLI}} \right\} . \quad (69)$$

Although v_{xc}^{KLI} appears on both sides, one can either iterate to self-consistency starting from (for example) an LDA approximation to Δv_k^{KLI} or recast these as a set of linear equations allowing Δv_k^{KLI} to be determined without knowing v_{xc}^{KLI} .

Results from representative calculations comparing OPM and KLI to LDA, GGA, and HF using exchange-only functionals have been studied systematically and are summarized in Refs. [4] and [53]. Note that in such comparisons the Hartree-Fock (HF) result serves as the “exact” answer. In most cases, exchange-only OPM is found to be a very good approximation to HF, e.g., agreement at one part in 10^{-6} for the ground-state energies of heavy closed-subshell atoms. Because exchange-only OPM is a more restricted variational minimization than Hartree-Fock, the HF results must always be more bound than OPM, but the small difference implies that the greater variational freedom for HF has little effect in practice. Furthermore, the KLI energies are very good approximations to the full OPM results; for this same example the KLI–OPM difference is systematically about 1/3 that of HF–OPM. The KLI energies are above OPM in all cases, as required because the full OPM energy is a minimum for local potentials. The deviation for even the largest atom is still very small. The level of agreement can be calibrated by comparison to LDA and GGA results; the latter are much better than the former, but sometimes an order of magnitude worse than KLI and without a systematic sign.

Other approximations related to KLI but with improvements have been proposed. The Common Energy Denominator Approximation (CEDA) [68] and the Localized Hartree-Fock (LHF) approximation [69] are the same as KLI except that only the energy differences for occupied-unoccupied pairs of states are approximated by an average, while the exact differences are kept for occupied-occupied pairs. CEDA is invariant under unitary transformations of the occupied orbitals, which is a plus, but

in practice the results are similar to KLI [53]. Yet another approximation is the effective local potential proposed by Staroverov et al. [70], which is efficient to implement numerically.

The good results that have been found using the KLI and similar approximations (for total energies) are encouraging because the corresponding potentials are far easier to calculate. KLI has been shown to be a sort of mean-field approximation to the full OEP, which accounts for its success [53]. However, more work is needed on applications beyond exchange-only functionals. There are no calculations yet that compare these approximations (and more extreme approximations such as the density matrix expansion, see Section 3.4) for nuclear systems, so drawing conclusions on the prospects would be premature.

3 DFT and *ab initio* wave function methods

The development of accurate *ab initio* functionals for orbital-based DFT that go beyond exchange-only (what is called the “correlation functional”) for Coulomb systems is the subject of much recent activity. Progress is being made although it is still an open question whether the most ambitious accuracy goals can be met (e.g., chemical accuracy). The extensive review by Kümmel and Kronik [53] provides a good idea of the state of the art in 2008 but we note that there are subsequent and ongoing advances.

For the nuclear problem, the development of analogous *ab initio* functionals suitable for orbital-based DFT is still in its infancy. Thus our “review” in this section will mainly look toward the future, considering first how to formulate an exchange-correlation functional in MBPT, neglecting some serious issues such as symmetry breaking. We then examine a specific implementation by Bartlett and collaborators for quantum chemistry that is based on requiring density invariance and which highlights how the convergence of the perturbation expansion for the functional can be improved by shifting more physics into the Kohn-Sham potential. These developments are based on applying MBPT at low order, so we next discuss how this is meaningful for nuclear interactions if they are transformed to low-momentum potentials. Finally, we review recent and ongoing efforts to apply the density matrix expansion to make *ab initio* energy calculations by expanding functionals about the uniform system (asymmetric nuclear matter). This also provides examples of how to deal with momentum space potentials, non-localities, and three-body forces, which will not be found in the Coulomb literature.

3.1 Goldstone many-body perturbation theory

A direct method to construct an orbital-based energy functional is to consider the Kohn-Sham potential $v_{\text{KS}}(\mathbf{x})$ as defining the single-particle potential (typically called $U(\mathbf{x})$ in the nuclear physics literature) that is used in Goldstone many-body perturbation theory (MBPT). This will give us a diagrammatic expansion for the energy as a functional of U that will depend on KS orbitals and eigenvalues. There are various alternative ways to formulate MBPT. For example, in the Coulomb DFT literature a formalism for perturbation theory based on coupling constant integration [1, 4] is typically used. Here we use the Goldstone formalism that historically led from “hard core” NN potentials to the hole-line expansion [71, 72, 73], but the end result is basically the same. Note that “perturbation theory” does not exclude infinite summations of diagrams in our functional, although we will argue in Section 3.3 that second-order perturbation theory is a good starting point for low-momentum nuclear interactions.

Our schematic discussion is compatible with the detailed, pedagogical expositions of the Goldstone-diagram expansion given in Refs. [71, 74, 32, 73]. We start with a division of the second-quantized, time-independent Hamiltonian:

$$\hat{H} = \hat{H}_0 + \hat{H}_1 , \quad (70)$$

where the separation is our choice. One might imagine taking \hat{H}_0 to be the kinetic energy plus the fixed external potential and \hat{H}_1 to be the interaction potential. Such a division will be invoked in Section 5.3 when we discuss the connection to the perturbation expansion using Green’s functions. However, for

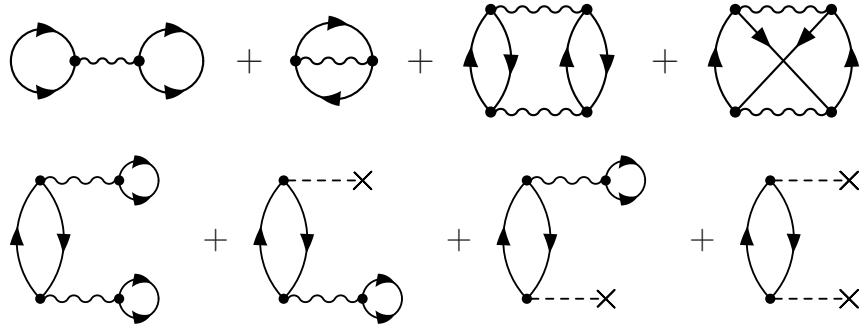


Figure 3: Goldstone diagrams at first and second order in \hat{H}_1 with a single-particle potential $-\hat{U}$ (dash lines) and a two-body potential \hat{V}_{NN} only (wiggle lines).

our applications, we will require \hat{H}_0 to be the sum of the kinetic energy¹⁰ and a single-particle potential (including any \hat{V}_{ext}), $\hat{H}_0 = \hat{T} + \hat{U}$. Then \hat{H}_1 corrects for the new part of \hat{U} , $\hat{H}_1 = \hat{V} - \hat{U} + \hat{V}_{\text{ext}}$. With this restricted form, the many-body ground- and excited-states of \hat{H}_0 will be simple to construct. The ground state of \hat{H}_0 , designated $|\Phi_0\rangle$, will be our reference state and our Fock space will be built from particles and holes with respect to it. More precisely, the complete set of orbitals defined by the single-particle potential establishes the single-particle basis for the Fock space, and second-quantized field operators are expanded in this basis. So $|\Phi_0\rangle = \prod_{\varepsilon_i \leq \varepsilon_F} a_i^\dagger |0\rangle$ is a Slater determinant of orbitals where $a_i(a_i^\dagger)$ is the destruction (creation) operator for the single-particle state i and $a_i|0\rangle = 0$ for all i and ε_F is the energy of the last filled level. The idea will be to identify \hat{U} with the Kohn-Sham potential [i.e., $\hat{U} = \hat{V}_{\text{KS}} = \int d\mathbf{x} v_{\text{KS}}(\mathbf{x})\hat{\rho}(\mathbf{x})$], which is to be determined self-consistently in accordance with Section 2. So the orbitals ϕ_i are then KS orbitals.

Goldstone's theorem expresses the energy of the ground state as

$$E = E_0 + \langle \Phi_0 | \hat{H}_1 \sum_{n=0}^{\infty} \left(\frac{1}{E_0 - \hat{H}_0} \hat{H}_1 \right)^n | \Phi_0 \rangle_{\text{connected}}, \quad (71)$$

where E_0 is the ground state energy of \hat{H}_0 ; that is, $\hat{H}_0|\Phi_0\rangle = E_0|\Phi_0\rangle$. (Note: These operators are in the Schrödinger picture.) The general idea of an n^{th} order contribution (see Fig. 4) is that we start with $|\Phi_0\rangle$ and apply \hat{H}_1 , which creates particles and holes. For a two-body potential, this is two particles and two holes (called “doubles” in quantum chemistry parlance), but in our case \hat{H}_1 in addition has one-particle–one-hole excitations (“singles”) as well as few-particle–few-hole excitations from few-body interactions (“triples” and beyond). The factor $(E_0 - \hat{H}_0)^{-1}$ propagates the state and then the next \hat{H}_1 hits. The proviso “connected” means that we do not have $|\Phi_0\rangle$ as an intermediate state; we only get back to it at the end after the final \hat{H}_1 .

Goldstone diagrams can be used to organize the contributions from Eq. (71). A set of rules is given in Ref. [71] for the general case of interest with nonzero \hat{U} . The diagrams that contribute in a finite system at first and second order in \hat{H}_1 are shown in Fig. 3 [75] (those in the second row vanish in uniform matter by momentum conservation). A sample diagram contributing to Eq. (71) is shown in Fig. 4. Lines with upward arrows are particles and those with downward arrows are holes; they will carry labels for the KS orbitals. By inserting complete sets of states, any diagram is reduced to products of matrix elements of \hat{H}_1 and energy denominators that are sums and differences of KS eigenvalues. For example, a general expression for the energy shift $E - E_0$ with $\hat{U} = 0$ is found to be (see Ref. [32] for

¹⁰For finite nuclei, we would subtract the center-of-mass kinetic energy \hat{T}_{cm} from \hat{T} .

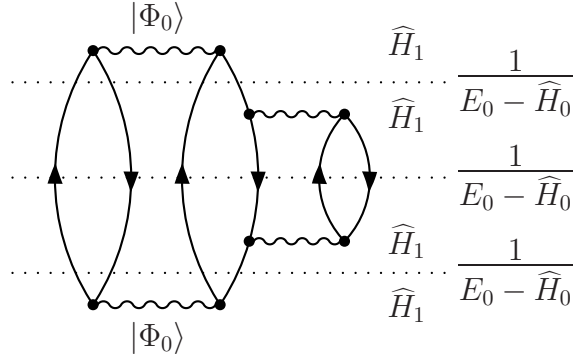


Figure 4: A Goldstone diagram contributing to Eq. (71) at fourth order in \widehat{H}_1 with a two-body potential only (wiggle lines) [31].

more details):

$$E - E_0 = \sum_{\text{connected}} \frac{(-1)^{n_L + n_h}}{2^{n_e}} \prod \frac{1}{-(\sum_a \epsilon_a - \sum_A \epsilon_A)} \prod \{ij|\widehat{V}_{\text{NN}}|kl\} , \quad (72)$$

where the matrix elements are antisymmetrized Hugenholtz matrix elements (and only the two-body interaction is included; the generalization to three-body and beyond is similar only with few-body matrix elements such as $\{ijk|\widehat{V}_{\text{NNN}}|lmn\}$). The energy denominator comes in between each successive interaction and includes all particle lines (“A”) and hole lines (“a”) cut by the dotted lines as in Fig. 4. The number of hole lines is n_h and the number of equivalent pairs is n_e , while n_L is the number of closed loops that the diagram with only direct matrix elements at each vertex would have.

A *perturbative* calculation applying Goldstone’s theorem (which is just a restatement to all orders of time-independent perturbation theory for the ground-state energy¹¹) is organized in the number of times \widehat{H}_1 is applied. Experience using nuclear potentials with strong short-range repulsion reveals that such calculations do not converge. This led to the development of the Brueckner-Bethe-Goldstone approach and the hole-line expansion. The latter is a prescription for infinite resummations of diagrams (e.g., summing the potential first into a G-matrix and then including all diagrams with a given number of independent hole lines [71]) along with constraints on the background potential \widehat{U} in order to cancel certain diagrams. These constraints are incompatible with the choice $\widehat{U} = \widehat{V}_{\text{KS}}$. However, with low-momentum interactions we are (apparently) free to choose \widehat{U} in this way and even a simple perturbative truncation (at sufficient density) is a reasonable approximation.

The matrix elements of the low-momentum potentials are typically given in momentum representation or, more appropriately for the present discussion, in a harmonic oscillator basis. Then the KS orbitals are expanded in the same basis so that matrix elements such as $\{ij|V_{\text{NN}}|kl\}$, which is in the orbital basis, can be evaluated. (Note: the necessary angular momentum recoupling is conventional; see for example Ref. [38].) To calculate $v_{\text{KS}}(\mathbf{x})$ according to the OEP prescription, we need to compute the

¹¹A perturbative expansion with the same \widehat{H}_0 (often called \widehat{H}_s in the DFT literature) and \widehat{H}_1 can be derived [4] using a coupling constant integration to adiabatically switch on \widehat{H}_1 as in Refs. [31, 32]. Thus $\widehat{H} = \widehat{H}_0 + \lambda \widehat{H}_1$ and

$$E - E_0 \equiv E_1 = \int_0^1 d\lambda \langle \Psi_0(\lambda) | \widehat{H}_1 | \Psi_0(\lambda) \rangle , \quad (73)$$

which is developed using the interaction picture time-evolution operator. Then E_{xc} is given by

$$E_{\text{xc}} = E_1 + \int d\mathbf{x} \rho(\mathbf{x}) v_{\text{xc}} . \quad (74)$$

functional derivatives of E_{Hxc} [see Eq. (33)] with respect to the orbitals and eigenvalues. The eigenvalues appear explicitly in the Goldstone expansion and the derivatives of the potential matrix elements can be carried out using the basis expansion without having to evaluate the matrix elements in coordinate space. For example, the two-body contribution from the Hartree-Fock terms is

$$\frac{\delta}{\delta\phi_i^*(\mathbf{x})} \left\{ \frac{1}{2} \sum_{j,k=1}^A [\langle jk|\widehat{V}_{\text{NN}}|jk\rangle - \langle jk|\widehat{V}_{\text{NN}}|kj\rangle] \right\} = \sum_{j,k=1}^A \phi_k(\mathbf{x}) [\langle jk|\widehat{V}_{\text{NN}}|ji\rangle - \langle jk|\widehat{V}_{\text{NN}}|ij\rangle]. \quad (75)$$

If the matrix element integrals are written out in coordinate space for a local $V_{\text{NN}}(\mathbf{x}, \mathbf{x}')$ and completeness of the orbitals used to remove the sum over k , the corresponding part of Eq. (17) is reproduced.

So we take [76]

$$\widehat{H}_0 = \widehat{H}_s = \widehat{T} + \int d\mathbf{x} \widehat{\rho}(\mathbf{x}) v_{\text{KS}}(\mathbf{x}), \quad (76)$$

where $v_{\text{KS}} = v_{\text{ext}} + v_{\text{H}} + v_{\text{xc}} \equiv v_{\text{ext}} + v_{\text{Hxc}}$. The KS energy and density are

$$E_0 = E_s = T_s + \int d\mathbf{x} \widehat{\rho}(\mathbf{x}) v_{\text{KS}}(\mathbf{x}) = \sum_i n_i \varepsilon_i, \quad (77)$$

$$\rho(\mathbf{x}) = \langle \Phi_0 | \widehat{\rho}(\mathbf{x}) | \Phi_0 \rangle = \sum_i n_i |\phi_i(\mathbf{x})|^2 \equiv \rho_{\text{KS}}(\mathbf{x}), \quad (78)$$

which is the exact density according to the conditions (to be) imposed on v_{KS} . (Note: $\widehat{\rho}(\mathbf{x}) = \widehat{\psi}^\dagger(\mathbf{x}) \widehat{\psi}(\mathbf{x})$ where the field operators are $\widehat{\psi}^\dagger(\mathbf{x}) = \sum_i \phi_i^*(\mathbf{x}) a_i^\dagger$ and $\widehat{\psi}(\mathbf{x}) = \sum_i \phi_i(\mathbf{x}) a_i^\dagger$.) Then we have

$$\widehat{H}_1 = \widehat{V} - \int d\mathbf{x} \widehat{\rho}(\mathbf{x}) v_{\text{Hxc}}(\mathbf{x}). \quad (79)$$

At this point, we can carry out the Goldstone expansion to any order or with whatever infinite summation we wish.

We note that because this expansion depends on $v_{\text{KS}}(\mathbf{x})$, it is a highly nonlinear functional equation, as E_{Hxc} depends on its own functional derivative. This is not in conflict with DFT because v_{Hxc} is a density functional, so

$$E_{\text{Hxc}} = E_{\text{H}} + E_{\text{xc}} = E_1 + \int d\mathbf{x} [v_{\text{H}}(\mathbf{x}) + v_{\text{xc}}(\mathbf{x})] \rho(\mathbf{x}) \quad (80)$$

is an implicit functional. Furthermore, it is the same nonlinearity as in the OPM equation. A perturbative approach to solving for the functional derivative $v_{\text{Hxc}}(\mathbf{x}) = \delta E_{\text{Hxc}}[\rho]/\delta \rho(\mathbf{x})$ leads to a linearization of the OPM equation. This will correspond to the inversion method discussed in Section 4. The details of such a perturbative expansion and the nonperturbative resummation of ring diagrams (the random phase approximation or RPA) is described by Engel (with references to the original literature) [4].

According to Engel the results for KS perturbation theory are not satisfactory. However, more recent developments have shown promise by improving the perturbation theory. We have emphasized that with low-momentum potentials, \widehat{U} can be chosen freely to allow the DFT constraints to hold. But there is still freedom in defining it, which can be used to significantly improve perturbative convergence in the Coulomb problem. We consider this in the next section.

3.2 Improved perturbation theory

In this section, we summarize the basic features of the approach to *ab initio* DFT under development by Bartlett and collaborators [58, 59]. In Ref. [59] they explain their strategy, which is closely in line

with the highly successful coupled cluster approach to electronic systems. A key part of the formulation as well as its numerical execution is to use a finite basis set (which is almost always chosen to be gaussians for finite systems in quantum chemistry so that all integrals can be done analytically). Above all, they emphasize that DFT should be formulated so that it converges in the limit of a full basis set,¹² as obtained for wave function methods (cf. the partial hierarchy of CC approximations: MBPT(2) < CCSD < CCSD(T) < full CI). They contrast this precept with conventional DFT approaches such as LDA or GGA or hybrid DFT (HDFT, which mixes semi-local GGA and non-local HF exchange functionals), which do not consistently predict better answers when applied in that order, even though they are claimed to be better approximations. That is, there is no definite hierarchy.

The Bartlett construction follows most cleanly by requiring that corrections to the density beyond the Kohn-Sham density, as calculated according to MBPT, must vanish. As noted in Section 2.4, this is an alternate but equivalent prescription for orbital-based *ab initio* DFT. The Hamiltonian is split as in the last section into $\hat{H} = \hat{H}_0 + \hat{H}_1$ using the Kohn-Sham potential to define the reference state. We will use $|\Phi_{\text{KS}}\rangle$ instead of $|\Phi_0\rangle$ to make this clear. The perturbative expansion for the energy is [58, 59]

$$E = E_0 + E^{(1)} + E^{(2)} + \dots \quad (81)$$

where (in quantum chemistry coupled cluster notation)

$$E_0 = \langle \Phi_{\text{KS}} | \hat{H}_0 | \Phi_{\text{KS}} \rangle = \sum_i n_i \varepsilon_i , \quad (82)$$

$$E^{(1)} = \langle \Phi_{\text{KS}} | \hat{H}_1 | \Phi_{\text{KS}} \rangle , \quad (83)$$

$$E^{(2)} = \langle \Phi_{\text{KS}} | \hat{H}_1 \hat{R}_0 \hat{H}_1 | \Phi_{\text{KS}} \rangle , \quad (84)$$

and so on. Here the operator \hat{R}_0 is

$$\hat{R}_0 = \hat{Q} \frac{1}{E_0 - \hat{H}_0} \hat{Q} , \quad (85)$$

with

$$\hat{Q} = \sum | \Phi_i^a \rangle \langle \Phi_i^a | + | \Phi_{ij}^{ab} \rangle \langle \Phi_{ij}^{ab} | + | \Phi_{ijk}^{abc} \rangle \langle \Phi_{ijk}^{abc} | + \dots , \quad (86)$$

which are singles, doubles, and higher excitations with respect to the reference KS state (which is a determinant). By convention, a, b, c are unoccupied and i, j, k are occupied in the KS state. We see that this agrees with the Goldstone expansion from before, because \hat{Q} ensures that only connected contributions are included (i.e., it is a complete set of states excluding $|\Phi_{\text{KS}}\rangle$).

Rather than use the functional derivative to calculate v_{KS} , the condition that the density be unchanged from the Kohn-Sham density is used. For calculating the exchange-only KS potential \hat{V}_{x} , this implies the density be unchanged to first order in perturbation theory. We expand the wave function and the density:

$$|\Psi\rangle = |\Phi_{\text{KS}}\rangle + |\Psi^{(1)}\rangle + |\Psi^{(2)}\rangle + \dots , \quad (87)$$

$$\rho = \rho_{\text{KS}} + \rho^{(1)} + \rho^{(2)} + \dots , \quad (88)$$

where the density is computed from the expectation value of $\hat{\rho}(\mathbf{x})$ (note that Bartlett et al. write this using $\hat{\delta}$, which is the same as $\hat{\rho}$):

$$\rho(\mathbf{x}) = \frac{\langle \Psi | \hat{\rho}(\mathbf{x}) | \Psi \rangle}{\langle \Psi | \Psi \rangle} . \quad (89)$$

¹²The diagonalization of the Hamiltonian including all possible particle-hole excitations in a given basis set is called “full CI”. That solution is an upper bound to the exact energy and reproducing it using that same basis set is considered to be an unambiguous measure of success in describing electron correlation [77].

So at leading order, we determine $v_{\mathbf{x}}(\mathbf{x})$ such that $\rho^{(1)}(\mathbf{x}) = 0$. Thus

$$\langle \Phi_{\text{KS}} | \widehat{\rho}(\mathbf{x}) | \Psi^{(1)} \rangle + \text{c.c.} = 0 , \quad (90)$$

where writing $\widehat{H}|\Psi\rangle = E|\psi\rangle$ to this order gives

$$(E_0 - \widehat{H}_0)|\Psi^{(1)}\rangle = (\widehat{H}_1 - E^{(1)})|\Phi_{\text{KS}}\rangle \quad (91)$$

and therefore

$$|\Psi^{(1)}\rangle = \widehat{R}_0(\widehat{H}_1 - E^{(1)})|\Phi_{\text{KS}}\rangle . \quad (92)$$

Substituting for $|\Psi^{(1)}\rangle$,

$$\rho^{(1)} = 0 = \langle \Phi_{\text{KS}} | \widehat{\rho}(\mathbf{x}) \widehat{R}_0 \widehat{H}_1 | \Phi_{\text{KS}} \rangle + \text{c.c.} , \quad (93)$$

and noting that at this order only single excitations contribute, we obtain

$$\begin{aligned} 0 &= \sum_{j,i,a} \langle i | \widehat{\rho}(\mathbf{x}) | a \rangle (\langle aj | \widehat{H}_1 | ij \rangle - \langle a | \widehat{V}_{\text{Hx}} | i \rangle) / (\varepsilon_i - \varepsilon_a) + \text{c.c.} \\ &= - \sum_{i,a} \phi_i^*(\mathbf{x}) \phi_a(\mathbf{x}) (\langle a | \widehat{K} | i \rangle + \langle a | \widehat{V}_{\text{x}} | i \rangle) / (\varepsilon_i - \varepsilon_a) + \text{c.c.} . \end{aligned} \quad (94)$$

where we have used $\langle \Phi_i^a | E_0 - \widehat{H}_0 | \Phi_i^a \rangle = \varepsilon_i - \varepsilon_a$. Here \widehat{K} is the conventional exchange (Fock) energy operator $\widehat{V}P_{12}$, where P_{12} is the particle-exchange operator.

Note that we cannot choose $\langle a | \widehat{K} | i \rangle = -\langle a | \widehat{V}_{\text{x}} | i \rangle$ because \widehat{V}_{x} must be local. We can think of Eq. (94) as the solution to a weighted least squares problem to replace the non-local \widehat{K} by the local \widehat{V}_{x} in the space spanned by $\{\phi_i^*, \phi_a\}$ [58]. This is a point-wise identity that can be written [with χ_s from Eq. (48)]

$$\int d\mathbf{x}' \chi_s(\mathbf{x}, \mathbf{x}') [v_{\text{x}}(\mathbf{x}') + K(\mathbf{x}')] = 0 , \quad (95)$$

which agrees with the OEP equation in Section 2; that is, we have rederived the OEP equation with exchange only. Here

$$K(\mathbf{x}) \phi_j(\mathbf{x}) = \int d\mathbf{x}' \rho(\mathbf{x}, \mathbf{x}') V(\mathbf{x}, \mathbf{x}') \phi_j(\mathbf{x}') \quad (96)$$

for a local potential with

$$\rho(\mathbf{x}, \mathbf{x}') = \sum_i n_i \phi_i^*(\mathbf{x}') \phi_i(\mathbf{x}) . \quad (97)$$

Details on solving Eq. (95) in matrix form are given in Refs. [58, 59] with pointers to the literature.

At second order, where the correlation potential first enters, one encounters issues with slow convergence. Here we simply sketch the problem and proposed solution to give the flavor. Working to second-order MBPT, the second order energy is straightforward to write but naturally more complex. One insists that $\rho^{(1)} + \rho^{(2)} = 0$ and this defines $\widehat{V}_c^{(2)}$ consistent to this order. The problem is that the perturbation $\widehat{H}_1^{(1)} - E^{(1)} = \widehat{V} - (\widehat{V}_{\text{H}} + \widehat{V}_{\text{x}}^{(1)}) - E^{(1)}$ (note: no \widehat{V}_c at this order) can have large, diagonal contributions [59]:

$$\langle \Phi_{\text{KS}} | \widehat{\rho}(\mathbf{x}) | \Phi_i^a \rangle \langle \Phi_i^a | (E_0 - \widehat{H}_0)^{-1} | \Phi_i^a \rangle \langle \Phi_i^a | \widehat{H}^{(1)} - E^{(1)} | \Phi_b^b \rangle \quad (98)$$

$$= - \left[\langle aj | \widehat{V}(1 - P_{12}) | bi \rangle - \delta_{ij} \langle a | \widehat{K} + \widehat{V}_{\text{x}} | b \rangle - \delta_{ab} \langle j | \widehat{K} + \widehat{V}_{\text{x}} | i \rangle \right] \frac{\phi_i(\mathbf{x}) \phi_a^*(\mathbf{x})}{\varepsilon_i - \varepsilon_a} . \quad (99)$$

Because we can have $a = b$ and $i = j$, these are diagonal elements of $\widehat{K} + \widehat{V}_{\text{x}}$, which make $\widehat{H}^{(1)}$ a larger perturbation than usual [58, 59]. The remedy is to resum diagonal and near-diagonal one-particle terms

into \hat{H}'_0 (this includes a rotation of the KS orbits so that off-diagonal terms in \hat{H}'_0 vanish). Most of the effect from the resummation comes with the replacement of KS denominator energies ε_p (p is either a particle or hole) with diagonal Fock matrix elements f_{pp} , where

$$f_{pp} = \langle p|f|p\rangle = \varepsilon_p - \langle p|\hat{K} + \hat{V}_{\text{xc}}|p\rangle . \quad (100)$$

The details are beyond the scope of this review but can be found in Ref. [78] along with results.

In summary, the key issue is that the freedom in how we split the Hamiltonian can be exploited to improve convergence of the perturbation series without sacrificing the form of *ab initio* DFT. In particular, rather than use the standard Kohn-Sham choice (called Görling-Levy perturbation theory [79, 80]), we shift as much physics as possible into \hat{H}'_0 . While far from a complete treatment, we hope we have conveyed the flavor of the Bartlett approach. As a side note, Bartlett et al. claim that observations made for conventional DFT that orbital energies are meaningless (other than the least bound) are mostly because functionals and potentials were not accurate.

3.3 Low-momentum interactions

The last two sections illustrate how exchange-correlation functions can be constructed for Coulomb systems for which many-body perturbation theory is applicable. This is irrelevant for nuclear physics unless we have similar control of MBPT. Here we highlight recent results that show that modern RG methods can be used to obtain a convergent expansion of nuclear matter properties by evolving to low-momentum interactions. There are various methods to achieve these interactions starting from phenomenological or EFT potentials (e.g., see Refs. [37, 81, 36]), which for our purposes here are equivalent. We simply cite two proof-of-principle results and refer the reader to the literature.

First we consider the uniform system. Despite a decades-old emphasis on infinite nuclear matter, most advances in microscopic nuclear structure theory over the last decade have been through expanding the reach of few-body calculations. This has unambiguously established the quantitative role of three-nucleon forces (3NF) for light nuclei ($A \leq 12$) [19, 20, 82, 22]. Until recently, few-body fits have not sufficiently constrained 3NF contributions at higher density such that nuclear matter calculations are predictive. Nuclear matter saturation is very delicate, with the binding energy resulting from cancellations of much larger potential and kinetic energy contributions. When a quantitative reproduction of empirical saturation properties has been obtained, it was imposed by hand through adjusting short-range three-body forces (see, for example, Refs. [83, 84]).

Progress for controlled nuclear matter calculations has long been hindered by the difficulty of the nuclear many-body problem when conventional nuclear potentials are used. But recent calculations [40] overcome the hurdles by combining controlled starting Hamiltonians based on chiral effective field theory (EFT) [85, 86] with renormalization group (RG) methods [35, 87] to soften the short-range repulsion and short-range tensor components of the initial chiral interactions [88]. By doing so, the convergence of many-body calculations is vastly accelerated [39, 89, 90].

Some key results are summarized in Fig. 5, which shows the energy per particle of symmetric matter as a function of Fermi momentum k_F , or the density $\rho = 2k_F^3/(3\pi^2)$. A grey square representing the empirical saturation point is shown in each of the nuclear matter figures. Its boundaries reflect the ranges of nuclear matter saturation properties predicted by phenomenological Skyrme energy functionals that most accurately reproduce properties of finite nuclei. The calculations of Fig. 5 start from the N³LO nucleon-nucleon (NN) potential (EM 500 MeV) of Ref. [85]. This NN potential is RG-evolved to low-momentum interactions $V_{\text{low } k}$ with a smooth $n_{\text{exp}} = 4$ regulator [87]. For each cutoff Λ , two couplings that determine the shorter-range parts of the N²LO 3NF [91, 92] are fit to the ³H binding energy and the ⁴He matter radius [82] using exact Faddeev and Faddeev-Yakubovsky methods as in Ref. [93].

The Hartree-Fock results show that nuclear matter is bound even at this simplest level. A calculation without approximations should be independent of the cutoffs, so the spread in Fig. 5 sets the scale

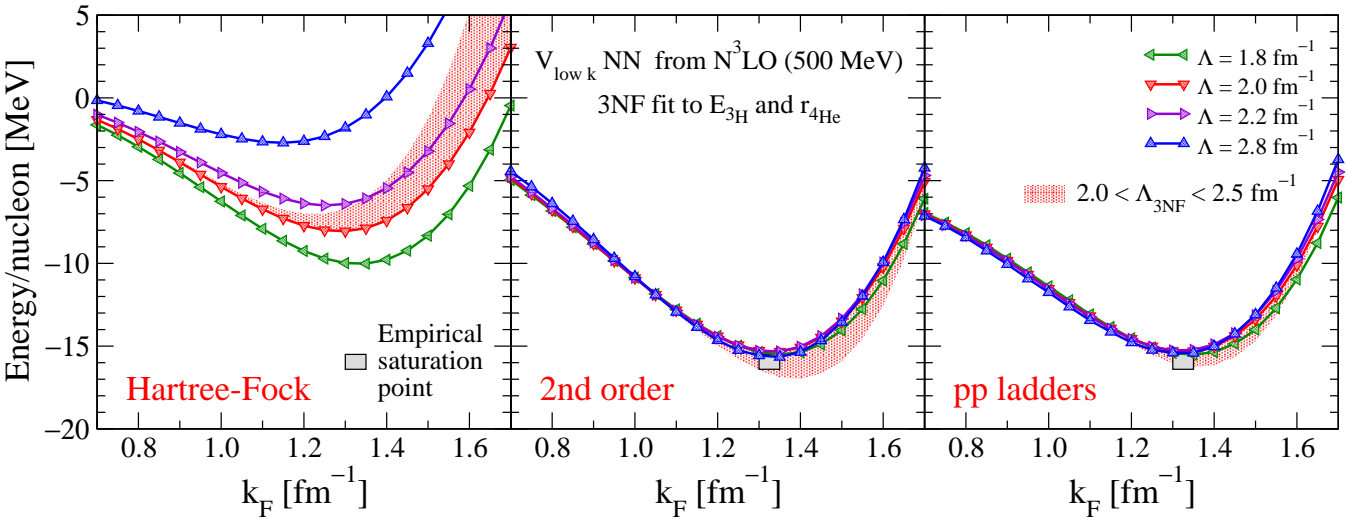


Figure 5: Nuclear matter energy per particle as a function of Fermi momentum k_F at the Hartree-Fock level (left) and including second-order (middle) and particle-particle-ladder contributions (right), based on evolved N^3LO NN potentials and 3NF fit to $E_{^3H}$ and $r_{^4He}$. Upper bounds to the theoretical uncertainties are estimated by the NN (lines) and 3N (band) cutoff variations [40].

for omitted many-body contributions (more precisely, it sets a lower bound to omitted contributions). The second-order results show a dramatic narrowing of this spread, with predicted saturation consistent with the empirical range. The narrowing happens across the full density range. This is strong evidence that these encouraging results are not fortuitous. The particle-particle-ladder sum is little changed from second order except at the lowest densities shown. The latter is not surprising because at very low density the presence of a two-body bound state necessitates a nonperturbative summation. Similar results are obtained using flow equations to evolve Hamiltonians, which is called the Similarity Renormalization Group (SRG) [94, 95, 36, 37] in nuclear physics.

The decrease in cutoff dependence in Fig. 5 with more complete approximations is necessary but not sufficient to conclude that the calculations are under control. Indeed, approximations that are independent of the cutoff will shift the answer but not widen the error band from cutoff variation. The theoretical errors arise from truncations in the initial chiral EFT Hamiltonian, the approximation of the 3NF, and the many-body approximations. The 3NF approximation is particularly uncertain because it involves long-range contributions independent of the cutoff. Many-body corrections to the current approximations include higher-order terms in the hole-line expansion and particle-hole corrections. An approach such as coupled cluster theory that can perform a high-level resummation including long-range correlations will ultimately be necessary for a robust validation.

These results, while not conclusive, open the door to ab-initio density functional theory (DFT) both directly (as in the last sections) but also based on expanding about nuclear matter [96] (next section). This is analogous to the application of DFT in quantum chemistry and condensed matter starting with the uniform electron gas in local-density approximations and adding constrained derivative corrections. Phenomenological energy functionals (such as Skyrme) for nuclei have impressive successes but lack a (quantitative) microscopic foundation based on nuclear forces and seem to have reached the limits of improvement with the current form of functionals [97, 98]. On the other hand, the theoretical errors of the calculations in Fig. 5, while impressively small on the scale of the potential energy per particle, are far too large to be quantitatively competitive with existing functionals. However, there is the possibility of fine tuning to heavy nuclei, of using EFT/RG to guide next-generation functional forms, and of benchmarking with ab-initio methods for low-momentum interactions. Overall, these results are

quite promising for a unified description of all nuclei and nuclear matter but much work is left to be done.

Calculations of finite nuclei by another group using soft potentials further support the use of MBPT. Roth and collaborators have developed a method using designed unitary transformations to remove short-range “hard core” and tensor correlations [99]. The approach is called the “Unitary Correlation Operator Method” or UCOM. The result is a soft Hamiltonian that shares the favorable features of the RG-based potentials. They have also shown close parallels (and some distinctions) of UCOM to the SRG approach [100, 101]. Using a UCOM NN potential, which is phase equivalent to a given initial Hamiltonian (in this case Argonne v_{18} [18]), they have calculated many nuclei (including heavy nuclei such as ^{208}Pb) in HF plus second- and third-order MBPT corrections. The energies and radii obtained seem to be remarkably converged at second order with good systematics [38]. Preliminary results from supplementing the NN potential by a contact 3-body interaction with fitted strength are very encouraging [102]. They have also examined corrections from particle-hole states in the RPA for closed-shell nuclei; these are found to be relatively small corrections [103].

Thus MBPT appears to be a viable candidate for calculating a nuclear exchange-correlation functional. However, there are three important caveats. Detailed comparisons with a method that does high-order resummations will be necessary before one can make robust conclusions. In this regard, converged calculations using soft potentials with coupled cluster and no-core-shell-model techniques are feasible now in ^{16}O including 3-body forces and soon¹³ in ^{40}Ca (NN-only calculations for CC are possible now even for an unevolved chiral EFT potential [25]). Second, tests of MBPT have so far been largely limited to spherical nuclei where pairing plays a small role. The final point to emphasize again is that corrections are *relatively* small, but not absolutely small and are large compared to the accuracy sought for functionals, so additional contributions must eventually be considered.

3.4 Density matrix expansion

While formally the construction of an *ab initio* DFT energy functional is well-defined based on a many-body perturbation expansion (resummed as needed) about a Kohn-Sham reference state, in practice the feasibility of using KS potentials from such a functional beyond Hartree-Fock has only recently been demonstrated. This is an ongoing area of research in quantum chemistry, with mixed results, and progress in nuclear physics will require many further developments. A more immediate route to a DFT functional based on microscopic nuclear interactions is to make a quasi-local expansion of the energy in terms of various densities, so that functional derivatives needed to define Kohn-Sham potentials are immediate. Of course, in doing so one sacrifices the full non-locality present in an orbital-based functional. An example of such an expansion is the density matrix expansion (DME) introduced by Negele and Vautherin [104, 105], which we describe here in some detail.

The strategy is to follow a path that will be compatible with current nuclear DFT technology but testable and systematically improvable. In this regard, the phenomenological nuclear energy density functionals of the Skyrme form are a good starting point to build on the MBPT with low-momentum interactions. Modern Skyrme functionals have been applied over a very wide range of nuclei, with quantitative success in reproducing properties of nuclear ground states and low-lying excitations [50, 106, 11]. Nevertheless, a significant reduction of the current global and local errors is a major goal [9]. One strategy is to improve the functional itself; the form of the basic Skyrme functional in use is very

¹³These calculations may require an approximation based on a normal-ordering truncation to treat the 3-body force [22], which has not been fully validated for these nuclei.

restricted, consisting of a sum of local powers of various nuclear densities, e.g., for $N = Z$ nuclei [47]:

$$E_{\text{Skyrme}}[\rho, \tau, \mathbf{J}] = \int d^3x \left\{ \frac{1}{2M}\tau + \frac{3}{8}t_0\rho^2 + \frac{1}{16}t_3\rho^{2+\alpha} + \frac{1}{16}(3t_1 + 5t_2)\rho\tau + \frac{1}{64}(9t_1 - 5t_2)(\nabla\rho)^2 - \frac{3}{4}W_0\rho\nabla \cdot \mathbf{J} + \frac{1}{32}(t_1 - t_2)\mathbf{J}^2 \right\}, \quad (101)$$

where the density ρ , the kinetic density τ , and the spin-orbit density \mathbf{J} are expressed as sums over single-particle orbitals. (Expressions for the Skyrme functional including isovector and more general densities can be found in Ref. [107].) Fits to measured nuclear data have given to date only limited constraints on possible density and isospin dependencies and on the form of the spin-orbit interaction. Even qualitative insight into these properties from realistic microscopic calculations could be beneficial in improving the effectiveness of the energy density functional.

A theoretical connection of the Skyrme functional to free-space NN interactions was made long ago by Negele and Vautherin using the density matrix expansion (DME) [104, 105, 108], but there have been few subsequent microscopic developments. The DME originated as an expansion of the Hartree-Fock energy constructed using the nucleon-nucleon G matrix [104, 105], which was treated in a local (i.e., diagonal in coordinate representation) approximation. Recently the DME has been revisited for spin-saturated nuclei using non-local low-momentum interactions in momentum representation [96], for which G matrix summations are not needed because of the softening of the interaction (see Section 3.3). When applied to a Hartree-Fock energy functional, the DME yields an energy functional in the form of a generalized Skyrme functional that is compatible with existing codes, by replacing Skyrme coefficients with density-dependent functions. As in the original application, a key feature of the DME is that it is not a pure short-distance expansion but includes resummations that treat long-range pion interactions correctly in a uniform system. However, we also caution that the Negele-Vautherin DME involves prescriptions for the resummations without a corresponding power counting to justify them.

In essence, the DME maps the orbital-dependent expressions for contributions to the interaction energy E_{int} of the type in Fig. 6(a) into a semi-local form, with explicit dependence on the local densities $\rho(\mathbf{R})$, $\tau(\mathbf{R})$, $\nabla^2\rho(\mathbf{R})$, and so on. This greatly simplifies the determination of the Kohn-Sham potential because the functional derivatives determining the KS potentials can be evaluated directly. The density matrix expansion (DME) for spin-saturated nuclei has been formulated for low-momentum interactions and applied to a Hartree-Fock energy functional including both NN and NNN potentials in Ref. [96]. The output is a set of functions of density that can replace density-independent parameters in standard Skyrme Hartree-Fock codes. Furthermore, the upgrade from Skyrme energy functional to DME energy functional can be carried out in stages. For example, the spin-orbit part and pairing can be kept in Skyrme form with the rest given by the DME. A further upgrade to orbital-based methods would only modify the same part of the code, although the increased computational load will be significant.

Here we outline how the density matrix expansion is carried out for a microscopic DFT at HF order using low-momentum (and non-local) two-body potentials. The relevant object we need to expand is E_{int} , which is expressed in terms of the Kohn-Sham orbitals and eigenvalues that comprise the Kohn-Sham single-particle propagators as in Section 3.1. For Hartree-Fock contributions only the orbitals enter. Higher-order contributions such as the ladder diagrams in the particle-particle channel can also be put approximately into the required form by averaging over the state dependence arising from the intermediate-state energy denominators (cf. the KLI approximation). Therefore, results presented here for the Hartree-Fock contributions to the functional can be generalized to approximately include selected higher-order contributions. However, a framework for systematic improvement is yet to be developed.

Before considering the DME derivation and its application to non-local low-momentum interactions, it is useful to first derive in some detail the starting expression for E_{HF} , the Hartree-Fock contribution to E_{int} . This introduces the basic notation and highlights the differences between most existing DME

studies, which are formulated with local interactions and in coordinate space throughout, and an approach formulated in momentum space and geared towards non-local potentials. For a local potential, the distinction between the direct (Hartree) and exchange (Fock) contributions is significant, and is reflected in the conventional decomposition of the DFT energy functional for Coulomb systems, which separates out the Hartree piece. For a non-local potential, the distinction is blurred because the Hartree contribution now involves the density matrix (as opposed to the density) and it is not useful to make this separation when the range of the interaction is comparable to the non-locality.¹⁴ Consequently, throughout this section we work instead with an antisymmetrized interaction.

For a general (i.e., non-local) free-space two-body potential \hat{V}_{NN} , E_{HF} is defined in terms of Kohn-Sham states [Eq. (11)] labeled by i and j ,

$$E_{\text{HF}} = \frac{1}{2} \sum_{ij}^A \langle ij | \hat{V}_{\text{NN}} (1 - P_{12}) | ij \rangle = \frac{1}{2} \sum_{ij}^A \langle ij | \hat{\mathcal{V}} | ij \rangle . \quad (102)$$

The summation is over the occupied states and the antisymmetrized interaction $\hat{\mathcal{V}} = \hat{V}_{\text{NN}}(1 - P_{12})$ has been introduced, with the exchange operator P_{12} equal to the product of operators for spin, isospin, and space exchange, $P_{12} = P_\sigma P_\tau P_r$. Note that the dependence of E_{HF} on the Kohn-Sham potential is implicit. By making repeated use of the completeness relation in space (\mathbf{r}), spin (σ), and isospin (τ),

$$\mathbb{1} = \sum_{\sigma\tau} \int d\mathbf{r} |\mathbf{r}\sigma\tau\rangle \langle \mathbf{r}\sigma\tau| , \quad (103)$$

E_{HF} can be written in terms of the coordinate space Kohn-Sham orbitals as

$$E_{\text{HF}} = \frac{1}{2} \sum_{ij} \sum_{\{\sigma\tau\}} \int d\mathbf{r}_1 \int d\mathbf{r}_2 \int d\mathbf{r}_3 \int d\mathbf{r}_4 \langle \mathbf{r}_1 \sigma_1 \tau_1 \mathbf{r}_2 \sigma_2 \tau_2 | \hat{\mathcal{V}} | \mathbf{r}_3 \sigma_3 \tau_3 \mathbf{r}_4 \sigma_4 \tau_4 \rangle \\ \times \phi_i^*(\mathbf{r}_1 \sigma_1 \tau_1) \phi_i(\mathbf{r}_3 \sigma_3 \tau_3) \phi_j^*(\mathbf{r}_2 \sigma_2 \tau_2) \phi_j(\mathbf{r}_4 \sigma_4 \tau_4) . \quad (104)$$

From the definition of the Kohn-Sham density matrix,

$$\rho(\mathbf{r}_3 \sigma_3 \tau_3, \mathbf{r}_1 \sigma_1 \tau_1) = \sum_i^A \phi_i^*(\mathbf{r}_1 \sigma_1 \tau_1) \phi_i(\mathbf{r}_3 \sigma_3 \tau_3) , \quad (105)$$

so Eq. (104) can be written as

$$E_{\text{HF}} = \frac{1}{2} \sum_{\{\sigma\tau\}} \int d\mathbf{r}_1 \cdots \int d\mathbf{r}_4 \langle \mathbf{r}_1 \sigma_1 \tau_1 \mathbf{r}_2 \sigma_2 \tau_2 | \hat{\mathcal{V}} | \mathbf{r}_3 \sigma_3 \tau_3 \mathbf{r}_4 \sigma_4 \tau_4 \rangle \rho(\mathbf{r}_3 \sigma_3 \tau_3, \mathbf{r}_1 \sigma_1 \tau_1) \rho(\mathbf{r}_4 \sigma_4 \tau_4, \mathbf{r}_2 \sigma_2 \tau_2) \\ = \frac{1}{2} \text{Tr}_1 \text{Tr}_2 \int d\mathbf{r}_1 \cdots \int d\mathbf{r}_4 \langle \mathbf{r}_1 \mathbf{r}_2 | \mathbf{V}^{1 \otimes 2} | \mathbf{r}_3 \mathbf{r}_4 \rangle \boldsymbol{\rho}^{(1)}(\mathbf{r}_3, \mathbf{r}_1) \boldsymbol{\rho}^{(2)}(\mathbf{r}_4, \mathbf{r}_2) , \quad (106)$$

where a matrix notation is used in the second equation and the traces denote summations over the spin and isospin indices for “particle 1” and “particle 2”. Hereafter we drop the superscripts on \mathbf{V} and $\boldsymbol{\rho}$ that indicate which space they act in as it will be clear from the context.

Expanding the $\boldsymbol{\rho}$ matrices on Pauli spin and isospin matrices we have

$$\boldsymbol{\rho}(\mathbf{r}_1, \mathbf{r}_2) = \frac{1}{4} [\rho_0(\mathbf{r}_1, \mathbf{r}_2) + \rho_1(\mathbf{r}_1, \mathbf{r}_2) \tau_z + \vec{S}_0(\mathbf{r}_1, \mathbf{r}_2) \cdot \vec{\sigma} + \vec{S}_1(\mathbf{r}_1, \mathbf{r}_2) \cdot \vec{\sigma} \tau_z] , \quad (107)$$

where we have assumed the absence of charge-mixing in the single-particle states and the components are obtained by taking the relevant traces of $\boldsymbol{\rho}$. From now on we consider only terms in the energy

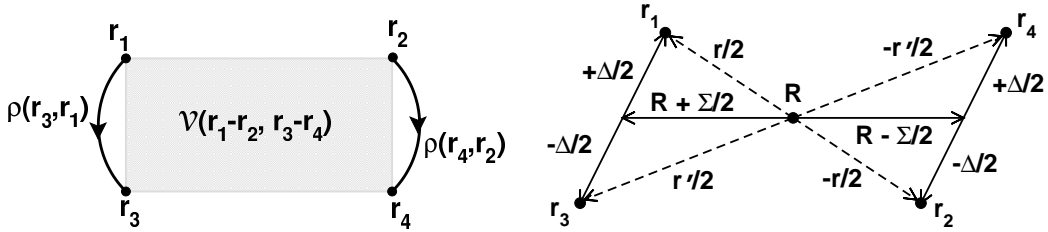


Figure 6: (a) Schematic diagram for approximations to E_{int} that can be expanded using the DME. (b) Coordinates appropriate for the DME applied to the Hartree-Fock potential energy with a non-local potential.

functional arising from products of the scalar-isoscalar (ρ_0) density matrices in Eq. (106), which are the relevant terms for spin-saturated systems with $N = Z$. Because there will be no confusion, we will drop the subscript “0” on the density matrices.

The first step is to switch to relative/center-of-mass (COM) coordinates (see Fig. 6). The free-space two-nucleon potential is diagonal in the COM coordinate, so the starting point for the DME of the two-body Hartree-Fock contribution from a non-local interaction is

$$E_{\text{HF}} = \frac{1}{32} \int d\mathbf{R} d\mathbf{r} d\mathbf{r}' \rho(\mathbf{R} + \frac{\mathbf{r}'}{2}, \mathbf{R} + \frac{\mathbf{r}}{2}) \rho(\mathbf{R} - \frac{\mathbf{r}'}{2}, \mathbf{R} - \frac{\mathbf{r}}{2}) \text{Tr}_{\sigma\tau}[\langle \mathbf{r} | \mathcal{V} | \mathbf{r}' \rangle], \quad (108)$$

where \mathcal{V} denotes the antisymmetrized interaction and the trace is defined as

$$\text{Tr}_{\sigma\tau}[\langle \mathbf{r} | \mathcal{V} | \mathbf{r}' \rangle] \equiv \sum_{\{\sigma\tau\}} \langle \mathbf{r} \sigma_1 \tau_1 \sigma_2 \tau_2 | \hat{V}(1 - P_{12}) | \mathbf{r}' \sigma_1 \tau_1 \sigma_2 \tau_2 \rangle. \quad (109)$$

The DME derivation of Negele and Vautherin (NV) [104] focuses on applications to local potentials, which satisfy $\langle \mathbf{r} | \hat{V} | \mathbf{r}' \rangle = \delta(\mathbf{r} - \mathbf{r}') \langle \mathbf{r} | \hat{V} | \mathbf{r}' \rangle$. While the original NV work included coordinate-space formulas applicable for non-local interactions, for low-momentum potentials it is advantageous to revisit and extend the original derivation to a momentum-space formulation. (Note that Kaiser et al. have shown how to use medium-insertions in momentum space in their application of the DME to chiral perturbation theory at finite density [109, 110, 111].)

For the momentum space formulation, we first rewrite the density matrices in Eq. (108) as

$$\rho(\mathbf{R} \pm \mathbf{r}'/2, \mathbf{R} \pm \mathbf{r}/2) = \rho(\mathbf{R}^{\pm} \pm \Delta/2, \mathbf{R}^{\pm} \mp \Delta/2), \quad (110)$$

where the vectors appearing on the right-hand side are defined by (see Fig. 6)

$$\mathbf{R}^{\pm} = \mathbf{R} \pm \frac{1}{2}\Sigma, \quad \Sigma = \frac{1}{2}(\mathbf{r}' + \mathbf{r}), \quad \Delta = \frac{1}{2}(\mathbf{r}' - \mathbf{r}). \quad (111)$$

Introducing the Fourier transform of \mathcal{V} in the momentum transfers conjugate to Σ and Δ ,

$$\mathbf{q} = \mathbf{k} - \mathbf{k}', \quad \mathbf{p} = \mathbf{k} + \mathbf{k}', \quad (112)$$

(where \mathbf{k}' , \mathbf{k} correspond to relative momenta) gives

$$E_{\text{HF}} = \frac{1}{32} \int d\mathbf{R} \int \frac{d\mathbf{q} d\mathbf{p}}{(2\pi)^6} F(\mathbf{R}, \mathbf{q}, \mathbf{p}) \text{Tr}_{\sigma\tau}[\tilde{\mathcal{V}}(\mathbf{q}, \mathbf{p})],$$

¹⁴However, it is useful to separate out the long-distance part of the potential, which is local, and treat its direct (Hartree) contribution exactly.

where we have defined

$$F(\mathbf{R}, \mathbf{q}, \mathbf{p}) \equiv \int d\Sigma d\Delta e^{i\mathbf{q}\cdot\Sigma} e^{i\mathbf{p}\cdot\Delta} \rho(\mathbf{R}^+ - \Delta/2, \mathbf{R}^+ + \Delta/2) \rho(\mathbf{R}^- + \Delta/2, \mathbf{R}^- - \Delta/2), \quad (113)$$

and

$$\tilde{\mathcal{V}}(\mathbf{q}, \mathbf{p}) \equiv 8 \int d\Sigma d\Delta e^{-i\mathbf{q}\cdot\Sigma} e^{-i\mathbf{p}\cdot\Delta} \langle \Sigma - \Delta | \mathcal{V} | \Sigma + \Delta \rangle. \quad (114)$$

The momenta \mathbf{q} and \mathbf{p} correspond to the momentum transfers for a local interaction in the direct and exchange channels. That is, the direct matrix element is a function of \mathbf{q} and the exchange is a function of \mathbf{p} . In contrast, for a non-local interaction the direct and exchange matrix elements depend on both \mathbf{q} and \mathbf{p} . This is the reason why we do not attempt to separate out the Hartree (direct) and Fock (exchange) contributions to E_{HF} , as is commonly done for local interactions.

The trace of Eq. (114) can be written in a more convenient form for the application of low momentum NN interactions as a sum over partial wave matrix elements (see Ref. [96] for more complete definitions),

$$\text{Tr}_{\sigma\tau}[\tilde{\mathcal{V}}(\mathbf{q}, \mathbf{p})] = 8\pi \sum_{lsj}' (2j+1)(2t+1) P_l(\hat{\mathbf{k}} \cdot \hat{\mathbf{k}}') \langle klsjt | V | k'lsjt \rangle, \quad (115)$$

where the primed summation means that it is restricted to values where $l+s+t$ is odd, with $\mathbf{k} = \frac{1}{2}(\mathbf{p}+\mathbf{q})$ and $\mathbf{k}' = \frac{1}{2}(\mathbf{p}-\mathbf{q})$. For simplicity we assume a charge-independent two-nucleon interaction, although charge-dependence can easily be included.

The expression Eq. (113) for E_{HF} is written in terms of off-diagonal density matrices constructed from the Kohn-Sham orbitals and so is an *implicit* functional of the density. To circumvent the application of the chain rule for the KS potentials, we apply Negele and Vautherin's DME to E_{HF} , resulting in an expression of the form

$$E_{\text{DME}}[\rho, \tau, \mathbf{J}] = \int d\mathbf{R} \mathcal{E}_{\text{DME}}(\rho(\mathbf{R}), \tau(\mathbf{R}), \mathbf{J}(\mathbf{R})), \quad (116)$$

with *explicit* dependence on the local quantities $\rho(\mathbf{R})$, $\tau(\mathbf{R})$, and $|\nabla\rho(\mathbf{R})|^2$ that we write for E_{HF} as

$$E_{\text{HF}} = \int d\mathbf{R} (A[\rho] + B[\rho]\tau + C[\rho](\nabla\rho)^2 + \dots). \quad (117)$$

(We have suppressed terms that go beyond the present limited discussion; also, when $N \neq Z$ these are functions of the isovector densities as well.) The goal is to find the coefficient functions in Eq. (117). The starting point of the DME is the formal identity [104]

$$\rho(\mathbf{R} + \mathbf{s}/2, \mathbf{R} - \mathbf{s}/2) = \sum_a \phi^*(\mathbf{R} + \mathbf{s}/2)\phi(\mathbf{R} - \mathbf{s}/2) = [e^{\mathbf{s}\cdot(\nabla_1 - \nabla_2)/2} \sum_a \phi^*(\mathbf{R}_1)\phi(\mathbf{R}_2)]_{\mathbf{R}_1=\mathbf{R}_2=\mathbf{R}}, \quad (118)$$

where ∇_1 and ∇_2 act on \mathbf{R}_1 and \mathbf{R}_2 , respectively, and the result is evaluated at $\mathbf{R}_1 = \mathbf{R}_2 = \mathbf{R}$. We assume here that time-reversed orbitals are filled pairwise, so that the linear term of the exponential expansion vanishes. After applying a Bessel-function expansion (which is simply the usual plane-wave expansion with real arguments), the angle-averaged density matrix takes the form

$$\hat{\rho}(\mathbf{R} + \mathbf{s}/2, \mathbf{R} - \mathbf{s}/2) = \frac{1}{sk_F(\mathbf{R})} \left[\sum_{n=0}^{\infty} (4n+3) j_{2n+1}(sk_F(\mathbf{R})) \mathcal{Q}_n \left(\left(\frac{\nabla_1 - \nabla_2}{2k_F(\mathbf{R})} \right)^2 \right) \right] \rho(\mathbf{R}_1, \mathbf{R}_2), \quad (119)$$

where \mathcal{Q} is related to the usual Legendre polynomial by $\mathcal{Q}(z^2) = P_{2k+1}(iz)/(iz)$ and an arbitrary momentum scale $k_F(\mathbf{R})$ has been introduced. Equation (119) is independent of k_F if all terms are kept,

but any truncation will give results depending on the particular choice for k_F . The standard LDA choice of Negele and Vautherin,

$$k_F(\mathbf{R}) = (3\pi^2 \rho(\mathbf{R})/2)^{1/3}, \quad (120)$$

is used here. Alternative choices for $k_F(\mathbf{R})$ may better optimize the convergence of truncated expansions of Eq. (119) and lead to a systematic power counting.

Following Negele and Vautherin, Eq. (119) is truncated to terms with $n \leq 1$, which yields the fundamental equation of the DME,

$$\hat{\rho}(\mathbf{R} + \frac{\mathbf{s}}{2}, \mathbf{R} - \frac{\mathbf{s}}{2}) \approx \rho_{SL}(k_F(\mathbf{R})s) \rho(\mathbf{R}) + s^2 g(k_F(\mathbf{R})s) \left[\frac{1}{4} \nabla^2 \rho(\mathbf{R}) - \tau(\mathbf{R}) + \frac{3}{5} k_F(\mathbf{R})^2 \rho(\mathbf{R}) \right], \quad (121)$$

where

$$\rho_{SL}(x) \equiv 3j_1(x)/x, \quad g(x) \equiv 35j_3(x)/2x^3, \quad (122)$$

and the kinetic energy density is $\tau(\mathbf{R}) = \sum_i |\nabla \phi_i(\mathbf{R})|^2$. If a short-range interaction is folded with the density matrix, then a truncated Taylor series expansion of Eq. (121) in powers of s would be justified and would produce a quasi-local functional. But the local k_F in the interior of a nucleus is typically greater than the pion mass m_π , so such an expansion would give a poor representation of the physics of the long-range pion exchange interaction.

Instead, the DME is constructed as an expansion about the exact nuclear matter density matrix. Thus, Eq. (121) has the important feature that it reduces to the density matrix in the homogeneous nuclear matter limit, $\rho_{NM}(\mathbf{R} + \mathbf{s}/2, \mathbf{R} - \mathbf{s}/2) = \rho_{SL}(k_F s) \rho$. As a result, the resummed expansion in Eq. (121) does not distort the finite range physics, as the long-range one-pion-exchange contribution to nuclear matter is exactly reproduced and the finite-range physics is encoded as non-trivial (e.g., non-monomial) density dependence in the resulting functional. The small parameters justifying this expansion emerge in the functionals as integrals over the inhomogeneities of the density. (See Section 4.3 and Ref. [112] for examples of estimated contributions to a functional for a model problem.)

In the case of a local interaction, the Fock term is schematically given by $W_F \sim \int d\mathbf{R} ds \rho^2(\mathbf{R} + \mathbf{s}/2, \mathbf{R} - \mathbf{s}/2) V(\mathbf{s})$, so a single application of Eq. (121) is sufficient to cast E_{HF} into the desired form. For a non-local interaction the calculation is more involved as two applications of the DME are required. There is arbitrariness in what is kept in higher orders of Σ^2 , which is used (following Negele and Vautherin) to “reverse engineer” the expansion so that the exact nuclear matter limit is always exactly reproduced by the leading term [104]. We emphasize that this is a prescription without established power counting or error estimates; as shown in Ref. [96], different prescriptions can lead to significant changes in nuclear observables. The end result for the product of two density matrices is [96]

$$\begin{aligned} \rho(\mathbf{R} + \frac{\mathbf{r}'}{2}, \mathbf{R} + \frac{\mathbf{r}}{2}) \rho(\mathbf{R} - \frac{\mathbf{r}'}{2}, \mathbf{R} - \frac{\mathbf{r}}{2}) &\approx \rho_{SL}^2(k_F \Delta) \rho^2 + \frac{1}{2} \Sigma^2 g(k_F \Sigma) \left(\rho \nabla^2 \rho \rho_{SL}(k_F \Delta) j_0(k_F \Delta) \right. \\ &\quad \left. - |\nabla \rho|^2 [j_0^2(k_F \Delta) + j_1^2(k_F \Delta)] \right) + 2\Delta^2 g(k_F \Delta) \rho_{SL}(k_F \Delta) \left(\frac{1}{4} \rho \nabla^2 \rho - \rho \tau + \frac{3}{5} k_F^2 \rho^2 \right). \end{aligned} \quad (123)$$

In the momentum space expression for E_{HF} , it remains to evaluate the Fourier transforms defined in Eq. (113) for the expanded density matrices in Eq. (123). Identifying the terms in Eq. (117) that give the DME functionals $A[\rho]$, $B[\rho]$, and $C[\rho]$, we have

$$A[\rho] = \frac{\rho^2}{16\pi k_F^3} \int_0^{2k_F} p^2 dp \text{Tr}_{\sigma\tau} [\tilde{\mathcal{V}}(0, \mathbf{p})] (I_1(\bar{p}) + \frac{6}{5} I_2(\bar{p})), \quad (124)$$

$$B[\rho] = -\frac{\rho}{8\pi k_F^5} \int_0^{2k_F} p^2 dp \text{Tr}_{\sigma\tau} [\tilde{\mathcal{V}}(0, \mathbf{p})] I_2(\bar{p}), \quad (125)$$

where $\text{Tr}_{\sigma\tau} [\tilde{\mathcal{V}}(0, \mathbf{p})]$ is given by a simple sum of diagonal matrix elements in the different partial waves,

$$\text{Tr}_{\sigma\tau} [\tilde{\mathcal{V}}(0, \mathbf{p})] = 8\pi \sum_{lsj} (2j+1)(2t+1) \langle \frac{p}{2} lsjt | V | \frac{p}{2} lsjt \rangle. \quad (126)$$

The primed sum is over all channels for which $l + s + t$ is odd.

In these expressions, the functions $I_j(\bar{p})$ and $I_j(\bar{q})$ are simple polynomials (and theta functions) in the scaled momenta $\bar{p} \equiv p/k_F$ and $\bar{q} \equiv q/k_F$:

$$I_1(\bar{p}) \equiv \int x^2 dx j_0(\bar{p}x) \rho_{\text{SL}}^2(x) = \frac{3\pi}{32}(16 - 12\bar{p} + \bar{p}^3) \theta(2 - \bar{p}) , \quad (127)$$

$$I_2(\bar{p}) \equiv \int x^4 dx j_0(\bar{p}x) \rho_{\text{SL}}(x) g(x) = -\frac{35\pi}{128}(\bar{p}^5 - 18\bar{p}^3 + 40\bar{p}^2 - 24\bar{p}) \theta(2 - \bar{p}) , \quad (128)$$

$$I_3(\bar{q}) \equiv \int x^4 dx j_0(\bar{q}x) g(x) = -\frac{35\pi}{8}(5\bar{q}^2 - 3) \theta(1 - \bar{q}) , \quad (129)$$

$$I_4(\bar{p}) \equiv \int x^2 dx j_0(\bar{p}x) j_0(x) \rho_{\text{SL}}(x) = \frac{3\pi}{8}(2 - \bar{p}) \theta(2 - \bar{p}) , \quad (130)$$

$$I_5(\bar{p}) \equiv \int x^2 dx j_0(\bar{p}x) [j_0^2(x) + j_1^2(x)] = \frac{\pi}{8\bar{p}}(4 - \bar{p}^2) \theta(2 - \bar{p}) . \quad (131)$$

Note that the trivial angular dependence of Eqs. (127)–(131) is a consequence of the angle averaging that is implicit with each application of the DME.

The contributions to E_{HF} that have gradients of the local density take the form

$$E_{\text{HF}}|_{|\nabla\rho|^2} = \int d\mathbf{R} (C_{\nabla^2\rho} \nabla^2 \rho(\mathbf{R}) + C_{|\nabla\rho|^2} |\nabla \rho(\mathbf{R})|^2) . \quad (132)$$

We can perform a partial integration on the $\nabla^2\rho$ terms to cast them into the canonical form proportional to only $|\nabla\rho|^2$; that is,

$$E_{\text{HF}}|_{|\nabla\rho|^2} = \int d\mathbf{R} |\nabla \rho(\mathbf{R})|^2 \left[C_{|\nabla\rho|^2} - \frac{d}{d\rho} C_{\nabla^2\rho} \right] , \quad (133)$$

so that

$$C[\rho] = C_{|\nabla\rho|^2} - \frac{d}{d\rho} C_{\nabla^2\rho} . \quad (134)$$

In practice it is efficient and accurate to calculate the derivative in Eq. (134) numerically rather than analytically. The expressions for $C_{|\nabla\rho|^2}$ and $C_{\nabla^2\rho}$ are

$$C_{|\nabla\rho|^2} = \frac{1}{32} \int \frac{d\mathbf{q} d\mathbf{p}}{(2\pi)^6} \left(-\frac{8\pi^2}{k_F^8} I_3(\bar{q}) I_5(\bar{p}) \right) \text{Tr}_{\sigma\tau}[\tilde{\mathcal{V}}(\mathbf{q}, \mathbf{p})] \quad (135)$$

$$= -\frac{1}{16\pi^2 k_F^8} \int_0^{k_F} q^2 dq \int_0^{2k_F} p^2 dp I_3(\bar{q}) I_5(\bar{p}) \tilde{\mathcal{V}}_{av}(q, p) , \quad (136)$$

$$\begin{aligned} C_{\nabla^2\rho} &= \frac{\rho}{32} \int \frac{d\mathbf{q} d\mathbf{p}}{(2\pi)^6} \left(\frac{1}{k_F^5} (2\pi)^4 \delta^3(\mathbf{q}) I_2(\bar{p}) + \frac{8\pi^2}{k_F^8} I_3(\bar{q}) I_4(\bar{p}) \right) \text{Tr}_{\sigma\tau}[\tilde{\mathcal{V}}(\mathbf{q}, \mathbf{p})] \\ &= \frac{\rho}{32\pi k_F^5} \int_0^{2k_F} p^2 dp I_2(\bar{p}) \text{Tr}_{\sigma\tau}[\tilde{\mathcal{V}}(0, \mathbf{p})] \\ &\quad + \frac{\rho}{16\pi^2 k_F^8} \int_0^{k_F} q^2 dq \int_0^{2k_F} p^2 dp I_3(\bar{q}) I_4(\bar{p}) \tilde{\mathcal{V}}_{av}(q, p) , \end{aligned} \quad (137)$$

where $\tilde{\mathcal{V}}_{av}(q, p)$ is the angle-averaged interaction,

$$\tilde{\mathcal{V}}_{av}(q, p) \equiv \frac{1}{2} \int d(\cos\theta) \text{Tr}_{\sigma\tau}[\tilde{\mathcal{V}}(\mathbf{q}, \mathbf{p})] , \quad (138)$$

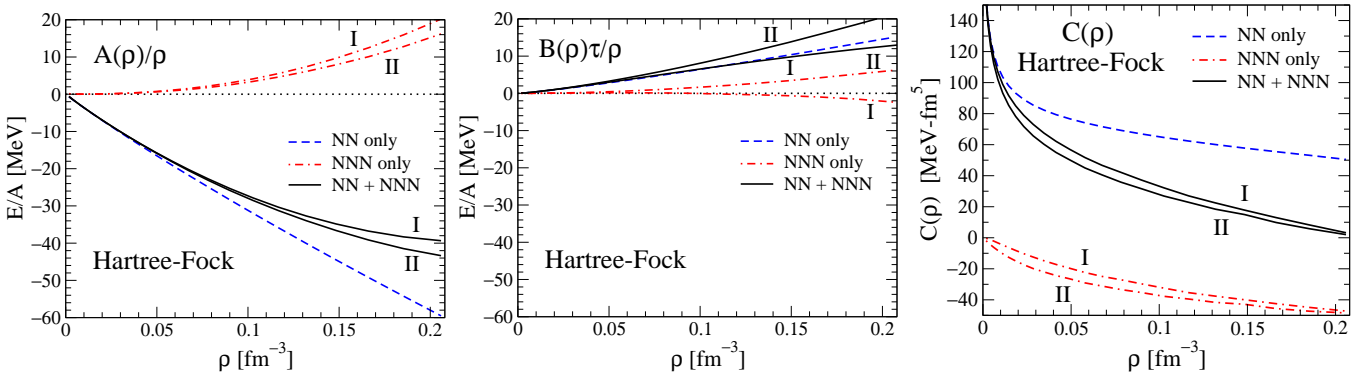


Figure 7: Contribution to the energy per particle in nuclear matter from the isoscalar coefficient functions $A(\rho)$, $B(\rho)$, and $C(\rho)$ as a function of the density from the DME applied to the Hartree-Fock energy calculated using $V_{\text{low } k}$ with $\Lambda = 2.1 \text{ fm}^{-1}$. The result including the NN interaction alone is compared to NN plus NNN interactions for two DME expansions (I and II, see Ref. [96]).

and $\tilde{\mathcal{V}}(\mathbf{q}, \mathbf{p})$ is given by Eq. (115). Note that care must be taken in the evaluation of $dC_{\nabla^2\rho}/d\rho$ if the vertex $\tilde{\mathcal{V}}(\mathbf{q}, \mathbf{p})$ is density-dependent or if the local Fermi momentum is not taken to be $k_F = (3\pi^2\rho/2)^{1/3}$.

These calculations are extended to (local) three-body forces with corresponding contributions to A , B , and C in Ref. [96] using the same type of expansions. Some representative numerical results given there are reproduced in Fig. 7, which illustrate the relative size of NN and NNN contributions and the truncation uncertainty introduced from different DME prescriptions. It is clear that the decreasing hierarchy of many-body contributions is maintained in the individual coefficient functions, but cancellations magnify the sensitivity to the three-body part and how the truncation is carried out.

These results are limited and do not yet touch on many of the most interesting aspects of microscopic DFT from low-momentum potentials. Topics that should be explored in the future include:

- Examine the resolution or scale dependence of the energy functional by evolving the input low-momentum potential. There will be dependence on the RG cutoff or flow parameter both from omitted physics and from intrinsic scale dependence. Calculations at least to second order are needed to separate these dependencies.
- Examine the isovector part of the functional. Contributions from the more interesting long-range (pion) parts of the free-space interactions can be isolated, allowing the derivation of analytic expressions for the dominant density dependence of the isovector DME coupling functions.
- Study the dependence of spin-orbit contributions on NN vs. NNN interactions. This includes the isospin dependence as well as overall magnitudes. The NN spin-orbit contributions arise from short-range interactions, whereas NNN contributions arise from the long-range two-pion exchange interaction. Therefore, we expect to find a rather different density dependence for the two types of spin-orbit contributions.
- Explore the contribution of tensor contributions, which have recently been reconsidered phenomenologically [113, 114].
- Understand the scaling of contributions from many-body forces. In particular, how does the four-body force (which is known at N^3LO in chiral EFT with conventional Weinberg counting) contribution at Hartree-Fock level impact the energy functional?

There are both refinements possible within the DME framework and generalizations that test its applicability and accuracy. Most immediately, the DME at the Hartree-Fock level can be directly extended

to approximately include second-order (or full particle-particle ladder) contributions by using averaged energies for the energy denominators.

In extending the first calculations from Ref. [96], the standard DME formalism from Negele and Vautherin [104] will also need to be modified. This formalism has problems even beyond the truncation errors from different DME prescriptions seen in Fig. 7, the most severe being that it provides an extremely poor description of the vector part of the density matrix. While the standard DME is reasonable at reproducing the scalar density matrices, even here the errors are sufficiently large that the disagreement with a full finite-range Hartree-Fock calculations can reach the MeV per particle level. Gebremariam and collaborators have traced both of these problems to an inadequate phase space averaging (PSA) used in the previous DME approaches [115]. In the derivation of the DME, one incorporates average information about the local momentum distribution into the approximation. The Negele-Vautherin DME uses the phase space of infinite nuclear matter to perform this averaging for the scalar part (and do not even average the vector part). However, the local momentum distribution in finite Fermi systems exhibits two striking differences from that of infinite homogeneous matter. First, mean-field calculations of nuclei show that the local momentum distribution exhibits a diffuse Fermi surface that is especially pronounced in the nuclear surface [116]. Second, the local momentum distribution is found to be anisotropic, with the deformation accentuated in the surface region of the finite Fermi system [117].

Motivated by previous studies of the Wigner distribution function in nuclei, Gebremariam et al. calculate the quadrupole deformation of the local momentum distribution using wave functions for that nucleus [115]. There are no free parameters. The improvements are substantial for the vector density matrices, typically reducing relative errors in integrated quantities by as much as an order of magnitude across many different isotope chains [115].

Future tests of the DME will include benchmarks against *ab initio* methods in the overlap region of light-to-medium nuclei. Additional information is obtained from putting the nuclei in external fields, which can be added directly to the DFT/DME functional. Work is in progress on comparisons to both coupled cluster and full configuration interaction calculations as part of the UNEDF project. A key feature is that the same Hamiltonian will be used for the microscopic calculation and the DME approximation to the DFT. The freedom to adjust (or turn off) external fields as well as to vary other parameters in the Hamiltonian permits detailed evaluations of the approximate functionals. In parallel there will be refined nuclear matter calculations; power counting arguments from re-examining the Brueckner-Bethe-Goldstone approach in light of low-momentum potentials will provide a framework for organizing higher-order contributions. These investigations should provide insight into how the energy density functional can be fine tuned for greater accuracy in a manner consistent with power counting and EFT principles.

4 DFT as Legendre transform

In this section, we turn from MBPT in second quantization formalism to the formulation of DFT using path integrals for effective actions of composite operators. This can be an intimidating formalism if unfamiliar but offers complementary advantages. For example:

- Effective actions are the natural theoretical framework for Legendre transforms [118, 119, 120], which is the underlying basis for DFT. These aspects tend to be hidden in the framework of Section 3.
- The path integral construction of DFT is transparent, such as the role and usefulness of additional densities/sources. (As for implementation, we rapidly discover the same necessity to evaluate functional derivatives that was treated in Section 2.)

- Path integral effective actions are particularly suited for symmetry breaking, such as encountered with pairing. The renormalization issues in the latter case are manifest rather than hidden.
- Connections to effective field theory (EFT) and power counting can be more accessible.
- The path integral formulation puts the DFT construction in a broader perspective, which can suggest connections and generalizations not apparent otherwise. For example, there are alternative effective actions using auxiliary fields or with a two-particle-irreducible nature. The latter may be related to more general EDF constructions as proposed in Ref. [16].
- The quantization of gauge theories was greatly facilitated by Faddeev-Popov and BRST methods using path integrals; the same techniques offer alternative possibilities for implementing collective coordinates to restore symmetries broken by the mean-field organization of DFT [121, 122].
- The path integral formulation can suggest different types of nonperturbative approximations, such as $1/N$ expansions, that might be needed for extensions beyond low-order nuclear MBPT (e.g., to handle long-range correlations).

Space does not permit a detailed exposition of the path integral formulation of DFT. Furthermore, in the short term the construction for nuclear DFT based on MBPT and the DME is probably cleanest in the formalism of Section 3. Therefore we focus on presenting the main ideas through analogy and schematic versions of the path integrals, and concentrate the EFT discussion on general issues such as power counting for functionals.

As stressed in Section 1, microscopic DFT follows naturally from calculating the response of a many-body system to external sources, as in Green’s function methods, only with local, static sources that couple to densities rather than fundamental fields. (Time-dependent sources can be used for certain excited states.) It is profitable to think in terms of a thermodynamic formulation of DFT, which uses the effective action formalism [32] applied to composite operators to construct energy density functionals [123, 124, 125]. The basic plan is to consider the zero temperature limit of the partition function \mathcal{Z} for the (finite) system of interest in the presence of external sources coupled to various quantities of interest (such as the fermion density). We derive energy functionals of these quantities by Legendre transformations with respect to the sources [29]. These sources probe, in a variational sense, configurations near the ground state.

The work by Lieb [126] on the Hohenberg-Kohn theorem [27] establishes that the real issue for DFT is the existence of the Legendre transform $F[\rho]$ of the ground state energy as a functional $E[v]$ of the potential. The details involve sophisticated mathematics (e.g., convex-functional analysis) that is not readily accessible; we recommend Ref. [29] by Kutzelnigg as a gateway to the mathematically rigorous literature behind DFT in terms of Legendre transformations.¹⁵ Fortunately, for our purposes the familiarity of physicists with Legendre transforms in the context of thermodynamics is all we need. We highly recommend Ref. [26] as an elementary introduction to DFT that carries the analogy to thermodynamics through various simple examples.

Effective actions are a natural framework to implement Legendre transformations, motivate approximations not obvious in MBPT, and consider generalizations. One limitation of DFT is the exclusive role of local potentials (sources) and densities, where locality is in reference to coordinate space. Kutzelnigg points out that this is in contrast to many-body methods that introduce a finite basis in which operators are expanded, for which local operators have no privileged place. In this sense, density matrix functional theory, as proposed for nuclei in Ref. [16], seems more natural [29]. By looking at effective actions as a broader context, the limitations and problems of local sources are apparent, but also the opportunities for generalizations.

¹⁵There are important formal details [30], such as that we need $E[v]$ to be concave to carry out the transform.

4.1 Analogy to Legendre transform in thermodynamics

We first preview DFT as an effective action [125] by recalling ordinary thermodynamics with N particles as temperature $T \rightarrow 0$. The thermodynamic potential is related to the grand canonical partition function, with the chemical potential μ acting as a source to change $N = \langle \hat{N} \rangle$,

$$\Omega(\mu) = -kT \ln Z(\mu) \quad \text{and} \quad N = -\left(\frac{\partial \Omega}{\partial \mu}\right)_{TV}. \quad (139)$$

Because Ω is convex, N is a monotonically increasing function of μ and we can *invert* to find $\mu(N)$ and apply a Legendre transform to obtain

$$F(N) = \Omega(\mu(N)) + \mu(N)N. \quad (140)$$

This is our (free) energy function of the particle number, which is analogous to the DFT energy functional of the density.¹⁶ Indeed, if we generalize to a spatially dependent chemical potential $J(\mathbf{x})$, then

$$Z(\mu) \longrightarrow Z[J(\mathbf{x})] \quad \text{and} \quad \mu N = \mu \int \psi^\dagger \psi \longrightarrow \int J(\mathbf{x}) \psi^\dagger \psi(\mathbf{x}). \quad (141)$$

Now Legendre transform from $\ln Z[J(\mathbf{x})]$ to $\Gamma[\rho(\mathbf{x})]$, where $\rho = \langle \psi^\dagger \psi \rangle_J$, and we have DFT with Γ simply proportional to the energy functional! [Note that $J(\mathbf{x}) \rightarrow v_{\text{ext}}(\mathbf{x})$ to match our previous notation.]

The functional Γ is a type of effective action [125]. An effective action is generically the Legendre transform of a generating functional with an external source (or sources). For DFT, we use a source to adjust the density (cf. using an external applied magnetic field to adjust the magnetization in a spin system). Consider first the simplest case of a single external source $J(\mathbf{x})$ coupled to the density operator $\hat{\rho}(x) \equiv \psi^\dagger(x)\psi(x)$ in the partition function

$$\mathcal{Z}[J] = e^{-W[J]} \sim \text{Tr } e^{-\beta(\hat{H}+J\hat{\rho})} \sim \int \mathcal{D}[\psi^\dagger] \mathcal{D}[\psi] e^{-\int [\mathcal{L} + J\psi^\dagger \psi]}, \quad (142)$$

for which we can construct a (Euclidean) path integral representation with Lagrangian \mathcal{L} [32]. (Note: because our treatment is schematic, for convenience we neglect normalization factors and take the inverse temperature β and the volume Ω equal to unity in the sequel.) The static density $\rho(\mathbf{x})$ in the presence of $J(\mathbf{x})$ is

$$\rho(\mathbf{x}) \equiv \langle \hat{\rho}(\mathbf{x}) \rangle_J = \frac{\delta W[J]}{\delta J(\mathbf{x})}, \quad (143)$$

which we invert to find $J[\rho]$ and then Legendre transform from J to ρ :

$$\Gamma[\rho] = -W[J] + \int d\mathbf{x} J(\mathbf{x})\rho(\mathbf{x}), \quad (144)$$

with

$$J(\mathbf{x}) = \frac{\delta \Gamma[\rho]}{\delta \rho(\mathbf{x})} \longrightarrow \left. \frac{\delta \Gamma[\rho]}{\delta \rho(\mathbf{x})} \right|_{\rho_{\text{gs}}(\mathbf{x})} = 0. \quad (145)$$

For static $\rho(\mathbf{x})$, $\Gamma[\rho]$ is proportional to the conventional Hohenberg-Kohn energy functional, which by Eq. (145) is extremized at the ground state density $\rho_{\text{gs}}(\mathbf{x})$ (and thermodynamic arguments establish that it is a minimum [124]).¹⁷

¹⁶Because v_{ext} is typically given rather than eliminated, for a closer analogy we would also define $\Omega_\mu(N) \equiv F(N) - \mu N$, which depends explicitly on both N and μ . This gives the grand potential when minimized with respect to N [26].

¹⁷A Minkowski-space formulation of the effective action with time-dependent sources leads naturally to an RPA-like generalization of DFT that can be used to calculate properties of collective excitations.

Consider the partition function in the zero-temperature limit of a Hamiltonian with time-independent source $J(\mathbf{x})$ [120]:

$$\widehat{H}(J) = \widehat{H} + \int J \psi^\dagger \psi . \quad (146)$$

If the ground state is isolated (and bounded from below),

$$e^{-\beta \widehat{H}} = e^{-\beta E_0} [|0\rangle\langle 0| + \mathcal{O}(e^{-\beta(E_1 - E_0)})] . \quad (147)$$

As $\beta \rightarrow \infty$, $\mathcal{Z}[J]$ yields the ground state of $\widehat{H}(J)$ with energy $E_0(J)$:

$$E_0(J) = \lim_{\beta \rightarrow \infty} -\frac{1}{\beta} \log \mathcal{Z}[J] = \frac{1}{\beta} W[J] . \quad (148)$$

Substitute and separate out the pieces:

$$E_0(J) = \langle \widehat{H}(J) \rangle_J = \langle \widehat{H} \rangle_J + \int J \langle \psi^\dagger \psi \rangle_J = \langle \widehat{H} \rangle_J + \int J \rho(J) . \quad (149)$$

Rearranging, the expectation value of \widehat{H} in the ground state generated by $J[\rho]$ is¹⁸

$$\langle \widehat{H} \rangle_J = E_0(J) - \int J \rho = \frac{1}{\beta} \Gamma[\rho] . \quad (150)$$

Now put it all together:

$$\frac{1}{\beta} \Gamma[\rho] = \langle \widehat{H} \rangle_J \xrightarrow{J \rightarrow 0} E_0 \quad \text{and} \quad J(x) = -\frac{\delta \Gamma[\rho]}{\delta \rho(x)} \xrightarrow{J \rightarrow 0} \left. \frac{\delta \Gamma[\rho]}{\delta \rho(x)} \right|_{\rho_{\text{gs}}(\mathbf{x})} = 0 . \quad (151)$$

So for static $\rho(\mathbf{x})$, $\Gamma[\rho]$ is proportional to the DFT energy functional F_{HK} . Furthermore, the true ground state (with $J = 0$) is a variational minimum, *so additional sources should be better than just one source coupled to the density* (as we will consider below).¹⁹ The simple, universal dependence on a non-zero external potential v follows directly in this formalism:

$$\Gamma_v[\rho] = W_v[J] - \int J \rho = W_{v=0}[J+v] - \int [(J+v) - v] \rho = \Gamma_{v=0}[\rho] + \int v \rho . \quad (152)$$

Thus allowing for non-zero v_{ext} is a trivial modification to $\Gamma[\rho]$.

There are a various paths to a DFT effective action:

1. The auxiliary field (Hubbard-Stratonovich) method [127, 128]: Couple $\psi^\dagger \psi$ to an auxiliary field φ , and eliminate all or part of $(\psi^\dagger \psi)^2$. Add a source term $J\varphi$ and perform a loop expansion about the expectation value $\phi = \langle \varphi \rangle$. A Kohn-Sham version uses the freedom of the expansion to require the density be unchanged at each order.
2. The inversion method [129, 124, 130, 131] yields a systematic Kohn-Sham DFT, based on an order-by-order expansion. For example, we can apply the EFT power counting for a dilute system.
3. Derive the functional with an RG approach [132]. This is briefly discussed in Section 6.

We will discuss here the inversion method, which connects most closely to the developments in Section 3.

¹⁸The functionals will change with resolution or field redefinitions; only stationary points are observables. This can be seen from Eq. (150), where $\Gamma[\rho]$ is not the expectation value of \widehat{H} in an eigenstate unless $J = J[\rho_{\text{gs}}]$.

¹⁹For the Minkowski-space version of this discussion, see Ref. [119].

4.2 Effective actions for composite operators

A formal constructive framework for Kohn-Sham DFT based on effective actions of composite operators can be carried out using the inversion method [123, 124, 130, 125, 133, 112, 134, 135]. This is an organization of the many-body problem that is based on calculating the response of a finite system to external, static sources rather than seeking the many-body wave function. It requires a tractable expansion (such as an EFT momentum expansion or many-body perturbation theory) that is controllable in the presence of inhomogeneous sources, which act as single-particle potentials. As already noted in Section 3.3, this is problematic for conventional internucleon interactions, for which the single-particle potential needs to be tuned to enhance the convergence of the hole-line expansion [71, 73], but is ideally suited for low-momentum interactions. Given an expansion, one can construct a free-energy functional in the presence of the sources and then Legendre transform order-by-order to the desired functional of the densities. Because these are complicated, non-local functionals and we require functional derivatives with respect to the densities, whose dependencies are usually only implicit, we will ultimately apply the methods of Section 2 to derive OEP equations.

The essential features of the inversion method can be illustrated without the involved path integral formalism by considering the Kohn-Luttinger-Ward (KLW) theorem [136, 137], which relates the perturbative calculation of diagrams using the finite-temperature Matsubara formalism in the zero-temperature limit to the calculation of diagrams using zero-temperature perturbation theory. A demonstration of the KLW theorem using an inversion method for the case of an electron gas presented in Ref. [31] can be adapted to any hierarchical expansion. Besides perturbation theory in the interaction, this includes an EFT expansion relevant to a natural short-distance interaction (which is an expansion in the Fermi momentum k_F times the effective range parameters a_s , r_s , and so on [138]) and nonperturbative (in diagrams) $1/N$ expansions [139].

The basic plan is to carry out order-by-order the conventional thermodynamic Legendre transformation already considered:

$$F(N) = \Omega(\mu) + \mu N , \quad (153)$$

with $\mu(N)$ obtained by inverting $N(\mu) = -(\partial\Omega/\partial\mu)_{TV}$. We expand each of the quantities in Eq. (153) about the non-interacting system:

$$\Omega(\mu) = \Omega_0(\mu) + \Omega_1(\mu) + \Omega_2(\mu) + \dots , \quad (154)$$

$$\mu = \mu_0 + \mu_1 + \mu_2 + \dots , \quad (155)$$

$$F(N) = F_0(N) + F_1(N) + F_2(N) + \dots , \quad (156)$$

where the subscript indicates the order of the expansion. (Note that the subscript is just a counting parameter that does not have to correspond to a *power series* in the expansion parameter; e.g., in the Coulomb case the expansion parameter is e^2 but Ω_2 has both an e^4 term and the correlation energy of order $e^4 \ln e$.) The non-interacting system refers to a system of zeroth order in the EFT expansion parameter. This means the zeroth-order system has no *internal* interactions among the particles, but it can include external sources (we exploit this freedom below).

The number of particles is

$$N(\mu, T, V) = - \left(\frac{\partial \Omega}{\partial \mu} \right)_{TV} = - \frac{\partial \Omega_0}{\partial \mu} - \frac{\partial \Omega_1}{\partial \mu} - \frac{\partial \Omega_2}{\partial \mu} + \dots \quad (157)$$

Note that we could simply use the *unexpanded* first equality in Eq. (157) together with the series in Eq. (154), because they define a parametric relation between N and Ω in terms of μ [31]. Instead, to mimic DFT we perform the inversion in Eq. (157) order-by-order, treating N as order zero in the expansion. (That is, we ensure there are no corrections to N at higher order.) This means that the

zeroth order equation,

$$N = - \left[\frac{\partial \Omega_0}{\partial \mu} \right]_{\mu=\mu_0}, \quad (158)$$

is the *only* equation to which N contributes (by construction). Thus the “exact” N is obtained from the non-interacting thermodynamic potential. This might not sound impressive, but the analogous situation holds when we generalize μ to be position dependent or coupled to the pair density in a finite system. In these cases, it is the exact, spatially dependent fermion or pair density (with appropriate renormalization conditions, see below) that is obtained from a non-interacting system with a single-particle potential that is the generalization of μ_0 . This is precisely the description of the Kohn-Sham system (see Refs. [133] and [112] for details on carrying out the DFT case without pairing).

Equation (158) determines $N(\mu_0)$ at any temperature, from which we can find $\mu_0(N)$ for any system for which we can identify Ω_0 (the inversion is unique because μ_0 is a monotonic function of N [31]). If we have a uniform system with no external sources, μ_0 is the chemical potential of a noninteracting Fermi gas at temperature T with density N/V . In particular, at $T = 0$ with no external potential and spin-isospin degeneracy ν ,

$$\mu_0(N) = (6\pi^2 N/\nu V)^{2/3} \equiv k_F^2/2M \equiv \varepsilon_F^0. \quad (159)$$

The first-order equation extracted from Eq. (157) has two terms, which lets us solve for μ_1 in terms of known (from diagrams) functions of μ_0 :

$$0 = \left[\frac{\partial \Omega_1}{\partial \mu} \right]_{\mu=\mu_0} + \mu_1 \left[\frac{\partial^2 \Omega_0}{\partial \mu^2} \right]_{\mu=\mu_0} \implies \mu_1 = - \frac{[\partial \Omega_1 / \partial \mu]_{\mu=\mu_0}}{[\partial^2 \Omega_0 / \partial \mu^2]_{\mu=\mu_0}}. \quad (160)$$

At second order, we can isolate and solve for μ_2 , eliminating μ_1 using (160). This pattern continues to all orders: μ_i is determined by functions of μ_0 only.

Now we apply the inversion to $F = \Omega + \mu N$:

$$\begin{aligned} F(N) &= \underbrace{\Omega_0(\mu_0) + \mu_0 N}_{F_0} + \underbrace{\mu_1 \left[\frac{\partial \Omega_0}{\partial \mu} \right]_{\mu=\mu_0} + \Omega_1(\mu_0) + \mu_1 N}_{F_1} \\ &\quad + \underbrace{\mu_2 \left[\frac{\partial \Omega_0}{\partial \mu} \right]_{\mu=\mu_0} + \mu_1 \left[\frac{\partial \Omega_1}{\partial \mu} \right]_{\mu=\mu_0} + \frac{1}{2} \mu_1^2 \left[\frac{\partial^2 \Omega_0}{\partial \mu^2} \right]_{\mu=\mu_0} + \Omega_2(\mu_0) + \mu_2 N}_{F_2} + \dots \end{aligned} \quad (161)$$

The $\mu_i N$ term always cancels with $\mu_i [\partial \Omega_0 / \partial \mu]_{\mu=\mu_0}$ in F_i for $i \geq 1$ because of Eq. (158), leaving

$$F(N) = F_0(N) + \underbrace{\Omega_1(\mu_0)}_{F_1} + \underbrace{\Omega_2(\mu_0) - \frac{1}{2} \frac{[\partial \Omega_1 / \partial \mu]_{\mu=\mu_0}^2}{[\partial^2 \Omega_0 / \partial \mu^2]_{\mu=\mu_0}}}_{F_2} + \dots, \quad (162)$$

where we have also used Eq. (160) to simplify F_2 . The expansion for F can be extended systematically, but this is all we need here. (Higher orders can be found by following the prescription in Refs. [140, 141].)

This construction is rather general. The Kohn-Luttinger-Ward theorem explores a particular case, the $T \rightarrow 0$ limit, in which the second term in F_2 in Eq. (162) cancels precisely against the anomalous diagram in Ω_2 , as illustrated in Fig. 8. This cancellation of derivative terms and anomalous diagrams occurs to all orders in the expansion. An analogous cancellation occurs in the Kohn-Sham DFT inversion [133]. The end result is an expression for the free-energy $F(N)$ in terms of the diagrams used for $\Omega_i(\mu)$, only evaluated with $\mu = \mu_0$ and excluding the anomalous diagrams (both of which simplify the evaluation of $F(N)$!). This is precisely the formalism used in Ref. [138] for a uniform low-density Fermi gas at zero temperature, where μ_0 appeared as the Fermi energy of Eq. (159).

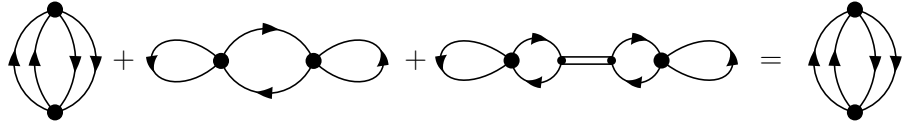


Figure 8: Cancellation of the anomalous diagram at NLO. The double lines represents the inverse of $[\partial^2 \Omega_0 / \partial \mu^2]_{\mu=\mu_0}$ in Eq. (162).

This procedure can be generalized rather directly [123, 124] to carry out the inversion from $\rho[J]$ to $J[\rho]$ needed for Eqs. (142)–(145). The idea again is to expand the relevant quantities in a hierarchy, here labeled by a counting parameter λ ,

$$W[J, \lambda] = W_0[J] + \lambda W_1[J] + \lambda^2 W_2[J] + \dots , \quad (163)$$

$$J[\rho, \lambda] = J_0[\rho] + \lambda J_1[\rho] + \lambda^2 J_2[\rho] + \dots , \quad (164)$$

$$\Gamma[\rho, \lambda] = \Gamma_0[\rho] + \lambda \Gamma_1[\rho] + \lambda^2 \Gamma_2[\rho] + \dots , \quad (165)$$

treating ρ as order unity (which is the same as requiring that there are no corrections to the zero-order density), and match order by order in λ to determine the J_i 's and Γ_i 's. Zeroth order is a noninteracting system with potential $J_0(x)$:

$$\Gamma_0[\rho] = -W_0[J_0] + \int d\mathbf{x} J_0(\mathbf{x})\rho(\mathbf{x}) \quad (166)$$

and

$$\rho(\mathbf{x}) = \frac{\delta W_0[J_0]}{\delta J_0(\mathbf{x})} . \quad (167)$$

Because ρ appears only at zeroth order, it is always specified from the non-interacting system according to Eq. (167); there are no corrections at higher order. *This is the Kohn-Sham system with the same density as the fully interacting system.*

What we have done is use freedom to split J into J_0 and $J - J_0$, which is the analog of introducing a single-particle potential \widehat{U} and splitting the Hamiltonian according to $\widehat{H} = (\widehat{T} + \widehat{U}) + (\widehat{V} - \widehat{U})$, as discussed in Section 3. Typically \widehat{U} is chosen to accelerate (or even allow) convergence of a many-body expansion (e.g., the Bethe-Brueckner-Goldstone theory [71, 72, 73]). For DFT, we need to choose it to ensure that the *density* is unchanged, order by order. Thus, we need the flexibility in the many-body expansion to choose \widehat{U} without seriously degrading the convergence; such freedom is characteristic of low-momentum interactions. (Note: If there is a non-zero external potential, it is simply included with J_0 .)

The path integral defined by W_0 (or Z_0 actually) is a gaussian, which is equal to a functional determinant that is evaluated by diagonalizing $W_0[J_0]$. To do so means to introduce Kohn-Sham orbitals ϕ_i and eigenvalues ε_i ,

$$[-\nabla^2/2m - J_0(\mathbf{x})]\phi_i = \varepsilon_i \phi_i \quad (168)$$

so that

$$\rho(\mathbf{x}) = \sum_{i=1}^A |\phi_i(\mathbf{x})|^2 . \quad (169)$$

Then Z_0 is the product and W_0 is the sum of the ε_i 's. Thus in the path integral formalism, the Kohn-Sham system arises naturally as the zeroth-order approximation to the problem. The organization is based on a saddlepoint evaluation about the system defined by J_0 (which still must be specified) and subsequent corrections.

The orbitals and eigenvalues are used to construct the Kohn-Sham Green's functions, which are used as the propagator lines in calculations the diagrams generated by $W_i[J_0]$. Finally, we find J_0 for

the ground state by truncating the chain at $\Gamma_{i_{\max}}$,

$$J_0 \rightarrow W_1 \rightarrow \Gamma_1 \rightarrow J_1 \rightarrow W_2 \rightarrow \Gamma_2 \rightarrow \dots \rightarrow W_{i_{\max}} \rightarrow \Gamma_{i_{\max}} \quad (170)$$

and completing the self-consistency loop that enforces $J(\mathbf{x}) = 0$:

$$J_0(\mathbf{x}) = - \sum_{i>0}^{i_{\max}} J_i(\mathbf{x}) = \sum_{i>0}^{i_{\max}} \frac{\delta \Gamma_i[\rho]}{\delta \rho(\mathbf{x})} \equiv \frac{\delta \Gamma_{\text{int}}[\rho]}{\delta \rho(\mathbf{x})}. \quad (171)$$

Note that the sum of the Γ_i 's is directly proportional to the desired energy functional. When transforming from W_i to Γ_i , there are additional diagrams that take into account the adjustment of the source to maintain the same density and also so-called anomalous diagrams (these are two-particle reducible). This is the most complicated part but corresponds directly to the extra terms in the KLW inversion [see Eqs. (161),(162) and Fig. 8]. A general discussion and Feynman rules for these diagrams are given in Refs. [124, 130, 131, 133].

We emphasize that even though solving for Kohn-Sham orbitals makes the approach look like a mean-field Hartree calculation, the approximation to the energy and density is *only* in the truncation of Eq. (171). It is a mean-field formalism in the sense of a conventional loop expansion, which is nonperturbative only in the background field while including further correlations perturbatively order-by-order in loops. The special feature of DFT is that the saddlepoint evaluation applies the condition that there are no corrections to the density. Once again, this is not ordinarily an appropriate expansion for internucleon interactions; it is the special features of low-momentum interactions that make them suitable.

To generalize the energy functional to accommodate additional densities such as τ and \mathbf{J} (which appear in the density matrix expansion for nuclei), we simply introduce an additional source coupled to each density. Thus, to generate a DFT functional of the kinetic-energy density as well as the density, add $\eta(\mathbf{x}) \nabla \psi^\dagger \cdot \nabla \psi$ to the Lagrangian and Legendre transform to an effective action of ρ and τ [134]:

$$\Gamma[\rho, \tau] = W[J, \eta] - \int d\mathbf{x} J(\mathbf{x})\rho(\mathbf{x}) - \int d\mathbf{x} \eta(\mathbf{x})\tau(\mathbf{x}). \quad (172)$$

The inversion method results in two Kohn-Sham potentials,

$$J_0(\mathbf{x}) = \left. \frac{\delta \Gamma_{\text{int}}[\rho, \tau]}{\delta \rho(\mathbf{x})} \right|_\tau \quad \text{and} \quad \eta_0(\mathbf{x}) = \left. \frac{\delta \Gamma_{\text{int}}[\rho, \tau]}{\delta \tau(\mathbf{x})} \right|_\rho, \quad (173)$$

where $\Gamma_{\text{int}} \equiv \Gamma - \Gamma_0$. The Kohn-Sham equation is now [134]

$$\left[-\nabla \frac{1}{M^*(\mathbf{x})} \nabla - J_0(\mathbf{x}) \right] \phi_i = \varepsilon_i \phi_i, \quad (174)$$

with an effective mass $1/2M^*(\mathbf{x}) \equiv 1/2M - \eta_0(\mathbf{x})$, just like in Skyrme HF (see also Ref. [142] for an early application to Coulomb systems). Generalizing to the spin-orbit or other densities (including pairing [143], see Section 5.1) proceeds analogously. We note that the variational nature of the effective action implies that adding sources will always improve the effectiveness of the energy functional.

The Feynman diagrams for W_i will in general include multiple vertex points over which to integrate. Further, the dependence on the densities will not be explicit except when we have Hartree terms with a local potential (that is, a potential diagonal in coordinate representation). One way to proceed is to calculate the Kohn-Sham potentials using a functional chain rule, e.g.,

$$J_0(\mathbf{R}) = \frac{\delta \widetilde{\Gamma}_{\text{int}}[\rho]}{\delta \rho(\mathbf{R})} = \int dy \left(\frac{\delta \rho(\mathbf{R})}{\delta J_0(y)} \right)^{-1} \frac{\delta \Gamma_{\text{int}}[\rho]}{\delta J_0(y)}, \quad (175)$$

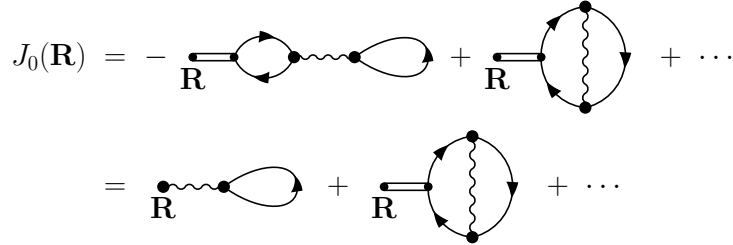


Figure 9: Schematic representation of Eq. (175) for a local potential, where the double-line symbol denotes the $(\delta\rho/\delta J_0)^{-1}$ term.

and steepest descent [124]. This is illustrated schematically for a local interaction in Fig. 9. We see that the Kohn-Sham potential is always just a function of \mathbf{R} but that the functional is generally very non-local. If zero-range interactions are used, these diagrams collapse into an expression for $J_0(\mathbf{R})$ that has no internal vertices, but this is no longer true for diagrams with more than one interaction. The orbital-based methods from Section 2 take the chain rule in Eq. (175) one step further, adding a functional derivative of the sources with respect to the ϕ_i 's (and ε_i 's) [4, 58, 54, 144], which can be applied directly to the functionals.

4.3 EFT and power counting for functionals

The expansion suggested by low-momentum interactions is perturbation theory in powers of the softened interaction \hat{V} . But it is also instructive to consider the simplest EFT example, a dilute system of fermions in a harmonic trap, interacting via natural-sized contact interactions [133, 112, 134]. (Natural-sized means that the scattering length is not fine-tuned to a large value compared to the effective range.) We can construct the effective action as a path integral by finding $W[J]$ order-by-order in an EFT expansion. For a dilute short-range system, the EFT Lagrangian for a nonrelativistic spin-1/2 fermion field with spin-independent interactions in Euclidean form is (t_E is the Euclidean time)

$$\begin{aligned} \mathcal{L}_E &= \psi^\dagger \left[\frac{\partial}{\partial t_E} - \frac{\vec{\nabla}^2}{2M} \right] \psi + \frac{C_0}{2} (\psi^\dagger \psi)^2 - \frac{C_2}{16} \left[(\psi \psi)^\dagger (\psi \vec{\nabla}^2 \psi) + \text{h.c.} \right] - \frac{C'_2}{8} (\psi \vec{\nabla} \psi)^\dagger \cdot (\psi \vec{\nabla} \psi) + \dots \\ &\equiv \psi^\dagger \left[\frac{\partial}{\partial t_E} - \frac{\vec{\nabla}^2}{2M} \right] \psi + \mathcal{L}_E^{\text{int}}(\psi^\dagger, \psi), \end{aligned} \quad (176)$$

where $\vec{\nabla} = \vec{\nabla} - \vec{\nabla}$ is the Galilean invariant derivative and h.c. denotes the Hermitian conjugate.²⁰ The terms proportional to C_2 and C'_2 contribute to *s*-wave and *p*-wave scattering, respectively, while the dots represent terms with more derivatives and/or more fields, as well as renormalization counterterms.

The Euclidean generating functional with chemical potential μ and external sources $\eta(x)$ and $\eta^\dagger(x)$ [32, 128]:

$$Z[\eta, \eta^\dagger; \mu] \equiv e^{-W[\eta, \eta^\dagger; \mu]} = \int D\psi_\alpha D\psi_\alpha^\dagger e^{-\int d^4x [\mathcal{L}_E - \mu \psi_\alpha^\dagger(x) \psi_\alpha(x) + \eta_\alpha^\dagger(x) \psi_\alpha(x) + \psi_\alpha^\dagger(x) \eta_\alpha(x)]}, \quad (177)$$

where $\int d^4x$ includes a dt_E integration that runs from $-\beta/2$ to $\beta/2$ (to facilitate the $\beta \rightarrow \infty$ limit) and anti-periodic boundary conditions are imposed. A conventional perturbative expansion is realized by removing the interaction terms from the path integral in (176) in favor of functional derivatives with respect to η and η^\dagger and performing the remaining Gaussian integration over ψ and ψ^\dagger [32, 128]:

$$Z[\eta, \eta^\dagger; \mu] = Z_0 e^{-\int d^4x \mathcal{L}_E^{\text{int}}[\delta/\delta\eta(x), -\delta/\delta\eta^\dagger(x)]} e^{\int d^4y d^4y' \eta^\dagger(y) \mathcal{G}_0(y, y') \eta(y')}, \quad (178)$$

²⁰We use units with $\hbar = 1$.

where the spin indices are implicit and we have introduced the noninteracting partition function Z_0 . Explicit expressions for the Green's function in coordinate and momentum space can be found in Ref. [32]. The linked-cluster theorem [32] shows that the difference of the interacting and noninteracting thermodynamic potentials Ω and Ω_0 is given by the sum of connected diagrams from the expansion of Z , with the external sources η^\dagger and η set to zero at the end:

$$\Omega(\mu, T, V) - \Omega_0(\mu, T, V) = \frac{1}{\beta}(W[0, 0; \mu] - W_0[0, 0; \mu]) . \quad (179)$$

In evaluating the Feynman diagrams for $W[J]$ and new diagrams for $\Gamma[\rho]$ order by order in the expansion (e.g., EFT power counting), the source $J_0(\mathbf{x})$ is now the background field. This means that propagators (lines) in the background field $J_0(\mathbf{x})$ are

$$G_{\text{KS}}^0(\mathbf{x}, \mathbf{x}'; \omega) = \sum_i \phi_i(\mathbf{x}) \phi_i^*(\mathbf{x}') \left[\frac{\theta(\varepsilon_i - \varepsilon_F)}{\omega - \varepsilon_i + i\eta} + \frac{\theta(\varepsilon_F - \varepsilon_i)}{\omega - \varepsilon_i - i\eta} \right] , \quad (180)$$

where $\phi_i(\mathbf{x})$ satisfies:

$$\left[-\frac{\nabla^2}{2M} + v_{\text{ext}}(\mathbf{x}) - J_0(\mathbf{x}) \right] \phi_i(\mathbf{x}) = \varepsilon_i \phi_i(\mathbf{x}) . \quad (181)$$

For example, if we apply this prescription to the short-range LO contribution (i.e., Hartree-Fock), we obtain

$$\begin{aligned} W_1[J_0] &= \frac{1}{2}\nu(\nu-1)C_0 \int d^3\mathbf{x} \int_{-\infty}^{\infty} \frac{d\omega}{2\pi} \int_{-\infty}^{\infty} \frac{d\omega'}{2\pi} G_{\text{KS}}^0(\mathbf{x}, \mathbf{x}; \omega) G_{\text{KS}}^0(\mathbf{x}, \mathbf{x}; \omega') \\ &= -\frac{1}{2} \frac{(\nu-1)}{\nu} C_0 \int d^3\mathbf{x} [\rho_{J_0}(\mathbf{x})]^2 , \end{aligned} \quad (182)$$

where ν is the spin-isospin degeneracy and

$$\rho_{J_0}(\mathbf{x}) \equiv \nu \sum_i^{\varepsilon_F} |\phi_i(\mathbf{x})|^2 . \quad (183)$$

Expressions for the other W_i 's proceed directly from conventional Feynman rules using the new propagator.

Given $W[J]$ as an EFT expansion, we perform the Legendre transformation,

$$\Gamma[\rho] = W[J] - \int J\rho , \quad (184)$$

by using the EFT power counting with the inversion method as described above, which gives us the means to invert to find $J[\rho]$ and to make an order-by-order inversion from $W[J]$ to $\Gamma[\rho]$ [129, 124, 130]. It proceeds by decomposing $J(\mathbf{x}) = J_0(\mathbf{x}) + J_{\text{LO}}(\mathbf{x}) + J_{\text{NLO}}(\mathbf{x}) + \dots$ as described earlier and fixing J_0 using

$$\rho(\mathbf{x}) = \frac{\delta W_0[J_0]}{\delta J_0(\mathbf{x})} \quad \text{and} \quad J_0(\mathbf{x})|_{\rho=\rho_{\text{gs}}} = \frac{\delta \Gamma_{\text{interacting}}[\rho]}{\delta \rho(\mathbf{x})} \Big|_{\rho=\rho_{\text{gs}}} . \quad (185)$$

Evaluating the functional derivatives is immediate if Γ is approximated so that the dependence on the density is explicit, as with the LDA or DME (see below). Otherwise we apply the OEP chain rule.

Consider the $T = 0$ local density approximation (LDA) for a dilute fermion gas with natural short-ranged interactions (meaning the scattering length a_0 is comparable in magnitude to the effective range r_0 and the p -wave scattering length a_p [138]). The energy density in the uniform system evaluates to:

$$\begin{aligned} \frac{E}{V} &= \rho \frac{k_F^2}{2M} \left[\frac{3}{5} + (\nu-1) \frac{2}{3\pi} (k_F a_0) + (\nu-1) \frac{4}{35\pi^2} (11 - 2 \ln 2) (k_F a_0)^2 \right. \\ &\quad \left. + (\nu-1) (0.076 + 0.057(\nu-3)) (k_F a_0)^3 + (\nu-1) \frac{1}{10\pi} (k_F r_0) (k_F a_0)^2 + (\nu+1) \frac{1}{5\pi} (k_F a_p)^3 + \dots \right] . \end{aligned} \quad (186)$$

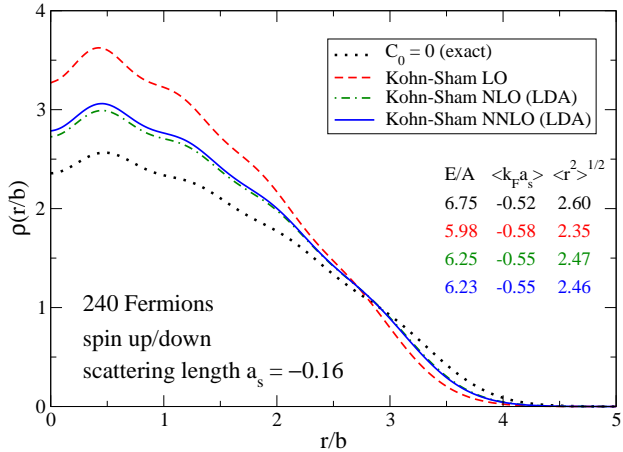


Figure 10: Density profile of a dilute system of fermions in a trap [133].

where $k_F a_0$, $k_F r_0$, and $k_F a_p$ are expansion parameters with $k_F = (6\pi^2 \rho / \nu)^{1/3}$. Using this relation to replace k_F everywhere by $\rho(\mathbf{x})$, we directly obtain the LDA expression for $\Gamma[\rho]$,

$$\begin{aligned} \Gamma[\rho] = & \int d^3x \left[T_{\text{KS}}(\mathbf{x}) + \frac{1}{2} \frac{(\nu - 1)}{\nu} \frac{4\pi a_0}{M} [\rho(\mathbf{x})]^2 + d_1 \frac{a_0^2}{2M} [\rho(\mathbf{x})]^{7/3} \right. \\ & \left. + d_2 a_0^3 [\rho(\mathbf{x})]^{8/3} + d_3 a_0^2 r_0 [\rho(\mathbf{x})]^{8/3} + d_4 a_p^3 [\rho(\mathbf{x})]^{8/3} + \dots \right]. \end{aligned} \quad (187)$$

The Kohn-Sham J_0 according to the EFT expansion follows immediately in the LDA from (185):

$$J_0(\mathbf{x}) = \left[-\frac{(\nu - 1)}{\nu} \frac{4\pi a_0}{M} \rho(\mathbf{x}) - c_1 \frac{a_0^2}{2M} [\rho(\mathbf{x})]^{4/3} - c_2 a_0^3 [\rho(\mathbf{x})]^{5/3} - c_3 a_0^2 r_0 [\rho(\mathbf{x})]^{5/3} - c_4 a_p^3 [\rho(\mathbf{x})]^{5/3} + \dots \right]. \quad (188)$$

where the $\{d_i\}$'s and $\{c_i\}$'s are given in Ref. [145]. Sample results at different EFT orders for a dilute Fermi gas in a harmonic oscillator trap are shown in Fig. 10. Note the systematic convergence with successive orders in the LDA average $\langle k_F a_s \rangle$ (and $a_s \equiv a_0$) for both the energy and density.

An important consequence of the systematic EFT approach is that we can also estimate individual terms in energy functionals. If we scale contributions to the energy per particle according to the average density or $\langle k_F \rangle$, we can make such estimates [133, 112]. This is shown in Fig. 11 for both the dilute trapped fermions, which is under complete control, and for phenomenological energy functionals for nuclei, to which a postulated QCD power counting is applied [146, 147]. In both cases the estimates²¹ agree well with the actual numbers (sometimes overestimating the contribution because of accidental cancellations), which means that truncation errors are understood. Understanding how such power counting can emerge from the MBPT-based DFT for nuclei is an important problem for future study.

4.4 Additional comments

The perspective of Legendre transforms clarifies many DFT issues [29]. For example:

- The Legendre transform formulation adds mathematical rigor to DFT claims. For example, one finds that a bijective mapping between v and ρ does not exist in general. However, it is not necessary for there to be such a mapping to have a Legendre transform; only the uniqueness of ρ given v is needed.

²¹The symbols with error bars are natural estimates with a factor of two spread in the order unity coefficient.

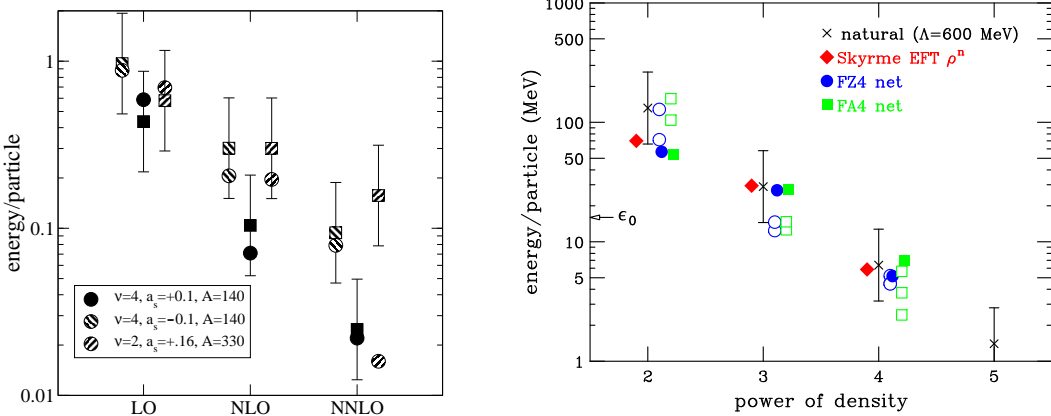


Figure 11: Estimates for energy functionals for a dilute fermions in a harmonic trap (left) and for phenomenological energy functionals for nuclei (right).

- For non-degenerate states, it is true that the density is the functional derivative of the energy with respect to the external potential. But this is not actually needed and so is not a problem for degenerate states; only the concavity of $E[v]$ is necessary.
- DFT is only variational with respect to ρ if we have the exact functional (i.e., never). Once there are approximations, it is no longer variational. This is not a cause for concern, as other successful many-body approaches such as coupled cluster are also not variational.

Additional useful comments on DFT and Legendre transforms can be found in Ref. [29].

5 Topics for nuclear DFT

In this section, we consider various topics specifically relevant to implementations of DFT for nuclei.

5.1 Pairing

Pairing is an important feature of finite nuclei that is absent from isolated atoms and molecules. Its inclusion in nuclear DFT based on microscopic interactions is a topic of much current activity. While there is some work on superconductivity in a Coulomb DFT framework, it is based on using non-local source terms to avoid divergences. The use of local densities for pairing is generally preferred for finite nuclei from a computational point of view. However, we note that recent results from hybrid EDF calculations using low-momentum potentials at lowest order, which suggest that an accurate *ab initio* DFT treatment of pairing is feasible [15], use non-local pairing fields. To use local pairing densities, we need a consistent generalization of the Skyrme-Hartree-Fock-Bogoliubov approach [106]. In fact, one can use functionals with local pairing fields as in phenomenological Skyrme functionals (that are based on zero-range effective interactions) by properly renormalizing [52, 148].

Pairing is an example of spontaneous symmetry breaking, which is naturally accommodated in an effective action framework [118, 119]. For example, consider testing for zero-field magnetization M in a spin system by introducing an external field H to break the rotational symmetry. Legendre transform the Helmholtz free energy $F(H)$:

$$\text{invert } M = -\partial F(H)/\partial H \implies \Gamma[M] = F[H(M)] + MH(M) . \quad (189)$$

Because $H = \partial\Gamma/\partial M \rightarrow 0$, we look for the stationary points of Γ to identify possible ground states, including whether the symmetry broken state is lowest. For pairing, the broken symmetry is a $U(1)$

[phase] symmetry for fermion number. We apply an external source that breaks the number symmetry, forcing $\psi\psi$ to have an expectation value. Then we turn that source off and see whether the expectation value (condensate) persists. (Note: we will only have actual spontaneous symmetry breaking in an infinite system.)

The textbook effective action treatment of pairing in condensed matter is to introduce a contact interaction [127, 128]: $g\psi^\dagger\psi^\dagger\psi\psi$, and perform a Hubbard-Stratonovich transformation with an auxiliary pairing field $\hat{\Delta}(x)$ coupled to $\psi^\dagger\psi^\dagger$, which eliminates the contact interaction. Then one constructs the one-particle-irreducible effective action $\Gamma[\Delta]$ with $\Delta = \langle\hat{\Delta}\rangle$, and looks for values for which $\delta\Gamma/\delta\Delta = 0$. To leading order in the loop expansion (which is a mean field approximation), this yields the BCS weak-coupling gap equation with gap Δ .

The natural alternative here is to use the inversion method for effective actions again [129, 124, 130]. Thus we introduce another external current $j(\mathbf{x})$, which is coupled to the fermion pair density $\psi\psi$ in order to explicitly break the phase symmetry. This is a natural generalization of normal-state Kohn-Sham DFT [51, 52, 149]. The generating functional has sources J, j coupled to the corresponding densities [143]:

$$Z[J, j] = e^{-W[J, j]} = \int D(\psi^\dagger\psi) e^{-\int d^4x [\mathcal{L} + J(x)\psi_\alpha^\dagger\psi_\alpha + j(x)(\psi_\uparrow^\dagger\psi_\downarrow^\dagger + \psi_\downarrow\psi_\uparrow)]}. \quad (190)$$

Densities are found by functional derivatives with respect to J and j :

$$\rho(x) \equiv \langle\psi^\dagger(x)\psi(x)\rangle_{J,j} = \left.\frac{\delta W[J, j]}{\delta J(x)}\right|_j, \quad (191)$$

and (note that κ is called ϕ in Ref. [143])

$$\kappa(x) \equiv \langle\psi_\uparrow^\dagger(x)\psi_\downarrow^\dagger(x) + \psi_\downarrow(x)\psi_\uparrow(x)\rangle_{J,j} = \left.\frac{\delta W[J, j]}{\delta j(x)}\right|_J. \quad (192)$$

(The source j would in general be complex, but it is sufficient for our purposes to take it to be real.) The effective action $\Gamma[\rho, \kappa]$ follows as in Section 4 by functional Legendre transformation:

$$\Gamma[\rho, \kappa] = W[J, j] - \int d^4x J(x)\rho(x) - \int d^4x j(x)\kappa(x), \quad (193)$$

and is proportional to the (free) energy functional $E[\rho, \kappa]$; at finite temperature, the proportionality constant is β . The sources are given by functional derivatives wrt ρ and κ :

$$\frac{\delta E[\rho, \kappa]}{\delta \rho(\mathbf{x})} = J(\mathbf{x}) \quad \text{and} \quad \frac{\delta E[\rho, \kappa]}{\delta \kappa(\mathbf{x})} = j(\mathbf{x}). \quad (194)$$

But the sources are zero in the ground state, so we determine the ground-state $\rho(\mathbf{x})$ and $\kappa(\mathbf{x})$ by stationarity:

$$\left.\frac{\delta E[\rho, \kappa]}{\delta \rho(\mathbf{x})}\right|_{\rho=\rho_{\text{gs}}, \kappa=\kappa_{\text{gs}}} = \left.\frac{\delta E[\rho, \kappa]}{\delta \kappa(\mathbf{x})}\right|_{\rho=\rho_{\text{gs}}, \kappa=\kappa_{\text{gs}}} = 0. \quad (195)$$

This is Hohenberg-Kohn DFT extended to pairing!

We need a method to carry out the Legendre transforms to get Kohn-Sham DFT; an obvious choice is to apply the Kohn-Sham inversion method again, with order-by-order matching in the counting parameter λ . Once again,

$$\text{diagrams} \implies W[J, j, \lambda] = W_0[J, j] + \lambda W_1[J, j] + \lambda^2 W_2[J, j] + \dots \quad (196)$$

$$\text{assume} \implies J[\rho, \kappa, \lambda] = J_0[\rho, \kappa] + \lambda J_1[\rho, \kappa] + \lambda^2 J_2[\rho, \kappa] + \dots \quad (197)$$

$$\text{assume} \implies j[\rho, \kappa, \lambda] = j_0[\rho, \kappa] + \lambda j_1[\rho, \kappa] + \lambda^2 j_2[\rho, \kappa] + \dots \quad (198)$$

$$\text{derive} \implies \Gamma[\rho, \kappa, \lambda] = \Gamma_0[\rho, \kappa] + \lambda \Gamma_1[\rho, \kappa] + \lambda^2 \Gamma_2[\rho, \kappa] + \dots \quad (199)$$

Start with the exact expressions for Γ and ρ

$$\Gamma[\rho, \kappa] = W[J, j] - \int J \rho - \int j \kappa , \quad (200)$$

and

$$\rho(x) = \frac{\delta W[J, j]}{\delta J(x)}, \quad \kappa(x) = \frac{\delta W[J, j]}{\delta j(x)} , \quad (201)$$

and plug in the expansions, with ρ, κ treated as order unity. Zeroth order is the Kohn-Sham system with potentials $J_0(\mathbf{x})$ and $j_0(\mathbf{x})$,

$$\Gamma_0[\rho, \kappa] = W_0[J_0, j_0] - \int J_0 \rho - \int j_0 \kappa , \quad (202)$$

so the *exact* densities $\rho(\mathbf{x})$ and $\kappa(\mathbf{x})$ are *by construction*

$$\rho(x) = \frac{\delta W_0[J_0, j_0]}{\delta J_0(x)}, \quad \kappa(x) = \frac{\delta W_0[J_0, j_0]}{\delta j_0(x)} . \quad (203)$$

Now introduce single-particle orbitals to diagonalize Γ_0 , which means solving

$$\begin{pmatrix} h_0(\mathbf{x}) - \mu_0 & j_0(\mathbf{x}) \\ j_0(\mathbf{x}) & -h_0(\mathbf{x}) + \mu_0 \end{pmatrix} \begin{pmatrix} u_i(\mathbf{x}) \\ v_i(\mathbf{x}) \end{pmatrix} = E_i \begin{pmatrix} u_i(\mathbf{x}) \\ v_i(\mathbf{x}) \end{pmatrix} \quad (204)$$

where

$$h_0(\mathbf{x}) \equiv -\frac{\nabla^2}{2M} + v_{\text{ext}}(\mathbf{x}) - J_0(\mathbf{x}) . \quad (205)$$

As expected, this is just like the Skyrme Hartree-Fock Bogoliubov (HFB) approach [47]. For *ab initio* DFT based on wave-function methods, Bogoliubov transformations lead to the same generalized Kohn-Sham equations.

The diagrammatic expansion of the W_i 's is the same as without pairing, except now lines in diagrams are KS Nambu-Gor'kov Green's functions [150],

$$\mathbf{G} = \begin{pmatrix} \langle T\psi_\uparrow(x)\psi_\uparrow^\dagger(x') \rangle_0 & \langle T\psi_\uparrow(x)\psi_\downarrow(x') \rangle_0 \\ \langle T\psi_\downarrow^\dagger(x)\psi_\uparrow^\dagger(x') \rangle_0 & \langle T\psi_\downarrow^\dagger(x)\psi_\downarrow(x') \rangle_0 \end{pmatrix} \equiv \begin{pmatrix} G_{\text{ks}}^0 & F_{\text{ks}}^0 \\ F_{\text{ks}}^{0\dagger} & -\tilde{G}_{\text{ks}}^0 \end{pmatrix} , \quad (206)$$

where the time-ordering is with respect to Euclidean time. In frequency space, the Kohn-Sham Green's functions are

$$G_{\text{ks}}^0(\mathbf{x}, \mathbf{x}'; \omega) = \sum_j \left[\frac{u_j(\mathbf{x}) u_j^*(\mathbf{x}')}{i\omega - E_j} + \frac{v_j(\mathbf{x}') v_j^*(\mathbf{x})}{i\omega + E_j} \right] , \quad (207)$$

$$F_{\text{ks}}^0(\mathbf{x}, \mathbf{x}'; \omega) = - \sum_j \left[\frac{u_j(\mathbf{x}) v_j^*(\mathbf{x}')}{i\omega - E_j} - \frac{u_j(\mathbf{x}') v_j^*(\mathbf{x})}{i\omega + E_j} \right] . \quad (208)$$

The Kohn-Sham self-consistency procedure involves the same iterations as in phenomenological Skyrme HF (or relativistic mean-field) when pairing is included. In terms of the orbitals, the fermion density is

$$\rho(\mathbf{x}) = 2 \sum_i |v_i(\mathbf{x})|^2 , \quad (209)$$

and the pair density is (warning: this is unrenormalized!)

$$\kappa(\mathbf{x}) = \sum_i [u_i^*(\mathbf{x}) v_i(\mathbf{x}) + u_i(\mathbf{x}) v_i^*(\mathbf{x})] . \quad (210)$$

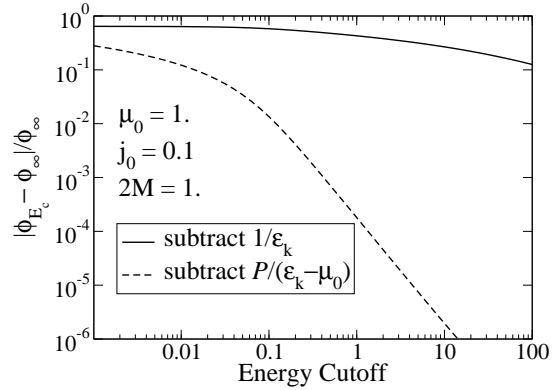
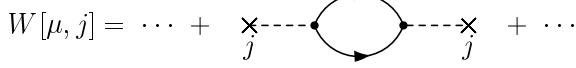


Figure 12: (a) Feynman diagram at second order in a perturbative expansion of $W[\mu, j]$ in j . (b) Convergence of the integral for the pair density in the uniform system for two subtractions as a function of an energy cutoff E_c in the integral.

The chemical potential μ_0 is fixed by $\int \rho(\mathbf{x}) = A$. Diagrams for $\Gamma[\rho, \kappa] \propto E_0[\rho, \kappa] + E_{\text{int}}[\rho, \kappa]$ yield the Kohn-sham potentials

$$J_0(\mathbf{x}) \Big|_{\rho=\rho_{\text{gs}}} = \frac{\delta E_{\text{int}}[\rho, \kappa]}{\delta \rho(\mathbf{x})} \Big|_{\rho=\rho_{\text{gs}}} \quad \text{and} \quad j_0(\mathbf{x}) \Big|_{\kappa=\kappa_{\text{gs}}} = \frac{\delta E_{\text{int}}[\rho, \kappa]}{\delta \kappa(\mathbf{x})} \Big|_{\kappa=\kappa_{\text{gs}}}. \quad (211)$$

So it appears that everything goes through smoothly as in the *ab initio* DFT without pairing.

Potential problems arise, however, because the use of local composite operators leads to new ultra-violet divergences even at the mean-field (Hartree-Fock) level when pairing is included. Divergences at this order are not encountered when coupling an external source to the fermion density $\psi^\dagger \psi$, but appear now because the composite operators $\psi \psi$ and $\psi^\dagger \psi^\dagger$ need additional renormalization [151]. The divergences at leading order are symptomatic of generic problems identified long ago by Banks and Raby [152] that arise with effective potentials of local composite operators. (It was to avoid these divergences in DFT that non-local sources were used in Refs. [153, 154].) These problems inhibited for many years the use of effective actions of composite operators but more recently Verschelde et al. [155, 156, 157] and Miransky et al. [158, 159, 160] have revived their use for relativistic field theories. In Ref. [143], it was shown how to identify and renormalize up to NLO the EFT from Section 4.3 when pairing was included.

The source of the divergences is found immediately when we try to carry out the DFT pairing calculation even for a *uniform* dilute Fermi system. The generating functional with constant sources μ and j for the EFT from Section 4.3 is:

$$\begin{aligned} e^{-W[\mu, j]} &= \int D(\psi^\dagger \psi) \exp \left\{ - \int d^4x \left[\psi_\alpha^\dagger \left(\frac{\partial}{\partial \tau} - \frac{\nabla^2}{2M} - \mu \right) \psi_\alpha \right. \right. \\ &\quad \left. \left. + \frac{C_0}{2} \psi_\uparrow^\dagger \psi_\downarrow^\dagger \psi_\downarrow \psi_\uparrow + j(\psi_\uparrow \psi_\downarrow + \psi_\downarrow^\dagger \psi_\uparrow^\dagger) \right] \right\} + \frac{1}{2} \zeta j^2 \right] \} \end{aligned} \quad (212)$$

(cf. adding an integration over an auxiliary field $\int D(\Delta^*, \Delta) e^{-\frac{1}{|C_0|} \int |\Delta|^2}$, then shifting variables to eliminate $\psi_\uparrow^\dagger \psi_\downarrow^\dagger \psi_\downarrow \psi_\uparrow$ for $\Delta^* \psi_\uparrow \psi_\downarrow$). There are new divergences because of j , e.g., expand W to $\mathcal{O}(j^2)$ [see Fig. 12(a)], which has the same linear divergence found in 2-to-2 scattering. (Equivalently, in coordinate space there is a $1/|\mathbf{r}_1 - \mathbf{r}_2|$ divergence in $\sum_i v_i^*(\mathbf{r}_1) u_i(\mathbf{r}_2)$ as it becomes local with $|\mathbf{r}_1 - \mathbf{r}_2| \rightarrow 0$.) To renormalize, we add the counterterm $\frac{1}{2} \zeta |j|^2$ to \mathcal{L} (see [120]), which is additive to W (cf. $|\Delta|^2$), so there is no effect on scattering.

We can follow a less formal and more numerically suitable procedure to renormalize the pair (anomalous) density,

$$\kappa(\mathbf{x}) = \sum_i [u_i^*(\mathbf{x})v_i(\mathbf{x}) + u_i(\mathbf{x})v_i^*(\mathbf{x})] \longrightarrow \infty , \quad (213)$$

which diverges for contact interactions in a finite system. This is to use the renormalized expression for κ in the uniform system,

$$\kappa = \int^{k_c} \frac{d^3 k}{(2\pi)^3} j_0 \left(\frac{1}{\sqrt{(\epsilon_k^0 - \mu_0)^2 + j_0^2}} - \frac{1}{\epsilon_k^0} \right) \xrightarrow{k_c \rightarrow \infty} \text{finite}, \quad (214)$$

which is cut off at momentum k_c , and apply this in a local density approximation (i.e., Thomas-Fermi):

$$\kappa(\mathbf{x}) = 2 \sum_i^{E_c} u_i(\mathbf{x})v_i(\mathbf{x}) - j_0(\mathbf{x}) \frac{M k_c(\mathbf{x})}{2\pi^2} \quad \text{with} \quad E_c = \frac{k_c^2(\mathbf{x})}{2M} + J(\mathbf{x}) - \mu_0 . \quad (215)$$

This procedure was worked out by Bulgac and collaborators in Refs. [52, 51, 149, 161]. Convergence is very slow as the energy cutoff E_c is increased, so Bulgac and Yu devised a different subtraction,

$$\kappa = \int^{k_c} \frac{d^3 k}{(2\pi)^3} j_0 \left(\frac{1}{\sqrt{(\epsilon_k^0 - \mu_0)^2 + j_0^2}} - \frac{\mathcal{P}}{\epsilon_k^0 - \mu_0} \right) \xrightarrow{k_c \rightarrow \infty} \text{finite} . \quad (216)$$

A comparison of convergence in the uniform system for the two subtraction schemes (214) and (216) [see Fig. 12] shows dramatic improvement for the Bulgac/Yu subtraction. Bulgac et al. have demonstrated that this works in finite systems [149] and it has been adopted for some Skyrme HFB implementations.

5.2 Broken symmetries

Ordinary nuclei are self-bound, which presents conceptual issues about whether Kohn-Sham DFT is well defined and practical problems on how to deal with the consequences of symmetry breaking by the KS potentials, which will not have all of the symmetries of the Hamiltonian [46].²² These broken symmetries include the $U(1)$ phase symmetry for fermion number and translational and rotational invariance. While restoring broken symmetries is a topic well-explored for mean-field approximations [46, 47], it has only recently been considered in a context relevant to *ab initio* DFT. Because no proven practical approaches are yet available, we simply point out the issues and current references.

The textbook discussions of how to restore mean-field broken symmetries tend to follow one of these two related lines of discussion:

- States related by a unitary transformation $U(\alpha)$ corresponding to a broken symmetry are degenerate:

$$|\phi \alpha\rangle = U(\alpha)|\phi\rangle \quad (217)$$

with $|\phi\rangle$ a “deformed” state, implies

$$\langle \phi \alpha | H_N | \phi \alpha \rangle = \langle \phi | H_N | \phi \rangle . \quad (218)$$

The degeneracy can be removed by diagonalizing in the subspace spanned by the degenerate states. The group parameter α for continuous groups can be considered a *collective coordinate*, which specifies the orientation in gauge space of the deformed state $|\phi\rangle$. A general strategy is to transform from $3A$ particle coordinates into collective and internal coordinates [47].

²²A state is one of broken symmetry if it does not have the quantum numbers of the eigenstates of the Hamiltonian (parity, particle number, angular momentum, linear momentum, isospin, and so on). Note that this does not mean it needs to be *invariant*, just that it can be labeled by definite quantum numbers [46].

- In finite systems, broken symmetries arise only as a result of approximations. This usually happens with variational calculations over trial wavefunctions that are too restricted; a mean-field approximation is an example. The symmetry can be restored by using a linear superposition of degenerate states:

$$|\psi\rangle = \int d\alpha f(\alpha)|\phi_\alpha\rangle, \quad (219)$$

which when minimized with respect to the $f(\alpha)$'s projects states of good symmetry [46]. (Because minimizing with respect to $|\phi\rangle$ and with respect to $f(\alpha)$ do not commute, there are two types of projection. It is most accurate to project first and then find the best deformed state corresponding to a given quantum number.) For example, particle number projection for EDF's is described in Refs. [162, 163].

When implemented, these approaches are sometimes considered to be beyond EDF, where there are only densities and not a wavefunction. From a different perspective, the restoration of broken symmetries of GCM-type configuration mixings should be considered as a “multi-reference” extension of the usual “single-reference” EDF implementation (see Refs. [12, 48, 49]). What about *ab initio* DFT as we have considered it?

For nuclear DFT, the conceptual question was highlighted by J. Engel [164], who pointed out that the ground state of a self-bound system, with a plane wave describing the center of mass, has a density distributed uniformly over space. Clearly this is not the density one wants to find from DFT, so there is a question of how to proceed. There are two separate considerations: i) Does Kohn-Sham DFT exist in a useful form for self-bound systems? ii) If so, how does one formulate and implement it? Engel and other authors have addressed this issue recently [164, 165, 166, 167, 168, 169], with a consensus that HK existence proofs for DFT are still well founded, but for *internal* densities (meaning independent of the center-of-mass motion when considering broken translational symmetry).²³ These authors also propose various schemes to carry out Kohn-Sham DFT that should be testable in the near future.

We have considered *ab initio* DFT from two viewpoints: MBPT using wave-function methods and effective actions with path integrals. How are these symmetry issues dealt with in these approaches? Wave function methods have several related strategies for dealing with the “center of mass” (COM) problem:

1. Isolate the “internal” degrees of freedom, typically by introducing Jacobi coordinates. Then the observables are by construction independent of the COM. This gets increasingly cumbersome with greater numbers of particles.
2. Work in a harmonic-oscillator Slater determinant basis, for which the COM decouples, and introduce a potential for the COM that allows its contribution to be subtracted.
3. Work with the internal Hamiltonian (i.e., subtract the COM kinetic energy T_{CM}) so that the COM part factors and does not contribute to observables to good approximation (see in particular Ref. [170] for coupled cluster calculations).

Versions of the first two possibilities are in fact among the ideas considered for DFT in Refs. [164, 165, 166, 167, 168, 169].

For the effective action approach, the issue of broken symmetry is familiar from the study of solitons [171, 32], where it arises as the problem of dealing with zero modes when calculating quantum fluctuations. The methods found in the literature are similar to the textbook approaches cited above. One compelling approach for *ab initio* DFT in the effective action formalism uses the Fadeev-Popov

²³In other contexts, such densities are called “intrinsic”, but this has a different meaning in the context of symmetry breaking, so “internal” is typically used instead.

construction (or BRST invariance [121]) to introduce collective coordinates through ghost degrees of freedom. This is worked out to some degree by Calzetta and Hu for broken particle number symmetry in Ref. [122], but a concrete implementation appropriate for nuclei remains to be formulated.

Thus, while dealing with broken symmetries in the DFT of self-bound nuclei is a topic of active investigation, the best way forward is not clear.

5.3 Single-particle energies

The only quantities obtained from Kohn-Sham DFT for ground states that are guaranteed to be the same as those obtained from many-body wave function calculations (at an equivalent level of approximation) are the total energies and the densities associated with the functionals.²⁴ Of course, measurable quantities that can be expressed as the differences of ground state energies are also reliable. For nuclear applications, one would like to establish a robust connection between KS eigenvalues and nuclear single-particle energies, but it is often observed that Kohn-Sham eigenvalues, except at the Fermi surface, are not physical. On the other hand, Bartlett et al. claim that with a sufficiently rich Coulomb DFT functional, the KS orbital eigenvalues can be good approximations to removal (ionization) energies [58, 59].

We can understand how improved approximations can happen by considering how the full self-consistent one-particle Green's function G , whose spectral density *is* physical, can be expressed in terms of the KS Green's function G_{KS} . We saw this earlier in the form of the Sham-Schlüter equation, Eq. (65); here we consider an alternative functional integral derivation and a diagrammatic representation to make some additional points. We add a non-local source $\xi(x', x)$ coupled to $\psi(x)\psi^\dagger(x')$ [we're in Minkowski space now with $x = (\mathbf{x}, t)$ so that we get real-time Green's functions]:

$$Z[J, \xi] = e^{iW[J, \xi]} = \int D\psi D\psi^\dagger e^{i \int d^4x [\mathcal{L} + J(x)\psi^\dagger(x)\psi(x) + \int d^4x' \psi(x)\xi(x, x')\psi^\dagger(x')]} . \quad (220)$$

Writing $\Gamma[\rho, \xi] = \Gamma_0[\rho, \xi] + \Gamma_{\text{int}}[\rho, \xi]$ and using functional properties of Legendre transforms,

$$G(x, x') = \left. \frac{\delta W}{\delta \xi} \right|_J = \left. \frac{\delta \Gamma}{\delta \xi} \right|_\rho = G_{\text{KS}}(x, x') + G_{\text{KS}} \left[\frac{1}{i} \frac{\delta \Gamma_{\text{int}}}{\delta G_{\text{KS}}} + \frac{\delta \Gamma_{\text{int}}}{\delta \rho} \right] G_{\text{KS}} , \quad (221)$$

which is represented diagrammatically in Fig. 13 [134]. (Note that these are the reducible self-energies here; so this is actually a rearranged Dyson-like equation that is equivalent to Eq. (65).)

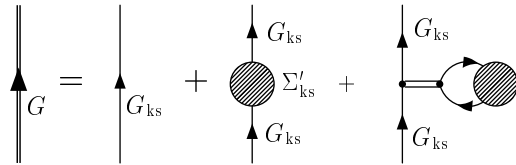
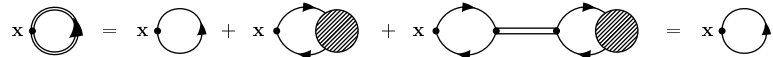


Figure 13: Full Green's function G in terms of the Kohn-Sham Green's function G_{KS} .

The Green's functions G and G_{KS} yield the same density *by construction*; that is, the Kohn-Sham density $\rho_{\text{KS}}(\mathbf{x}) = -i\nu G_{\text{KS}}^0(x, x^+)$ equals the full density $\rho(\mathbf{x}) = -i\nu G(x, x^+)$. Here is a simple diagrammatic demonstration (the double line is minus the inverse of a single particle-hole ring):



²⁴Note that these densities are not necessarily observables; e.g., the nuclear proton density is related to the measured charge density by a model dependent prescription, although this model dependence is generally considered to be negligible.

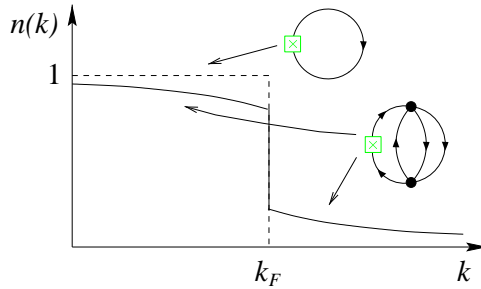


Figure 14: Schematic momentum occupation number $n(k)$ for mean-field (Hartree-Fock) and with correlations.

But other single-particle properties (e.g., the spectrum) are generally different, because the last two diagrams in Fig. 13 will not cancel exactly. However, we can make them cancel more closely by redefining the Kohn-Sham system as described in Section 3.2. In the effective action approach, we find that adding sources does exactly this. For example, in the dilute Fermi gas EFT from Section 4.3, the single-particle spectrum from a functional with ρ and τ densities was shown to be closer to the exact spectrum (e.g., at the HF level) than a functional based on ρ alone (see Ref. [112] for details). This is consistent with the Bartlett et al. claim. More generally, we can use the Kohn-Sham basis in constructing the full G .

One final note regarding Green’s functions. The comparison of Kohn-Sham DFT and “mean-field” models often leads to misunderstandings, as when considering “occupation numbers”, because of a confusion between G and G_{KS} . Figure 14 suggests that occupation numbers are equal to 0 or 1 if and only if correlations are *not* included. The Kohn-Sham propagator *always* has a “mean-field” structure, which means that (in the absence of pairing) the Kohn-Sham occupation numbers in the normal state are always 0 or 1. But correlations are certainly included in $\Gamma[\rho]!$ (In principle, all correlations can be included; in practice, certain types like long-range particle-hole correlations may be largely omitted because of limitations of the functional.) Further, $n(\mathbf{k}) = \langle a_{\mathbf{k}}^\dagger a_{\mathbf{k}} \rangle$ is resolution dependent (not an observable!); the operator related to experiment is more complicated. Additional discussion on these issues can be found in [172].

5.4 Improving empirical EDF’s

The technology for calculating with phenomenological energy density functionals such as those of the Skyrme form is already well developed and still improving. For example, machinery exists to calculate the entire mass table using a Skyrme form of the energy functional in a single day (examples of current capabilities are given in Refs. [106, 8, 173]). These calculations are quite successful, achieving root-mean-squared errors better than 2 MeV for the measured nuclides [11]. (See Ref. [45] for a state-of-the-art Gogny EDF.) Figures 15 and 16 show examples of both the successes and limitations of current Skyrme functionals. In particular, the trend is toward good reproduction of experimental data where it exists, but extrapolations toward the driplines where there is no data become uncertain and sensitive to poorly constrained parts of the functional. Improving the reliability of extrapolation is, of course, a prime motivation for *ab initio* DFT.

There are substantial and diverse efforts in progress to improve the functionals in use. Most of these, even if not directly motivated by ties to microscopic *ab initio* input, will make such connections more likely. In particular these efforts include:

- Generalizing the Skyrme functional. By making the functional a more complete representation of the possible physics, one gets closer to the systematics and model independence characteristic of effective field theory. Work in this direction includes adding tensor interactions [175, 113, 176], time-odd components [177, 178], and gradient and density corrections [178].

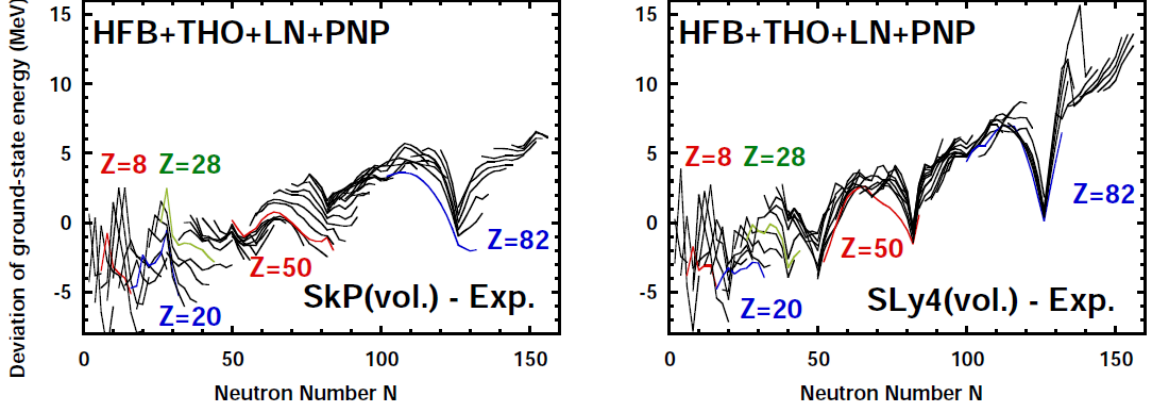


Figure 15: Deviations from experiment of Skyrme-Hartree-Fock EDF predictions for ground-state energies by two functionals [174].

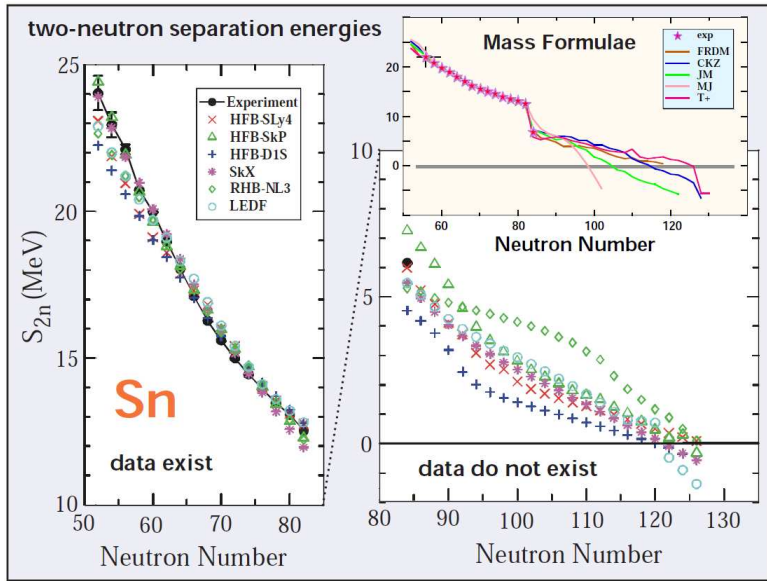


Figure 16: Extrapolation of predictions from Skyrme-Hartree-Fock functionals and mass formulas for two-neutron separation energies in tin isotopes [174].

- Correlation studies. By studying systematically the errors from empirical functionals, clues for the important microscopic physics are unearthed. One example is the study of odd-even mass differences [173, 179] and other examples are described in Refs. [97, 98, 180].
- Non-empirical approaches to pairing. At present these are hybrid calculations using a Skyrme EDF for the particle-hole part but a separable low-momentum potential at leading order to describe pairing [14]. The predictions of pairing gaps are remarkably consistent with those extracted from experiments (from three-point formulas using energies of adjacent nuclei as input) [14, 15, 16]. A systematic investigation of theoretical corrections is underway.
- New constraints from *ab initio* theory. As noted earlier, microscopic many-body calculations of symmetric nuclear matter are less valuable than constraints from stable nuclei. However, the isovector parts of the empirical functionals are much less constrained by data and this is where the microscopic calculations should be most reliable. For example, Monte Carlo calculations of energies and densities for neutrons in traps (generally with AFMC). The trap serves as a variable

$v_{\text{ext}}(\mathbf{x})$, so these calculations become benchmarks for testing or fitting empirical energy functionals. Note that constraints can be significantly more than realized by comparison to uniform neutron matter. Such a program is being carried out with GFMC/AFMC and NCSM calculations as part of the UNEDF project [9].

- Development of EDF without explicit underlying Hamiltonians. The strategy and distinction of EDF from DFT are described in Ref. [12], as well as challenges [13]. The insights gained and techniques being developed [12, 48, 49] will carry over to *ab initio* DFT.
- Long-range correlations. With current EDF's, the incorporation of long-range correlation effects is handled separately from the functional calculations [11, 41]. The outlook for directly including this physics in an *ab initio* approach with OEP is unclear, but there are precedents in Coulomb OEP (e.g., the Coulomb ring sum describing the high-density expansion of the electron gas can be included).
- Merging a variant of the density matrix expansion (DME) and empirical functionals. The comparison of the DME-I and DME-II curves in Fig. 7 gives us an estimate of the truncation error in the expansion applied to the NNN terms because these prescriptions differ in the contributions of higher-order terms in the expansion. Indeed, it has been verified that suppressing these terms by hand brings the predictions for the A and B coefficients into agreement [96]. The qualitative difference for the NNN-only contribution to B is large, but the actual coefficient itself is small, so this should not be alarming. However, because the combination of A and B and the kinetic energy to obtain the nuclear matter energy per particle involves strong cancellations, the spread in Fig. 7 is large on the scale of nuclear binding energies.

These differences motivate a generalization of the Negele-Vautherin DME following the discussion in Ref. [181]. In this approach, the expansion of the scalar density matrix takes the factorized form

$$\rho(\mathbf{R} + \frac{\mathbf{s}}{2}, \mathbf{R} - \frac{\mathbf{s}}{2}) = \sum_n \Pi_n(k_F s) \langle \mathcal{O}_n(\mathbf{R}) \rangle , \quad (222)$$

where

$$\langle \mathcal{O}_n(\mathbf{R}) \rangle = \{\rho(\mathbf{R}), \tau(\mathbf{R}), \nabla^2 \rho(\mathbf{R}), \dots\} , \quad (223)$$

and k_F is a momentum scale typically taken to be $k_F(\mathbf{R})$ as in Eq. (120). Similar expansions are made for the other components of the density matrix. Input from finite nuclei can be used to determine the Π_n functions, which can be viewed as general resummations of the DME expansion. A program to merge these developments with empirical Skyrme functionals is underway [115].

Almost all of the major developments are only recently begun, so many new results can be expected in the coming years.

6 Summary and outlook

The quest for an understanding of *all* nuclei based on microscopic few-body interactions among nucleons is being attacked from multiple directions. In this review, we have considered *ab initio* density functional theory for nuclei, defined as DFT based on a realistic nuclear Hamiltonian (meaning one that accurately reproduces few-body data) and orbitals that satisfy equations with local Kohn-Sham potentials. This is an ambitious undertaking and one which will not be realized without significant further developments in nuclear structure calculations. Nevertheless, the prospects are good for making microscopic connections to empirical functionals in the short term and building on them steadily.

We base this optimism in part on the successful advances in *ab initio* DFT for Coulomb-based systems by quantum chemists and condensed matter physicists. We believe nuclear physicists will profit from greater attention paid to Coulomb DFT developments. At the same time, we recognize that these advances have taken many years to realize and may not be readily transferred to the nuclear domain. Indeed, we have argued that strong analogies between Coulomb and nuclear systems are really only apparent when one considers low-momentum interactions, so that the correlations induced by more conventional (local or almost local) interactions are tamed from the outset. As one strives for greater accuracy, the differences between atoms or molecules and nuclei are likely to become more significant.

Perdew and collaborators describe for Coulomb DFT a “Jacob’s Ladder” of increasingly sophisticated “nonempirical” functionals stretching toward the heaven of chemical accuracy. In Ref. [43], five rungs of the ladder are identified (see also [182]):

1. The local density approximation (LDA) with both spin densities $\rho_{\uparrow}(\mathbf{x})$ and $\rho_{\downarrow}(\mathbf{x})$ as ingredients (usually called LSDA).
2. The generalized gradient approximation (GGA), which adds dependence on $\nabla\rho_{\uparrow}(\mathbf{x})$ and $\nabla\rho_{\downarrow}(\mathbf{x})$ to the LSDA functional.
3. The meta-GGA adds dependence on (some subset of) $\nabla^2\rho_{\uparrow}(\mathbf{x})$, $\nabla^2\rho_{\downarrow}(\mathbf{x})$, $\tau_{\uparrow}(\mathbf{x})$, and $\tau_{\downarrow}(\mathbf{x})$. Note that the kinetic energy densities are actually non-local functionals of the ordinary density, although only semi-local functionals of the occupied KS orbitals.
4. Hyper-GGA, which includes the exact exchange energy density calculated with the (occupied) orbitals.
5. Full orbital-based DFT, which in addition to exact exchange uses unoccupied orbitals. For example, this might include the random phase approximation (RPA) with Kohn-Sham orbitals to address long-range correlations.

An important aspect of the overall approach is “constraint satisfaction” as opposed to data fitting, which is why the functionals are called nonempirical [182]. Climbing this ladder has been a decades-long effort by quantum chemists with much development in progress on the last rung.

We can imagine a corresponding ladder for nuclear DFT climbing toward a universal energy density functional tied to microscopic nuclear Hamiltonians (and ultimately to QCD) that predicts known nuclear properties more accurately than currently possible and robustly predicts unknown properties with plausible theoretical error estimates. The rungs might look like this:

1. Present-day Skyrme EDF’s, which are mostly empirical (i.e., fit to properties of selected medium-to-heavy nuclei), such as described in Ref. [11].
2. Generalized Skyrme interactions, with additional gradient and density dependences, with new constraints from microscopic theory (e.g., neutron drops).
3. Functionals that merge the long-range parts of the microscopic NN and NNN interactions prescribed by chiral EFT, converted to semi-local form with a variant of the density matrix expansion (DME), with a Skyrme functional. The short-range parameters should be refit to nuclear properties and theoretical constraints.
4. A complete functional based on a variant of DME applied to a low-momentum potential that is evolved from chiral EFT NN and NNN interactions.
5. Full orbital-based DFT based on low-momentum interactions.

This ladder is tied to our restriction to local Kohn-Sham potentials and so naturally builds on Skyrme EDF's. An alternative ladder could build on non-local potentials (e.g., on Gogny-type EDF's) that arise from derivatives with respect to density matrices rather than densities; see Refs. [13, 16] for discussions along these lines. Just as in the Coulomb ladder, one hopes for monotonic improvements at each rung, but this may not always be the case. (Of course, rungs will shift or more will be added as progress is made.)

Rather than climb slowly over the course of decades, nuclear physicists are trying to catch up rapidly by attacking all of the higher rungs in parallel [8, 9, 10]. As described in Section 5.4, there are extensive ongoing efforts to explore the second rung, including more general density dependence and higher-order gradients [9, 10], while projects on both rungs three and four have recently been started as part of the UNEDF project [8]. The last rung is in the exploratory stage with tests started in one dimension with nuclear-like interactions for both self-bound and trapped systems to explore the accuracy of the KLI (and related) approximations compared to a full OEP treatment of such systems and to establish the limitations of semi-local expansions such as the DME.

While the last two rungs can be purely predictive if only few-body data is used to determine the input Hamiltonian, it is likely that fine-tuning to heavier nuclei will be needed to reach the accuracy goals. This is because even the best *ab initio* nuclear structure calculations at present only achieve about 1% accuracy in ground-state energies for a small fraction of the table of nuclides, while nuclear EDF's such as Skyrme functionals easily surpass this over most of the table. Indeed, the comparatively high accuracy of nuclear EDF may imply that a different organization of the problem (e.g., based on a finite-density effective field theory of nuclei) may be needed.

There are many important open questions to be addressed in the course of these projects (see also Ref. [13]). Among them are those highlighted in Section 5 on symmetry breaking and restoration, single-particle levels, and pairing; these will be relevant for all rungs of the ladder. At the top of the ladder we can ask: Which of the problems encountered in Coulomb DFT that motivate orbital-based functionals have analogs in nuclear DFT? E.g., what is the impact of self-interaction and missing derivative discontinuities? Another class of open questions concerns the input Hamiltonian: For low-momentum potentials, how accurate will many-body perturbation theory be? What corrections/summations will be needed to reach the desired accuracy for nuclear DFT? Are four-body forces necessary? The list of problems yet to solve might be intimidating, especially given the many decades already spent attacking nuclear structure, but the coherence of the current effort and the dramatic advances of just the last few years give hope that they can be overcome.

We have taken a broad view at what *ab initio* density functional theory could be but our discussion has been far from an exhaustive treatment. By focusing our discussion on orbital-based DFT for nonrelativistic Hamiltonians we have excluded various alternative paths to *ab initio* DFT. Here are some of the other approaches that are relevant to the wider nuclear DFT effort:

- The perturbative in-medium results from low-momentum potentials suggest that an alternative EFT power counting may be appropriate at nuclear matter densities. Kaiser and collaborators have proposed a perturbative chiral EFT approach to nuclear matter and then to finite nuclei through an energy functional [183, 109, 111, 184, 185] (see also [186]). They consider Lagrangians both for nucleons and pions and for nucleons, pions, and Δ 's, and fit parameters to nuclear saturation properties. They construct a loop expansion for the nuclear matter energy per particle, which leads to an energy expansion of the form

$$E(k_F) = \sum_{n=2}^{\infty} k_F^n f_n(k_F/m_\pi, \Delta/m_\pi) , \quad [\Delta = M_\Delta - M_N \approx 300 \text{ MeV}] \quad (224)$$

where each f_n is determined from a finite number of in-medium Feynman diagrams, which incorporate the long-distance physics. All powers of k_F/m_π and Δ/m_π are kept in the f_n 's because these

ratios are not small quantities [187]. A semi-quantitative description of nuclear matter is found even with just the lowest two terms without Δ 's and adding Δ 's brings uniform improvement (e.g., in the neutron matter equation of state). There are open questions about power counting and convergence, but many promising avenues to pursue. By applying the DME in momentum space to this expansion they derive a Skyrme-like energy functional for nuclei, which has also been merged with a treatment of strong scalar and vector mean fields. [109, 110, 111, 184, 185].

- The Superfluid Local Density Approximation (SLDA) and extensions developed by Bulgac and collaborators [149, 188, 189, 190] have been applied with great success to systems of trapped cold fermionic atoms with large scattering lengths. The SLDA is an extension of DFT to superfluid system that uses a semi-local energy density with parameters determined by matching to numerically accurate Monte Carlo simulations of uniform systems. Extensive further development of the SLDA for nuclear systems is in progress.
- We have noted that the Kohn-Sham DFT emphasis on locality in coordinate space is not so natural in many-body formulations. In particular, the nuclear shell model is naturally considered in the space of orbitals. Papenbrock has applied the Legendre transform formulation of DFT to energy functionals based on shell-model occupation numbers. That is, a functional of the density now becomes a function of the occupation numbers in the model space. He and his collaborators have shown the usefulness of this in solvable models (the pairing Hamiltonian [191] and the three-level Lipkin model [56]). The functional is orbital-based and thus non-local in density. For applications to nuclei, the idea is to generalize the Duflo-Zuker mass formula [192, 193] to a functional of occupation numbers, with values determined from the minimization of the functional. With 10 parameters, an RMS value of deviation for masses of about 2000 nuclei is just over 1 MeV.
- Schwenk and Polonyi have proposed an alternative approach to *ab initio* but orbit-free DFT (i.e., not Kohn-Sham) using a clever renormalization group (RG) evolution [132]. The idea is to introduce an effective action for a nucleus with a low-momentum interaction included with a multiplicative factor λ and a confining background potential (e.g., a harmonic oscillator trap) with a factor $(1 - \lambda)$. As λ flows from 0 to 1, the background potential is turned off and the interactions, with associated many-body correlations, are turned on. This evolution is dictated by an RG equation in λ . Work is in progress to implement this approach for a realistic nucleus [194].
- There is a large body of work on covariant approaches to nuclear DFT, which cannot be adequately summarized here. Fortunately, there are many reviews that highlight DFT connections, including Refs. [195, 196, 197, 147, 198, 199], to supplement our brief discussion. Covariant DFT invokes a different organization of the nuclear many-body problem that is particularly compelling because of the coupling of spin-orbit and central components dictated by relativity. In particular, the characteristic feature of relativistic approaches to nuclei is large isoscalar Lorentz scalar and vector mean fields, several hundred MeV in magnitude at nuclear densities, which cancel to provide nuclear binding but add to produce spin-orbit splittings.

Relativistic mean-field models were originally motivated as the Hartree approximation to a more complete theory, but a more recent interpretation of the largely empirical functionals is as relativistic versions of Kohn-Sham DFT [196]. The mean fields serve as local Kohn-Sham potentials in Dirac equations for the orbitals. This picture is consistent with a microscopic derivation within an effective action formulation as in Section 4 with sources coupled to each of the relativistic densities or currents or to corresponding meson-like auxiliary fields [147] (this is in contrast to implementations of relativistic electronic DFT for heavy atoms, which include only the vector four-current [4]). Application of a loop expansion with proper renormalization gives the possibility of a systematic microscopic expansion [200, 201]. Other ongoing efforts to provide more

ab initio aspects including a connection to free-space NN scattering derive relativistic EDF with density dependent meson-baryon vertex functionals, derived from the Dirac-Brueckner theory (see Refs. [202, 203, 204] and references cited therein).

These more microscopic approaches do not at present have the close connection to few-body data and to *ab initio* structure calculations of light nuclei that is possible with the non-relativistic approaches we have considered. However, the wide phenomenological successes and complementary nature of covariant nuclear DFT motivate further work toward incorporating additional microscopic constraints. In the process, most of the challenges confronting nonrelativistic DFT discussed above are being attacked in parallel for covariant DFT. This includes the issues of realistic pairing interactions [205, 206, 207], coupling to particle-hole vibrations [208], and symmetry breaking/restoration [209, 210, 211].

Each of these avenues has the potential to make a significant impact on nuclear DFT.

Acknowledgments

We thank S. Bogner, T. Duguet, and A. Schwenk for useful discussions. This work was supported in part by the National Science Foundation under Grant No. PHY-0653312 and the UNEDF SciDAC Collaboration under DOE Grant DE-FC02-07ER41457.

References

- [1] R.M. Dreizler and E. Gross, Density Functional Theory (Springer, Berlin, 1990).
- [2] R.G. Parr and Y. Weitao, Density-Functional Theory of Atoms and Molecules (International Series of Monographs on Chemistry) (Oxford University Press, USA, 1994).
- [3] W. Koch and M.C. Holthausen, A Chemist's Guide to Density Functional Theory, 2nd Edition (Wiley-VCH, 2001).
- [4] C. Fiolhais, F. Nogueira and M. Marques, editors, A Primer in Density Functional Theory (Springer, Berlin, 2003).
- [5] R.M. Martin, Electronic Structure: Basic Theory and Practical Methods (Cambridge University Press, 2004).
- [6] J. Kohanoff, Electronic Structure Calculations for Solids and Molecules: Theory and Computational Methods (Cambridge University Press, 2006).
- [7] M. Head-Gordon and E. Artacho, Physics Today 61 (2008) 58.
- [8] G.F. Bertsch, D.J. Dean and W. Nazarewicz, SciDAC Review 6 (2007) 42.
- [9] UNEDF website, <http://unedf.org>.
- [10] FIDIPRO website, <https://www.jyu.fi/fysiikka/en/research/accelerator/fidipro>.
- [11] M. Bender, P.H. Heenen and P.G. Reinhard, Rev. Mod. Phys. 75 (2003) 121.
- [12] D. Lacroix, T. Duguet and M. Bender, Phys. Rev. C 79 (2009) 044318.
- [13] T. Duguet et al., (2006), arXiv:nucl-th/0606037.

- [14] T. Duguet and T. Lesinski, Eur. Phys. J. ST 156 (2008) 207.
- [15] K. Hebeler et al., (2009), arXiv:0904.3152.
- [16] T. Duguet and T. Lesinski, (2009), arXiv:0907.1043.
- [17] E. Epelbaum, H.W. Hammer and U.G. Meissner, (2008), arXiv:0811.1338.
- [18] R.B. Wiringa, V.G.J. Stoks and R. Schiavilla, Phys. Rev. C51 (1995) 38.
- [19] S.C. Pieper and R.B. Wiringa, Ann. Rev. Nucl. Part. Sci. 51 (2001) 53.
- [20] S.C. Pieper, Nucl. Phys. A 751 (2005) 516.
- [21] P. Navratil et al., (2009), arXiv:0904.0463.
- [22] G. Hagen et al., Phys. Rev. C76 (2007) 034302.
- [23] G. Hagen et al., Phys. Rev. C76 (2007) 044305.
- [24] S.C. Pieper, (2007), arXiv:0711.1500.
- [25] G. Hagen et al., Phys. Rev. Lett. 101 (2008) 092502.
- [26] N. Argaman and G. Makov, Am. J. Phys. 68 (2000) 69.
- [27] P. Hohenberg and W. Kohn, Phys. Rev. 136 (1964) B864.
- [28] M. Levy, Phys. Rev. A26 (1982) 1200.
- [29] W. Kutzelnigg, J. Mol. Struct. 768 (2006) 163.
- [30] H. Eschrig, The Fundamentals of Density Functional Theory (Edition am Gutenbergplatz, Leipzig, 2003).
- [31] A.L. Fetter and J.D. Walecka, Quantum Many-Particle Systems (McGraw-Hill, New York, 1972).
- [32] J.W. Negele and H. Orland, Quantum Many-Particle Systems (Addison-Wesley, Redwood City, CA, 1988).
- [33] W.H. Dickhoff and D. Van Neck, Many-Body Theory Exposed!: Propagator Description of Quantum Mechanics in Many-Body Systems; 2nd ed. (World Scientific, Singapore, 2005).
- [34] J.P. Perdew et al., Journal of Chemical Theory and Computation 5 (2009) 902.
- [35] S.K. Bogner, T.T.S. Kuo and A. Schwenk, Phys. Rept. 386 (2003) 1.
- [36] S.K. Bogner, R.J. Furnstahl and R.J. Perry, Phys. Rev. C 75 (2007) 061001.
- [37] R. Roth et al., Phys. Rev. C 72 (2005) 034002.
- [38] R. Roth et al., Phys. Rev. C 73 (2006) 044312.
- [39] S.K. Bogner et al., Nucl. Phys. A 763 (2005) 59.
- [40] S.K. Bogner et al., (2009), arXiv:0903.3366.
- [41] M. Bender and P.H. Heenen, Eur. Phys. J. A25 (2005) 519.

- [42] J.P. Perdew, Physical Review B 33 (1986) 8822.
- [43] J. Perdew and S. Kurth, Density functionals for non-relativistic coulomb systems in the new century, A Primer in Density Functional Theory, pp. 1–55, Springer, 2003.
- [44] F. Chappert, M. Girod and S. Hilaire, Phys. Lett. B668 (2008) 420.
- [45] S. Goriely et al., Phys. Rev. Lett. 102 (2009) 242501.
- [46] J.P. Blaizot and G. Ripka, Quantum Theory of Finite Systems (MIT Press, Cambridge, MA, 1985).
- [47] P. Ring and P. Schuck, The Nuclear Many-Body Problem (Springer, Berlin, 2005).
- [48] M. Bender, T. Duguet and D. Lacroix, Phys. Rev. C 79 (2009) 044319.
- [49] T. Duguet et al., Phys. Rev. C 79 (2009) 044320.
- [50] J. Dobaczewski, W. Nazarewicz and P.G. Reinhard, Nucl. Phys. A 693 (2001) 361.
- [51] A. Bulgac, Phys. Rev. C65 (2002) 051305.
- [52] A. Bulgac and Y. Yu, Phys. Rev. Lett. 88 (2002) 042504.
- [53] S. Kümmel and L. Kronik, Rev. Mod. Phys. 80 (2008).
- [54] A. Görling, J. Chem. Phys. 123 (2005) 062203.
- [55] J. Grotendorst, S. Blügel and D. Marx, editors, Computational Nanoscience: Do It Yourself! (, 2006).
- [56] M.G. Bertolli and T. Papenbrock, Phys. Rev. C78 (2008) 064310.
- [57] A. Görling, Phys. Rev. A 54 (1996) 3912.
- [58] R.J. Bartlett, V.F. Lotrich and I.V. Schweigert, J. Chem. Phys. 123 (2005) 062205.
- [59] R.J. Bartlett, I.V. Schweigert and V.F. Lotrich, J. Mol. Struct. THEOCHEM 771 (2006) 1.
- [60] S. Stringari and D.M. Brink, Nucl. Phys. A304 (1978) 307.
- [61] J.P. Perdew et al., Phys. Rev. Lett. 49 (1982) 1691.
- [62] S. Kurth, C.R. Proetto and K. Capelle, Journal of Chemical Theory and Computation 5 (2009) 693.
- [63] L. Sham and M. Schlüter, Phys. Rev. Lett. 51 (1983) 1888.
- [64] M.E. Casida, Phys. Rev. A 51 (1995) 2005.
- [65] S. Kümmel and J.P. Perdew, Phys. Rev. B 68 (2003) 035103.
- [66] A. Hesselmann et al., J. Chem. Phys. 127 (2007) 054102.
- [67] J.B. Krieger, Y. Li and G.J. Iafrate, Phys. Lett. A 146 (1990) 256.
- [68] O.V. Gritsenko and E.J. Baerends, Phys. Rev. A 64 (2001) 42506.

- [69] F. Della Sala and A. Görling, *J. Chem. Phys.* 115 (2001) 5718.
- [70] V. Staroverov, G. Scuseria and E. Davidson, *J. Chem. Phys.* 125 (2006) 081104.
- [71] B.D. Day, *Rev. Mod. Phys.* 39 (1967) 719.
- [72] R. Rajaraman and H.A. Bethe, *Rev. Mod. Phys.* 39 (1967) 745.
- [73] M. Baldo, editor, Nuclear Methods and the Nuclear Equation of State (World Scientific, Singapore, 1999).
- [74] B.D. Day, *Rev. Mod. Phys.* 50 (1978) 495.
- [75] R.L. Becker, A.D. MacKellar and B. Morris, *Phys. Rev.* 174 (1968) 1264.
- [76] L. Sham, *Phys. Rev. B* 32 (1985) 3876.
- [77] R.J. Bartlett and M. Musial, *Reviews of Modern Physics* 79 (2007) 291.
- [78] R.J. Bartlett et al., *J. Chem. Phys.* 122 (2005) 0341045.
- [79] A. Görling and M. Levy, *Phys. Rev. A* 50 (1994) 196.
- [80] A. Görling and M. Levy, *Int. J. Quantum Chem.* 56 (1995) 385.
- [81] S.K. Bogner and R.J. Furnstahl, *Phys. Lett. B* 639 (2006) 237.
- [82] P. Navratil et al., *Phys. Rev. Lett.* 99 (2007) 042501.
- [83] A. Akmal, V.R. Pandharipande and D.G. Ravenhall, *Phys. Rev. C* 58 (1998) 1804.
- [84] A. Lejeune, U. Lombardo and W. Zuo, *Phys. Lett. B* 477 (2000) 45.
- [85] D.R. Entem and R. Machleidt, *Phys. Rev. C* 68 (2003) 041001.
- [86] E. Epelbaum, W. Glöckle and U.G. Meissner, *Nucl. Phys. A* 747 (2005) 362.
- [87] S.K. Bogner et al., *Nucl. Phys. A* 784 (2007) 79.
- [88] S.K. Bogner et al., *Nucl. Phys. A* 773 (2006) 203.
- [89] S.K. Bogner et al., *Nucl. Phys. A* 801 (2008) 21.
- [90] S. Bacca et al., (2009), arXiv:0902.1696.
- [91] U. van Kolck, *Phys. Rev. C* 49 (1994) 2932.
- [92] E. Epelbaum et al., *Phys. Rev. C* 66 (2002) 064001.
- [93] A. Nogga, S.K. Bogner and A. Schwenk, *Phys. Rev. C* 70 (2004) 061002.
- [94] S.D. Glazek and K.G. Wilson, *Phys. Rev. D* 48 (1993) 5863.
- [95] F. Wegner, *Ann. Phys. (Leipzig)* 3 (1994) 77.
- [96] S.K. Bogner, R.J. Furnstahl and L. Platter, *Eur. Phys. J. A* 39 (2009) 219.
- [97] G.F. Bertsch, B. Sabbey and M. Uusnakki, *Phys. Rev. C* 71 (2005) 054311.

- [98] M. Kortelainen et al., Phys. Rev. C77 (2008) 064307.
- [99] R. Roth et al., Nucl. Phys. A 788 (2007) 12.
- [100] H. Hergert and R. Roth, Phys. Rev. C75 (2007) 051001.
- [101] R. Roth, S. Reinhardt and H. Hergert, Phys. Rev. C77 (2008) 064003.
- [102] H. Hergert and R. Roth, private communication.
- [103] C. Barbieri et al., (2006), arXiv:nucl-th/0608011.
- [104] J.W. Negele and D. Vautherin, Phys. Rev. C 5 (1972) 1472.
- [105] J.W. Negele and D. Vautherin, Phys. Rev. C 11 (1975) 1031.
- [106] M.V. Stoitsov et al., Phys. Rev. C68 (2003) 054312.
- [107] E. Perlinska et al., Phys. Rev. C69 (2004) 014316.
- [108] F. Hofmann and H. Lenske, Phys. Rev. C57 (1998) 2281.
- [109] N. Kaiser, S. Fritsch and W. Weise, Nucl. Phys. A 724 (2003) 47.
- [110] N. Kaiser, Phys. Rev. C 68 (2003) 014323.
- [111] S. Fritsch, N. Kaiser and W. Weise, Nucl. Phys. A 750 (2005) 259.
- [112] A. Bhattacharyya and R.J. Furnstahl, Nucl. Phys. A 747 (2005) 268.
- [113] T. Lesinski et al., Phys. Rev. C76 (2007) 014312.
- [114] D.M. Brink and F. Stancu, Phys. Rev. C75 (2007) 064311.
- [115] B. Gebremariam, S. Bogner and T. Duguet, in preparation.
- [116] M. Durand, V.S. Ramamurthy and P. Schuck, Phys. Lett. B 113 (1982) 116.
- [117] A. Bulgac and J.M. Thompson, Phys. Lett. B 383 (1996) 127.
- [118] M.E. Peskin and D.V. Schroeder, An Introduction to Quantum Field Theory (Addison-Wesley, Reading, USA, 1995).
- [119] S. Weinberg, The Quantum Theory of Fields: vol. II, Modern Applications (Cambridge University Press, New York, 1996).
- [120] J. Zinn-Justin, Quantum Field Theory and Critical Phenomena (Oxford University Press, New York, 2002).
- [121] D.R. Bes and J. Kurchan, The Treatment of Collective Coordinates in Many-Body Systems (World Scientific, Singapore, 1990).
- [122] E. Calzetta and B.L. Hu, (2005), arXiv:cond-mat/0508240.
- [123] R. Fukuda et al., Prog. Theor. Phys. 92 (1994) 833.
- [124] M. Valiev and G.W. Fernando, (1997), arXiv:cond-mat/9702247.

- [125] J. Polonyi and K. Sailer, Phys. Rev. B 66 (2002) 155113.
- [126] E.H. Lieb, Int. J. Quantum Chem. (1983) 243.
- [127] N. Nagaosa, Quantum Field Theory in Condensed Matter Physics (Springer-Verlag, Berlin, 1999).
- [128] M. Stone, The Physics of Quantum Fields (Springer-Verlag, Berlin, 2000).
- [129] R. Fukuda et al., Prog. Theor. Phys. Suppl. 121 (1995) 1.
- [130] M. Valiev and G.W. Fernando, Phys. Lett. A 227 (1997) 265.
- [131] M. Rasamny, M. Valiev and G.W. Fernando, Phys. Rev. B58 (1998) 9700.
- [132] A. Schwenk and J. Polonyi, (2004), arXiv:nucl-th/0403011.
- [133] S.J. Puglia, A. Bhattacharyya and R.J. Furnstahl, Nucl. Phys. A 723 (2003) 145.
- [134] A. Bhattacharyya and R.J. Furnstahl, Phys. Lett. B 607 (2005) 259.
- [135] R.J. Furnstahl, J. Phys. G 31 (2005) S1357.
- [136] W. Kohn and J.M. Luttinger, Phys. Rev. 118 (1960) 41.
- [137] J.M. Luttinger and J.C. Ward, Phys. Rev. 118 (1960) 1417.
- [138] H.W. Hammer and R.J. Furnstahl, Nucl. Phys. A 678 (2000) 277.
- [139] R.J. Furnstahl and H.W. Hammer, Annals Phys. 302 (2002) 206.
- [140] K. Okumura, Int. J. Mod. Phys. A 11 (1996) 65.
- [141] S. Yokojima, Phys. Rev. D51 (1995) 2996.
- [142] A. Bulgac, C. Lewenkopf and V. Mickrjukov, Phys. Rev. B 52 (1995) 16476.
- [143] R.J. Furnstahl, H.W. Hammer and S.J. Puglia, Annals Phys. 322 (2007) 2703.
- [144] E.J. Baerends and O.V. Gritsenko, J. Chem. Phys. 123 (2005) 062202.
- [145] R.J. Furnstahl, (2007), arXiv:nucl-th/0702040.
- [146] R.J. Furnstahl and J.C. Hackworth, Phys. Rev. C56 (1997) 2875.
- [147] R.J. Furnstahl, Lect. Notes Phys. 641 (2004) 1.
- [148] P.J. Borycki et al., Phys. Rev. C73 (2006) 044319.
- [149] Y. Yu and A. Bulgac, Phys. Rev. Lett. 90 (2003) 222501.
- [150] A.A. Abrikosov, L.P. Gorkov and I.E. Dzyaloshinski, Methods of Quantum Field Theory in Statistical Physics (Prentice-Hall, Englewood Cliffs, NJ, 1963).
- [151] J. Collins, Renormalization (Cambridge University Press, New York, 1986).
- [152] T. Banks and S. Raby, Phys. Rev. D 14 (1976) 2182.
- [153] L. Oliveira, E. Gross and W. Kohn, Phys. Rev. Lett. 60 (1988) 2430.

- [154] S. Kurth et al., Phys. Rev. Lett. 83 (1999) 2628.
- [155] H. Verschelde, Phys. Lett. B 351 (1995) 242.
- [156] H. Verschelde, S. Schelstraete and M. Vanderkelen, Phys. Lett. B 76 (1997) 161.
- [157] K. Knecht and H. Verschelde, Phys. Rev. D 64 (2001) 085006.
- [158] V.A. Miransky, Int. J. Mod. Phys. A8 (1993) 135.
- [159] V.A. Miransky and K. Yamawaki, Phys. Rev. D55 (1997) 5051.
- [160] V.P. Gusynin, V.A. Miransky and A.V. Shpigin, Phys. Rev. D58 (1998) 085023.
- [161] Y. Yu and A. Bulgac, (2003), arXiv:nucl-th/0302007.
- [162] M.V. Stoitsov et al., Phys. Rev. C76 (2007) 014308.
- [163] J. Dobaczewski et al., Phys. Rev. C76 (2007) 054315.
- [164] J. Engel, Phys. Rev. C75 (2007) 014306.
- [165] B.G. Giraud, B.K. Jennings and B.R. Barrett, Phys. Rev. A78 (2008) 032507.
- [166] N. Barnea, Phys. Rev. C76 (2007) 067302.
- [167] B.G. Giraud, Phys. Rev. C77 (2008) 014311.
- [168] B.G. Giraud, Phys. Rev. C78 (2008) 014307.
- [169] J. Messud, M. Bender and E. Suraud, (2009), arXiv:0904.0162.
- [170] G. Hagen, T. Papenbrock and D.J. Dean, (2009), arXiv:0905.3167.
- [171] R. Rajaraman, Solitons and Instantons (North Holland, New York, 1982).
- [172] R.J. Furnstahl and H.W. Hammer, Phys. Lett. B 531 (2002) 203.
- [173] G.F. Bertsch et al., Phys. Rev. C79 (2009) 034306.
- [174] W. Nazarewicz, private communication.
- [175] B.A. Brown et al., Phys. Rev. C74 (2006) 061303.
- [176] M. Zalewski et al., Phys. Rev. C77 (2008) 024316.
- [177] J. Dobaczewski and J. Dudek, Phys. Rev. C52 (1995) 1827.
- [178] B.G. Carlsson, J. Dobaczewski and M. Kortelainen, Phys. Rev. C78 (2008) 044326.
- [179] W.A. Friedman and G.F. Bertsch, (2009), arXiv:0812.2006.
- [180] J. Toivanen et al., Phys. Rev. C78 (2008) 034306.
- [181] J. Dobaczewski, (2003), arXiv:nucl-th/0301069.
- [182] J.P. Perdew et al., J. Chem. Phys. 123 (2005) 062201.

- [183] N. Kaiser, S. Fritsch and W. Weise, Nucl. Phys. A 697 (2002) 255.
- [184] P. Finelli et al., Nucl. Phys. A 770 (2006) 1.
- [185] P. Finelli et al., Nucl. Phys. A 791 (2007) 57.
- [186] M. Lutz, B. Friman and C. Appel, Phys. Lett. B 474 (2000) 7.
- [187] N. Kaiser, M. Muhlbauer and W. Weise, Eur. Phys. J. A 31 (2007) 53.
- [188] A. Bulgac and Y. Yu, Int. J. Mod. Phys. E13 (2004) 147.
- [189] A. Bulgac, Phys. Rev. A76 (2007) 040502.
- [190] A. Bulgac and M.M. Forbes, (2008), arXiv:0808.1436.
- [191] T. Papenbrock and A. Bhattacharyya, Phys. Rev. C75 (2007) 014304.
- [192] J. Duflo and A.P. Zuker, Phys. Rev. C52 (1995) 23.
- [193] J. Duflo and A.P. Zuker, (1995), arXiv:nucl-th/9505011.
- [194] J. Braun, J. Polonyi and A. Schwenk, in preparation.
- [195] P. Ring, Prog. Part. Nucl. Phys. 37 (1996) 193.
- [196] B.D. Serot and J.D. Walecka, Int. J. Mod. Phys. E 6 (1997) 515.
- [197] R.J. Furnstahl and B.D. Serot, Comments Nucl. Part. Phys. 2 (2000) A23.
- [198] D. Vretenar and W. Weise, Lect. Notes Phys. 641 (2004) 65.
- [199] D. Vretenar, Eur. Phys. J. ST 156 (2008) 37.
- [200] J. McIntire, Y. Hu and B.D. Serot, Nucl. Phys. A794 (2007) 166.
- [201] Y. Hu, J. McIntire and B.D. Serot, Nucl. Phys. A794 (2007) 187.
- [202] H. Lenske et al., Prepared for 11th International Conference on Nuclear Reaction Mechanisms, Varenna, Italy, 12-16 Jun 2006.
- [203] H. Lenske et al., Prog. Part. Nucl. Phys. 59 (2007) 114.
- [204] S. Hirose et al., Phys. Rev. C75 (2007) 024301.
- [205] M. Serra and P. Ring, Phys. Rev. C65 (2002) 064324.
- [206] Y. Tian, Z.y. Ma and P. Ring, Phys. Rev. C79 (2009) 064301.
- [207] Y. Tian, Z.Y. Ma and P. Ring, Phys. Lett. B676 (2009) 44.
- [208] E. Litvinova, P. Ring and V. Tselyaev, Phys. Rev. C75 (2007) 064308.
- [209] J.A. Sheikh et al., Phys. Rev. C66 (2002) 044318.
- [210] T. Niksic, D. Vretenar and P. Ring, Phys. Rev. C73 (2006) 034308.
- [211] J.M. Yao et al., (2009), arXiv:0903.5027.